UNDERSTANDING HETEROGENEOUS COPPER CATALYSTS FOR COUPLING REACTIONS IN ORGANIC SYNTHESIS

A Dissertation
Presented to
The Academic Faculty

By

Linda Al-Hmoud

In Partial Fulfillment
Of the Requirements for the Degree
Doctor of Philosophy in the
School of Chemical & Biomolecular Engineering

Georgia Institute of Technology
December, 2014

UNDERSTANDING HETEROGENEOUS COPPER CATALYSTS FOR COUPLING REACTIONS IN ORGANIC SYNTHESIS

Approved by:

Dr. Christopher W. Jones, Advisor
School of Chemical & Biomolecular Engineering
Georgia Institute of Technology

Dr. Pradeep K. Agrawal
School of Chemical & Biomolecular Engineering
Georgia Institute of Technology

Dr. Z. John Zhang
School of Chemistry & Biochemistry
Georgia Institute of Technology

Dr. Andreas S. Bommarius
School of Chemical & Biomolecular Engineering
Georgia Institute of Technology

Dr. Jake Soper
School of Chemistry & Biochemistry
Georgia Institute of Technology

Date Approved:
July 16, 2014

To my wonderful husband, Muaz Nimer,
and my awesome children, Mohammad and Sara.

ACKNOWLEDGEMENTS

I want to start by thanking Allah, my god, for providing me with all what I needed to go through this long journey and finish this thesis. Without His help and guidance, everything would be much harder.

Who does not thank people, does not thank God. Therefore, I would like to thank my advisor, Dr. Christopher Jones. His support, patience on my cluelessness, and continuous encouragement were crucial to my success. There were definitely hard times when I felt that I was going through an endless tunnel, but sharing those concerns with Dr. Jones and discussing the different aspects, as well as his understanding for my situation, helped me go over those challenging times and continue. I would also like to thank my committee members. Their open doors and willingness to help let me feel more confident about what I am doing. My chemistry background was limited and therefore Dr. Zhang and Dr. Soper were so helpful in enriching my knowledge. Also, I would like to thank the Jones group members; the discussions we had together, whether they were about science or about life in general, enriched my experience in the US a lot.

PhD journey is tough, and for a married woman with two children, it is even more challenging. Without the endless support, patience, love, and unconditional help and understanding I got from my wonderful husband, Muaz Nimer, my life would be unbearable. Muaz sacrificed his job to accompany me to the US and help me chase my dream. He was the one person who I shared with him everything; good and bad. His wisdom and prudence helped me go over many obstacles. I cried to him, and celebrated my little successes with him too. And, I will not forget to thank my children Mohammad and Sara, who were mature enough and patient, and who lived with me some really tough moments without adding any more hardness.

My family and friends in Jordan and here in Atlanta, GA were part of this achievement. Thank you my parents for believing in me, and thinking that “I can do it”. Thank you my

father, Hazem Al-Hmoud, for doing every possible thing to help me getting to the US and start my degree. You knew that this 10 years old girl's dream will once be true! Thank you my mother for your love and prayers. Thank you my sisters and brothers for keep reminding me that I can do it, and for being proud of my here and there little achievements. Thank you my mother-in-law for your prayers and remote support. Thank you my sisters- and brothers-in-law for your continuous encouragement. Thank you my friends in Jordan for keep asking about me, and for keep saying "we are waiting for you Dr. Linda"! Thank you my friends here in Atlanta, GA, who became our new family. Without you being around, I and my little family would have been so lonely and our experience in this new country would not be as enjoyable as it was.

I would also like to thank University of Jordan for giving me this opportunity and supporting me. In the University of Jordan, I want to thank the faculty members in the Department of Chemical Engineering, who once were my teachers, and will soon be my colleagues. Among them, I will never forget Dr. Salaheddin Al-Sayed (RIP), my MS advisor, who was the Chemical Engineering department chair in 2008 and chose me for this scholarship. I wish he was still alive to see me holding my degree and coming back to my department.

Last but not least, I would like to thank Georgia Tech, and the School of Chemical & Biomolecular Engineering for giving me this opportunity of being part of its innovative environment, and providing me with all the facilities and support needed to achieve my goal. Also, the initial support I got from Dr. Amyn Teja, the Associate Chair for Graduate Studies, when I started the program in 2008, along with the continuous help from the administrative staff in the school made my life much easier.

This will never come to an end, and I wish that I can list all individual names, because every single person in my life had a role and I consider you all as significant part of this achievement. Thank you!

TABLE OF CONTENTS

ACKNOWLEDGEMENTS iv
LIST OF TABLES ix
LIST OF FIGURES x
SUMMARY xiv

CHAPTER 1 INTRODUCTION 1
1.1 Copper Catalysis 1
1.2 Homogeneous and Heterogeneous Catalysis 3
1.3 Objectives and Outline 4

CHAPTER 2 COPPER (II) EXCHANGED NAY ZEOLITE AS A LIGAND-FREE CATALYST FOR AMINATION OF ARYL IODIDE WITH IMIDAZOLE – STABILITY AND HETEROGENEITY ASSESSMENT 6
2.1 Introduction 6
2.2 Experimental Details 11
2.2.1 Synthesis of Cu(II) Exchanged Zeolite 11
2.2.2 Characterization 12
2.2.3 Catalytic C-N Cross Coupling reaction of Imidazole with Aryl Iodide 12
2.3 Results and Discussion 13
2.3.1 Catalyst Characterization 13
2.3.2 Catalytic Reactivity 14
2.3.3 Shape Selectivity Test 15
2.3.4 Stability of Copper Exchanged Zeolite 17
2.4 Conclusions 20

CHAPTER 3 COPPER OXIDE SUPPORTED ON MESOPOROUS CERIUM OXIDE AS A LIGAND-FREE CATALYST FOR N-ARYLATION OF IODOBENZENE WITH BENZYLAMINE – ACTIVITY AND HETEROGENEITY ASSESSMENT 21
3.1 Introduction 21
3.2 Experimental Details 24
3.2.1 Catalyst Preparation 24
3.2.1.1 Synthesis of Mesoporous CeO_2 24
3.2.1.2 Supporting CuO on Mesoporous CeO_2 25
3.2.2 Characterization 25
3.2.3 Catalytic N-Arylation (C-N Cross Coupling Reaction) 26
3.3 Results and Discussion 26
3.3.1 Catalyst Characterization 26
3.3.2 Catalytic Reactivity 28
3.3.2.1 Effect of Catalyst Loading 28
3.3.2.2 Effect of Added Base 30
3.3.2.3 Comparing the Catalytic Activity of CuO Nanoparticles and Ceria-Supported CuO 34
3.3.3 Catalyst Recyclability and Heterogeneity 35
3.3.3.1 Testing Copper Leaching 35
3.3.3.2 Why Does Copper Leach? 36
3.3.3.3 Hot Filtration Test 40
3.3.3.4 Recyclability Test 42
3.4 Conclusions 44

CHAPTER 4 REACTION PATHWAYS OVER COPPER AND CERIUM OXIDE CATALYSTS FOR DIRECT SYNTHESIS OF IMINES FROM AMINES UNDER AEROBIC CONDITIONS 46
4.1 Introduction 46
4.2 Experimental Details 47
4.2.1 Catalyst Preparation 47
4.2.2 Characterization 48

4.2.3 Catalytic Conversion of Benzylamine to N-Benzylidenebenzylamine 49
4.3 Results and Discussion 50
4.3.1 Catalyst Characterization 50
4.3.2 Catalytic Reactivity 58
4.3.3 Proposed Reaction Pathway 75
4.4 Conclusions 79

CHAPTER 5 AN INVESTIGATION OF THE EFFECT OF SUPPORT, TEMPERATURE, AND SOLVENT ON THE HOMOGENEITY/ HETEROGENEITY OF SOLID COPPER CATALYSIS 81
5.1 Introduction 81
5.2 Experimental Details 87
5.2.1 Catalysts Preparation 87
5.2.1.1 Synthesis of Mesoporous γ-Al_2O_3 87
5.2.1.2 Supporting CuO on Mesoporous γ-Al_2O_3 87
5.2.1.3 Supporting CuO on Mesoporous TiO_2 88
5.2.2 Materials Characterization 89
5.2.3 Catalytic Oxidative Homocoupling of Terminal Alkynes 90
5.3 Results and Discussion 90
5.3.1 Catalyst Characterization 90
5.3.2 Catalyst Heterogeneity Evaluation 91
5.3.2.1 Effect of Temperature on Copper Leaching and Reactivity 92
5.3.2.2 Effect of Support and Support Interaction with Copper Oxide on Copper Leaching 100
5.3.2.3 Effect of Solvent and Reactant on Copper Leaching 108
5.3.3 Does Recyclability Mean Heterogeneity? 109
5.4 Conclusions 111

CHAPTER 6 CONCLUDING REMARKS AND SUGGESTED FUTURE WORK .. 113

REFERENCES 115

LIST OF TABLES

Table 2.1 Elemental analysis of Cu(II)Y before and after reaction using K_2CO_3 as a base 17
Table 2.2 Elemental analysis of Cu(II)Y before and after reaction using Cs_2CO_3 as a base 19
Table 3.1 Elemental analysis of fresh and used 9CuO-CeO_2 catalyst 36
Table 3.2 Leaching test and effect of different reactants/reagents 37
Table 4.1 Physical properties of the composite CuO-CeO_2 catalysts, CuO nanoparticles, and CeO_2 support 50
Table 4.2 H_2-TPR analysis results of for three supported CuO catalysts, CeCu(II)01, CeCu(II)05, CeCu(II)09, and CuO nanoparticles 57
Table 4.3 Rates of reaction over the various catalysts 61
Table 5.1 Catalyst characterization 91
Table 5.2 Effect of temperature on copper leaching 94
Table 5.3 Effect of temperature on copper leaching when using TiO_2 as a support 104
Table 5.4 Copper and titanium contents of fresh and recycled 10CuO-TiO_2 catalyst 110

LIST OF FIGURES

Figure 1.1 Different copper catalyzed coupling reactions 2
Figure 2.1 Supported copper catalysts 9
Figure 2.2 Cu(phen)(PPh_3)Br complex tethered on NaY zeolite[53] 9
Figure 2.3 X-ray diffraction patterns of Cu(II)-Y zeolite before (red) and after (blue) the catalytic reaction 13
Figure 2.4 Kinetic behavior of C-N cross coupling reaction between 4-iodoanisole and imidazole (1.2 eq.), in DMF (3 mL per mmol 4-iodoanisole), using Cu(II)Y (10 mol% copper) as a catalyst, K_2CO_3 (2 eq.) as a base, at 120 °C under N_2. 14
Figure 2.5 Kinetic behavior of C-N cross coupling reaction between imidazole and 4-iodoanisole (a and b) or 5-iodo-1,2,3-trimethoxybenzene (c and d), using Cu(II)Y and K_2CO_3 (a and c) or CuO nanoparticles and t-BuOK (b and d), at 120 °C 16
Figure 2.6 PXRD patterns of fresh and used Cu(II)Y catalyst when using K_2CO_3 as a base 18
Figure 2.7 PXRD patterns of fresh and used Cu(II)Y catalyst when using Cs_2CO_3 as a base 19
Figure 3.1 PXRD patterns for ceria-supported CuO catalyst (9CuO-CeO_2), bare mesoporous CeO_2 support and commercial CuO nanoparticles 27
Figure 3.2 TEM image of ceria-supported CuO catalyst (9CuO-CeO_2) 28
Figure 3.3 Kinetic behavior of C-N cross coupling reaction between iodobenzene, benzylamine (1.2 eq.), in DMSO (1 mL per mmol iodobenzene), using 9CuO-CeO_2 (5 and 10 mol% copper) as a catalyst, and two different bases (KOH (a) and K_2CO_3 (b), 1 eq.) at 110 °C under N_2, to form N-benzylaniline. 29
Figure 3.4 Kinetic behavior of phenol and diphenylether formation using from iodobenzene and KOH (2 eq.), using 9CuO-CeO_2 (5mol% copper) as the catalyst, in DMSO (0.5 mL per mmol iodobenzene), at 130 °C under N_2. 31
Figure 3.5 PXRD patterns for ceria-supported CuO catalyst (9CuO-CeO_2); fresh (gray), used with KOH (red), and used with K_2CO_3 (blue). 33
Figure 3.6 PXRD patterns for ceria-supported CuO catalyst (9CuO-CeO_2); fresh and after treatment with DMSO, DMSO with KOH, and DMSO with K_2CO_3. 34

Figure 3.7 Kinetic behavior of C-N cross coupling reaction between iodobenzene and benzylamine (1.2 eq.), in DMSO (1 mL per mmol iodobenzene), using 9CuO-CeO_2 and CuO nanoparticles (10 mol% Cu) as catalysts, and two different bases (KOH (a) and K_2CO_3 (b), 1 eq.) at 110 °C under N_2, to form N-benzylaniline. 35
Figure 3.8 PXRD pattern of CuO nanoparticles after running C-N cross coupling reaction using KOH (purple) or K_2CO_3 (green) as a base 40
Figure 3.9 Hot filtration test (a) without and (b) with adding KOH to the filtrate receiving flask 42
Figure 3.10 Recyclability of 9Cu-CeO_2 catalyst with and without regeneration, using 5 mol% copper and KOH as a base, at 110 °C under N_2 44
Figure 4.1 Powder XRD patterns for bare CeO_2 and CeCu(II)09 catalyst 51
Figure 4.2 SEM images with (a) Cu mapping, and (b) Ce mapping of CeCu(II)09 catalyst 53
Figure 4.3 Pore size distribution of CeO_2 support and the synthesized CuO/CeO_2 catalysts calculated by the BDB-FHH method from nitrogen physisorption data at 77 K 54
Figure 4.4 H_2-TPR profiles of catalysts CeCu(II)01, CeCu(II)05, CeCu(II)09, and CuO nanoparticles 57
Figure 4.5 Kinetic profiles for the oxidative coupling of benzylamine using the bare ceria support (CeO_2-meso), unsupported CuO nanoparticles (CuO-np), a physical mixture of CuO nanoparticles and ceria (CeCu-PM), and the CeCu(II)09 material, as catalysts. Conditions: benzylamine (3 mmol), catalyst (5 mol% Cu), DMSO (3 ml), 110 °C, air. 59
Figure 4.6 Kinetic profiles for the oxidative coupling of benzylamine using the bare ceria support, followed by addition of unsupported CuO nanoparticles after 20 h. Reaction carried at 110°C under aerobic atmosphere. 64
Figure 4.7 Kinetic profiles for the oxidative coupling of benzylamine using the bare ceria support, followed by addition of "solid" and "soluble" copper species derived from CuO nanoparticles after 5.5 h. Reaction carried at 110 °C under aerobic atmosphere. 66
Figure 4.8 Kinetic profiles for the oxidative coupling of benzylamine using CeCu(II)09 catalysts and the effect of Cu concentration in the solution on the product yield. Conditions: benzylamine (3 mmol), catalyst (5 mol% Cu), DMSO (3 ml), 110 °C, air. 68
Figure 4.9 Kinetic profiles for the oxidative coupling of benzylamine using ceria-supported catalysts with different Cu(II) loadings: CeCu(II)01, CeCu(II)05 and CeCu(II)09. Conditions: benzylamine (3 mmol), catalyst (5 mol% Cu), DMSO (3 ml), 110 °C, air. 69

Figure 4.10 Comparison between mesoporous CeO_2 (172 mol%) and CeCu(II)01 as catalysts, and their effect on the kinetic profiles of the oxidative coupling of benzylamine. Reaction carried at 110 °C under aerobic atmosphere. .. 70
Figure 4.11 Comparison between bare CeO_2, and dry bare CeO_2 as catalysts, and their effect on the initial rate of amine oxidative coupling reaction. 72
Figure 4.12 Kinetic profiles for the oxidative coupling of benzylamine over two cycles using the CeCu(II)09 catalyst. Conditions: benzylamine (3 mmol), catalyst (5 mol% Cu), DMSO (3 ml), 110 °C, air. 74
Figure 4.13 Powder XRD patterns of fresh and used CeCu(II)09 catalysts 75
Figure 4.14 Effect of adding 0.5 equivalents of water on the kinetic profiles of oxidative coupling of benzylamine using CuO, CeO_2, and CeCu(II)09 as catalysts. Reaction carried at 110°C under aerobic atmosphere. 78
Figure 5.1 Effect of temperature on the homocoupling reaction of ethynylbenzene using 10CuO-Al_2O_3 (CuAl) and CuO nanoparticles (CuNP) as catalysts. Experiments run at 80 °C are denoted by (H) and experiments run at room temperature are denoted by (C). Figure (a) represents the conversion of ethynylbenzene and figure (b) represents the desired product (DPBD) yield, as a function of time. 93
Figure 5.2 Effect of temperature on copper leaching from CuO nanoparticles (CuNP) and from the γ-Al_2O_3 support (CuAl), for the homocoupling reaction of ethynylbenzene. Figure (a) represents the conversion of ethynylbenzene and figure (b) represents the desired product (DPBD) yield, as a function of time. The first letter represents the mixing temperature and the second letter represents the reaction temperature; (H) is for 80 °C and (C) is for room temperature. 95
Figure 5.3 Comparison of ESI MS spectra of pure piperidine, piperidine decanted after mixing it with CuO nanoparticles at 80 °C (CuNP-H), and piperidine decanted after mixing it with CuO nanoparticles at room temperature (CuNP-C) overnight. 98
Figure 5.4 Anticipated copper-piperidine complexes formed by mixing copper oxide with piperidine at high temperature (80 °C). 98
Figure 5.5 TEM images of (a) CuO nanoparticles after stirring them in water at room temperature and decanting liquid water, and (b) commercial CuO nanoparticles 99
Figure 5.6 Particle size distribution of commercial CuO nanoparticles (red) and CuO nanoparticles after stirring them in water at room temperature overnight and separating them by centrifugation (CuNP-C) 99
Figure 5.7 H_2-TPR profiles of 10CuO-Al_2O_3 and 10CuO-TiO_2 101
Figure 5.8 XRD patterns of 10CuO-Al_2O_3 and 10CuO-TiO_2 103

Figure 5.9 Effect of support and temperature on the catalytic activities of CuO supported on γ-Al_2O_3 (CuAl) and on TiO_2 (CuTi) in ethynylbenzene homocoupling at room temperature (C) and 80 °C (H) 105
Figure 5.10 Effect of temperature on copper leaching from γ-Al_2O_3 support (CuAl) and from TiO_2 support (CuTi) at room temperature (C) and at 80 °C (H) 106
Figure 5.11 Comparison between the activities of soluble copper from copper acetate, CuAC, with copper from (a) solid 10CuO-Al_2O_3 and with copper from (b) 10CuO-TiO_2 at the same concentration 107
Figure 5.12 Comparison between the catalytic activities of solid catalysts (a) 10CuO-Al_2O_3 and (b) 10CuO-TiO_2 with copper leached from the same catalyst 108
Figure 5.13 Recyclability test of 10CuO-TiO_2 for oxidative homocoupling of ethynylbenzene at room temperature 110

SUMMARY

Copper is an inexpensive, earth-abundant, non-toxic metal that is found to have widespread applications in catalysis. Ullmann and Ullmann-type reactions and Glaser-Hay oxidative coupling of terminal alkynes are some of the well-established copper catalyzed coupling reactions used for the construction of important organic molecules, including pharmaceuticals, commodity chemicals and polymers. Those reactions have been mainly performed homogeneously, where the removal of residual copper from the reaction mixture is a challenge. Therefore, many researchers tried supporting copper precatalysts in order to help recover, and thus reduce final product contamination. Some studies showed that copper leached significantly from the support, with others showing that leached copper has a role in the catalysis. Nevertheless, many studies reported that the used supported catalysts were recyclable and claimed catalyst's heterogeneity. In most cases, the nature of the truly active copper species is still not clear.

The objectives of this thesis were (1) to assess the heterogeneity/homogeneity of active copper species in popular catalytic C-N coupling reactions with already studied catalysts, mainly a copper exchanged zeolite and copper oxide nanoparticles, and (2) to use the collected information in designing a truly heterogeneous (stable and recyclable) catalyst.

Initially, and because of its shape selectivity characteristics, copper-exchanged NaY zeolite, Cu(II)Y, was chosen to study the heterogeneity of copper catalyzed amination of aryl iodide with imidazole. The collected results from conducted shape selectivity tests indicated that Cu(II)Y might be heterogeneous catalyst, but because of the used base, that is crucial for this C-N coupling reaction, the crystallinity of the zeolite structure was diminished. Therefore, it was important to support copper on a framework that is stable

under the basic conditions required for this type of reaction if a heterogeneous, recyclable catalyst were to be achieved. For this purpose, cerium oxide was chosen, and copper oxide supported on cerium oxide, CuO-CeO_2, was investigated as a potential heterogeneous catalyst for C-N coupling reaction. This investigation included the role of each reaction reagent in facilitating copper leaching into solution. It was found that copper leached from the support and it was demonstrated through hot filtration tests that the leached copper species was the main active catalyst. Leaching was caused by the solvent (DMSO) as well as the used reactants and the base. Similar conclusions were drawn when this CuO-CeO_2 catalyst was used for the direct synthesis of imines from amines under aerobic conditions. Although this CuO-CeO_2 catalyst has the advantages of being more recoverable and active than unsupported CuO nanoparticles at similar copper loadings, it is not fully recyclable, as the copper catalysis occurs in solution.

These findings meant that designing a truly heterogeneous catalyst for this reaction is a challenging task. Understanding the effect of each individual factor of this complicated system might help in achieving the second goal - designing a truly heterogeneous catalyst. Therefore, further studies were carried out to understand the effect of reaction conditions, including temperature, base, support, and solvent, on copper leaching. Homocoupling of terminal alkynes was chosen as a model reaction for this study, and CuO was supported on TiO_2 (10CuO-TiO_2) and on γ-Al_2O_3 (10CuO-Al_2O_3). It was found that copper interaction with the support affects the extent of leaching as well as the nature and activity of leached species. High temperature also facilitates copper leaching especially when a ligating amine, like piperidine, is present in the system.

CHAPTER 1

INTRODUCTION

1.1 Copper Catalysis

Copper-catalyzed reactions are widely used for the construction of important organic molecules, including pharmaceuticals, commodity chemicals and polymers. Copper is an inexpensive, earth-abundant, non-toxic metal that is found to have widespread applications in catalysis. For example, since their discovery at the turn of the twentieth century[3], copper-catalyzed cross-coupling reactions, Ullmann and Ullmann-type reactions, have been extensively studied. Such reactions serve as versatile methods for synthesizing biaryl linkages as well as for constructing the carbon–heteroatom bonds of aryl amines, aryl ethers and aryl thioether derivatives.[4] Glaser-Hay oxidative coupling of terminal alkynes,[5–11] coupling of terminal alkynes with aryl and vinyl halides, Sonogashira coupling,[12–15] and azide–alkyne cycloaddition,[16–21] Figure 1.1, are other types of well-established copper catalyzed coupling reactions.

Along with copper, palladium has been also used extensively in the construction of those types of carbon–carbon and carbon–heteroatom bonds. Advancements in copper chemistry have often stimulated improvements in palladium-catalyzed processes, and vice versa, leading to a wide range of robust, synthetically valuable and often complementary synthetic methods. Nevertheless, copper offers some potential advantages over palladium. Copper is cheaper and less toxic. More importantly, copper chemistry is rich because the metal can easily access Cu^0, Cu^I, Cu^{II}, and Cu^{III} oxidation states, allowing it to react through one-electron or two-electron processes. As a result, both

radical pathways and powerful two-electron bond-forming pathways via organometallic intermediates can occur.[4] Palladium also has multiple oxidation states; Pd^0, Pd^{II}, and Pd^{IV}, but its chemistry can only proceed through two-electron processes.

Ullmann-Type Reaction

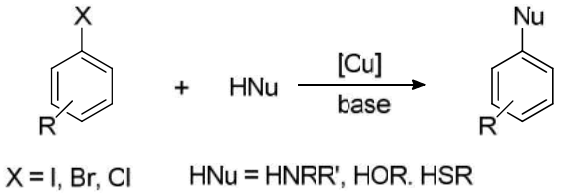

Glaser-Hay Terminal Alkyne Oxidative Coupling

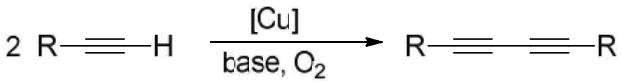

Sonogashira Coupling Reaction

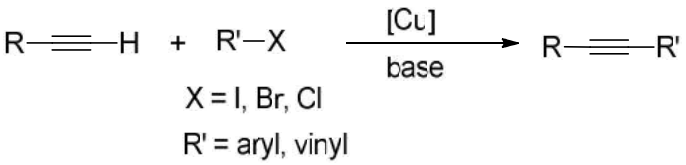

Azide–Alkyne Cycloaddition

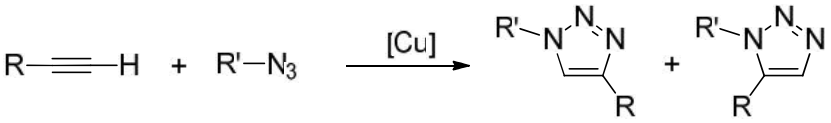

Figure 0.1 Different copper catalyzed coupling reactions

1.2 Homogeneous and Heterogeneous Catalysis

Palladium-catalyzed aromatic C-N bond forming reactions, or Buchwald-Hartwig amination reactions, have been one of the most important discoveries in synthetic organic chemistry and palladium catalysis in the last decades.[22–24] These reactions can be carried out under mild conditions with a large variety of amines and aryl halide substrates. Because of this tolerance, palladium catalysis has found increased popularity in pharmaceutical chemistry, where complicated molecules are synthesized. On the other hand, strict guidelines set for active pharmaceutical ingredients (APIs) limit the level of heavy metals in the final drug substances. All the aforementioned reactions, Figure 1.1, have been mainly performed homogeneously, and with homogeneous catalysis, removal of residual heavy metals like palladium from the reaction mixture is a challenge. This led scientists to seek to heterogeneously catalyze the reactions by supporting palladium on carbon or oxide supports, by using palladium ion-exchanged supports, or by binding palladium to polymeric supports.[25] These pathways reduced the amount of palladium in APIs, but solubilization and leaching of palladium from the support still routinely occur and further purification is still needed.[26] Palladium leaching and solubilization in coupling reactions were studied extensively, and previous work in the Jones group showed that when using many supported palladium precatalysts for Suzuki and Heck coupling, catalysis was often solely associated with leached palladium.[27]

Researchers have also supported copper precatalysts in order to help recover and recycle the catalyst, and reduce final product contamination. Some studies showed that copper leached significantly from the support,[1,2] and others showed that leached copper has at least partial role in the catalysis.[28] Other studies mainly reported that the used supported

catalysts were recyclable and claimed catalyst's heterogeneity based on absence of copper in reaction mixture after filtering out the catalyst.[29–31] The nature of the truly active copper species – leached copper, solid copper, or both – is still not clear in most cases.

1.3 Objectives and Outline

Copper, when combined with appropriate soluble ligands, has been shown to be an active homogeneous catalyst for wide range of reactions.[32–39] However, the benefits of heterogeneous catalysis continuously attract researchers to the design and preparation of heterogeneous catalysts. These benefits include ease of catalyst recovery and recycling, leading to more economical final product purification. To design a truly heterogeneous recyclable catalyst, understanding of homogeneity versus heterogeneity aspects is required. That is, does the catalytic turnover take place on the surface of a solid copper metal or oxide catalyst, with copper species that are solubilized under reaction conditions, or with both types of species? The first objective of this study was to assess the heterogeneity/homogeneity of active copper species in popular catalytic C-N coupling reactions with already studied catalysts, mainly a copper exchanged zeolite and copper oxide nanoparticles.[40,41] This investigation included the role of each reaction reagent in potentially facilitating copper leaching into solution. The second objective was to use the information collected about the aforementioned catalysts to design a truly heterogeneous (stable and recyclable) catalyst for C-N cross coupling reactions.

The outline of this thesis is as follows. In Chapter 2, the heterogeneity of copper-exchanged NaY zeolite as a catalyst for amination of aryl iodide with imidazole is

illustrated, as well as the investigation of this catalyst's stability. The results from Chapter 2 led to the choice of cerium oxide as a support for a copper precatalyst, and the results of this work are shown in Chapter 3. Running some control experiments led to the discovery that the ceria-supported copper catalyst was also an efficient aerobic oxidation catalyst to form N-benzylidenebenzylamine from benzylamine. Thorough study on this reaction and the role of copper and ceria-support was carried out and the results are illustrated in Chapter 4. Further studies were carried out to understand copper as a catalyst in the homocoupling of terminal alkynes, and the effect of reaction conditions, including temperature, base, support, and solvent, on copper leaching. These results are shown in Chapter 5. Some concluding remarks are presented in Chapter 6.

CHAPTER 2

COPPER (II) EXCHANGED NaY ZEOLITE AS A LIGAND-FREE CATALYST FOR AMINATION OF ARYL IODIDE WITH IMIDAZOLE – STABILITY AND HETEROGENEITY ASSESSMENT

2.1 Introduction

Aryl-nitrogen bond forming cross-coupling reactions are among the most common methods used in synthesizing numerous compounds in the biological, material, and pharmaceutical sciences. Copper has been used for decades in stoichiometric C-N coupling reactions (classical Ullmann-condensation reaction). However, due to the Ullmann reaction's restrictions, including harsh reaction conditions (mainly high temperatures, more than 200 °C), the need for stoichiometric amount of copper, a limited range of suitable substrates, and the moderate yields usually obtained, it has not been employed to its full potential for a long time.[42]

To improve this system and overcome these restrictions, considerable research efforts have focused on developing copper/ligand complexes that can be used to catalyze Ullmann-type reactions, the aromatic nucleophilic coupling reaction between nucleophiles and aryl halides, under conditions milder than those being used in the classical Ullmann couplings. In 2001, important breakthroughs were achieved by two research groups with the discovery of efficient new copper/ligand systems for the formation of C-C, C-N, and C-O bonds. Those important discoveries enabled the use of

only catalytic amounts of copper under mild conditions (90–110 °C), and thus have led to a revival of interest in Ullmann-type reactions.[42,43]

Since then, many research groups have worked on the development of more efficient copper/ligand systems that can be used to catalyze these reactions under conditions milder than those being used in the classical Ullmann and Ullmann-type reactions. These reactions used metal salts coupled with ligands and thus were thought to occur homogeneously, and typically, nothing was mentioned about reusable/recyclable catalysts in the early development.[34–36,38,39]

In parallel, some research efforts focused on designing and utilizing *ligand-free* copper catalysts to decrease the cost and the toxicity of the process. In these examples, copper(I) oxide (Cu_2O)[44,45] and copper(I) halide salts[46] were used to catalyze a variety of N-arylation reactions.

Homogeneous catalyst systems are not easy to separate from the products, recover, and recycle, and thus they often generate unnecessary waste. To explore recyclable heterogeneous catalysts, solid copper (II) oxide (CuO) nanoparticles have been studied for C-N bond forming reactions.[41,47] Jammi et al[41] used CuO nanoparticles to catalyze about 70 different C-N, C-O, and C-S cross-coupling reactions under mild, ligand-free conditions. By conducting some heterogeneity assessment tests, they claimed that the C-O coupling reaction between phenol and iodobenzene may occur heterogeneously on the copper oxide nanoparticles surface. They also claimed that there was no leaching of soluble copper species into solution, and that the catalyst was recyclable without loss of activity. These claims could be an important advance, but more evidence, consideration of the effect of reactants, and more conclusive experiments like hot filtration test are

needed to support it and to understand the nature of the working catalyst, as the presented data were inconclusive with regard to heterogeneity, in my opinion.

Also, in efforts to synthesize another type of heterogeneous catalyst, several supported copper catalysts were prepared by Kantam's group and employed for the N-arylation of aryl halides[40,48–52] (Figure 2.1). In most cases, they showed that the synthesized catalysts can be reused for several cycles with some copper leaching and loss of activity, but without any convincing kinetic studies that could strongly substantiate claims of heterogeneity. In one study,[40] Kantam et al reported using Cu(II) exchanged NaY zeolite (microporous, anionic aluminosilicate with exchangeable cations, vide infra) as a catalyst for the N-arylation of nitrogen heterocycles with aryl halides. The catalyst was recycled four times, and claimed to be effective under recycling with minimal loss of activity. They also noticed some leaching of the copper (2-6%) from the zeolite after each reaction cycle. Patil et al[53] synthesized heterogenized analogs of a homogenous copper complex (Figure 2.2) by either encapsulating or tethering it to NaY zeolite and other supports. They used the different catalysts for the amination of iodobenzene by aniline, Scheme 2.1. They tested their catalytic activity and selectivity towards diphenylamine. They found that catalyst's selectivity was dependent on the method of catalyst synthesis; encapsulating the copper complex gave higher selectivity towards diphenylether (DPA), while the tethered copper complex was more selective towards triphenylamine (TPA). They assigned that to the shape selectivity of NaY zeolite they used. The recyclability of the catalyst was also studied, but with only end point analysis; no kinetic studies were presented.

(a) Silica supported copper catalysts[49] (b) Copper exchanged apatite[50]

Figure 2.1 Supported copper catalysts

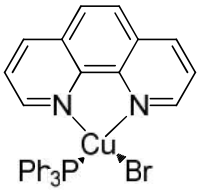

Figure 2.2 Cu(phen)(PPh_3)Br complex tethered on NaY zeolite[53]

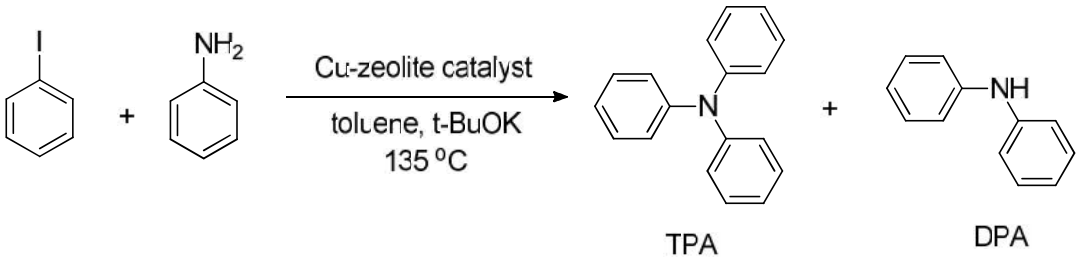

Scheme 2.1 Amination of iodobenzene with aniline[53]

Zeolites are of the class of microporous solids known as "molecular sieves" because of their ability to selectively sort molecules based primarily on size exclusion processes. This ability is due to their regular pore structure on the molecular level. In addition, they are often used as catalysts in different industries, and as solid acids (in the H^+ form rather than the Na^+ form). Inspired by the results of Kantam and Patil, and with the hope to understand the heterogeneity/homogeneity of the active copper species in the catalytic C-N coupling reactions, this study was conducted to test the hypothesis that copper catalyzed C-N bond forming reactions are homogeneously catalyzed by soluble, molecular copper species, regardless of the nature of the catalyst or the precursor used. That is, it was hypothesized that leached, molecular copper species in homogeneous solution catalyze this reaction. Therefore, starting with Cu(II) exchanged zeolite, copper ions must leach from the zeolite to catalyze the reaction. NaY zeolite was chosen mainly because it was the catalyst tested by Kantam and Patil, and because it has moderate pore size (7.4 Å), allowing small molecules to easily diffuse and react inside the pores, and preventing larger molecule from diffusing and completing the coupling reaction. For this study, a Cu(II) exchanged NaY zeolite was used as a catalyst for the C-N cross coupling reaction of imidazole with 4-iodoanisole, Scheme 2.2, and with 5-Iodo-1,2,3-trimethoxybenzene, Scheme 2.3. The latter reaction is expected to be sufficiently sterically constrained to not occur to a large extent in the zeolite micropores.

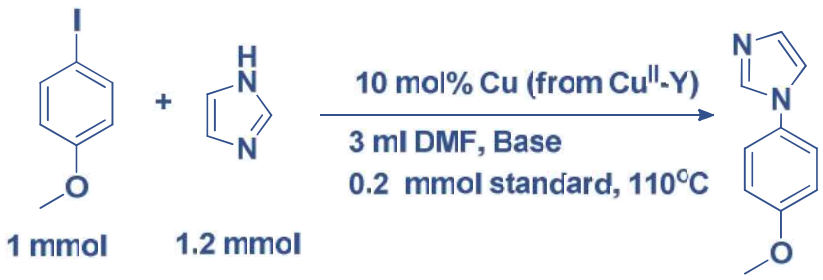

Scheme 2.2 C-N cross coupling reaction of imidazole with 4-iodoanisole

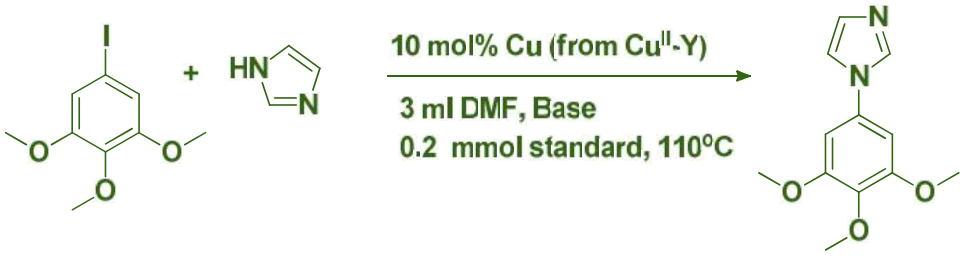

Scheme 2.3 C-N cross coupling reaction of imidazole with 5-Iodo-1,2,3-trimethoxybenzene

2.2 Experimental Details

2.2.1 Synthesis of Cu(II) Exchanged Zeolite

Cu(II) exchanged zeolite (referred to hereafter as Cu(II)Y was prepared using an ion-exchange method. NaY zeolite (10 g) was mixed with 150 mL of 0.1 M aqueous solution of copper (II) acetate at room temperature for 24 h. The material was recovered by filtration and washed with 0.01 M aqueous solution of copper (II) acetate. The wet blue zeolite was then transferred to an oven, dried at 120 °C (1 °C/min ramp) for 3 h under

flowing air, and then calcined at 550 °C (1 °C/min ramp) for another 3 h, also under flowing air.

Commercial CuO nanoparticles (Sigma-Aldrich, S_{BET} = 16 g/m^2) were used as received for comparison purposes.

2.2.2 Characterization

Powder X-ray diffraction (PXRD) was carried out with a PAnalytical X'Pert PRO diffractometer operating with Cu Kα radiation and an X'celerator RTMS detector. A step size of 0.002° 2θ and a scan rate of 10 s per step were used. Elemental analysis by ICP-AES was carried out by ALS Environmental Division (Tucson, AZ).

2.2.3 Catalytic C-N Cross Coupling reaction of Imidazole with Aryl Iodide

In a typical reaction, the catalyst Cu(II)Y (0.10 eq. Cu relative to aryl iodide), was added to a 25-mL two-neck round bottom flask containing 1 mmol iodobenzene (112 μL), 1.2 mmol benzylamine (131 μL), 2 mmol base (either potassium tert-butoxide or potassium carbonate), 3 mL solvent (either DMSO or DMF), and 0.2 mmol diethylene glycol dibutyl ether (123 μL) as an internal standard. The round bottom flask was attached to a condenser, evacuated and backfilled with nitrogen gas twice, and then immersed in a preheated oil bath, at 120 °C, to start the reaction. Samples of the reaction mixture were taken at specified times, filtered over silica gel column and diluted with dichloromethane, and the limiting reactant (iodobenzene) conversion was determined by GC-FID, and

calculated by comparing the reactant to the internal standard peak area ratio to the ratio at the beginning of the reaction. The identity of the product was verified by GC-MS.

2.3 Results and Discussion

2.3.1 Catalyst Characterization

Elemental analysis of the prepared catalyst showed that it contains 6.0 wt % Cu with Cu/Al ratio of 0.255 mol/mol. The PXRD pattern for the fresh Cu(II)Y catalyst is shown in Figure 2.3 (in blue). The PXRD patterns of NaY zeolite and Cu(II)Y are the same, and two characteristic peaks of crystalline CuO at 2θ = 35.5° and 38.9° cannot be identified. This means that copper was most probably ion exchanged and is present as cationic Cu(II).

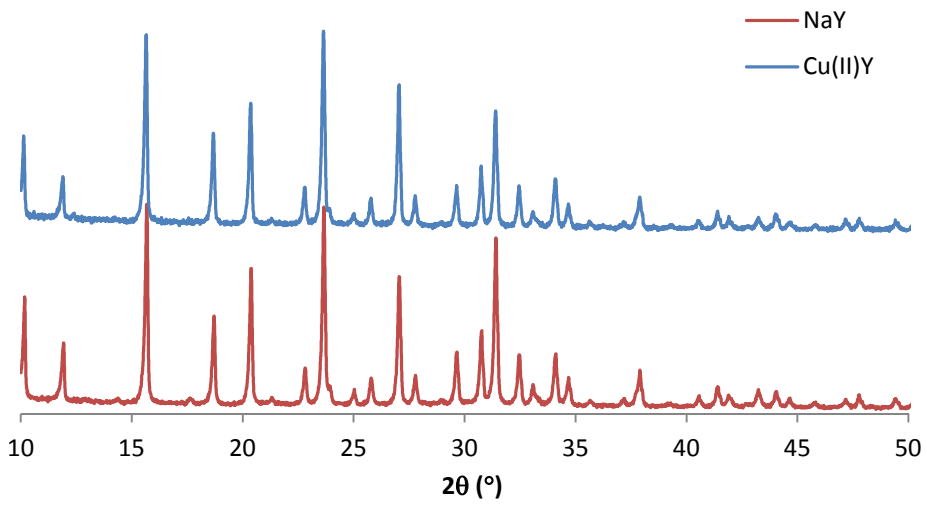

Figure 2.3 X-ray diffraction patterns of Cu(II)-Y zeolite before (red) and after (blue) the catalytic reaction

2.3.2 Catalytic Reactivity

The activity of Cu(II)Y as a catalyst for C-N bond forming reaction between 4-iodoanisole and imidazole, Scheme 2.2, was evaluated and the kinetic curve is shown in Figure 2.4. An induction period of about 6 hours can be noticed, after which the rate of the reaction increases. The limiting reactant (4-iodoanisole) conversion reached a maximum of 70% after 50 hours. The induction period might indicate that some time was needed either for copper to leach from the zeolite and activate the reaction, or for the reactants to diffuse inside the zeolite pores and react, and thus further investigation was required.

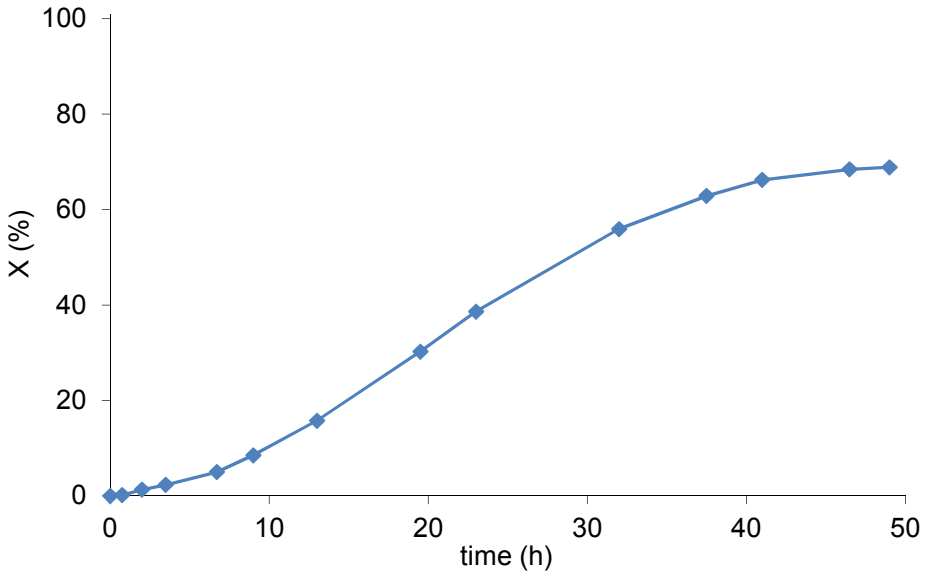

Figure 2.4 **Kinetic behavior of C-N cross coupling reaction between 4-iodoanisole and imidazole (1.2 eq.), in DMF (3 mL per mmol 4-iodoanisole), using Cu(II)Y (10 mol% copper) as a catalyst, K_2CO_3 (2 eq.) as a base, at 120 °C under N_2.**

2.3.3 Shape Selectivity Test

Shape selectivity tests can be used to understand the homogeneity/ heterogeneity of this copper catalysis. As mentioned earlier, NaY zeolite has a pore diameter of 7.4 Å, and to perform this test, a reactant bigger than this diameter must be used for comparison to the standard reaction. Scheme 2.3 shows the reaction that was used to perform this shape selectivity test. As estimated by ChemBioDraw Ultra 14® software, the minimum dimension of the limiting reactant, 5-iodo-1,2,3-trimethoxybenzene, is 8 Å, larger than the zeolite pore size.

Figure 2.5 shows that when using Cu(II)Y as a catalyst, the reaction between imidazole and 5-iodo-1,2,3-trimethoxybenzene is much slower than that with 4-iodoanisloe. For comparison, the same reactions were run using CuO nanoparticles. Potassium carbonate was found to be ineffective as base with CuO nanoparticles, and thus t-BuOK was used instead. Potassium tert-butoxide (t-BuOK) is a very strong base, and could not be used with Cu(II)Y zeolite, as it destroys its structure. Therefore, although the comparison between the CuO nanoparticles and Cu(II)Y performance as catalysts would not be perfect, some conclusions could be drawn.

In the case of CuO nanoparticles, where the copper is readily available to activate the reaction, 5-iodo-1,2,3-trimethoxybenzene was more active as a reactant than 4-iodoanisole, with initial rate of 3.8 mmol/(mmol Cu.h) compared to 1.6 mmol/(mmol Cu.h). With two more electron donating groups, it was expected for 5-iodo-1,2,3-trimethoxybenzene to be more active than 4-iodoanisloe in the cross coupling reaction. Comparing that with the kinetic curves of Cu(II)Y catalysis, it can be seen that reaction with 5-iodo-1,2,3-trimethoxybenzene is much slower than that with 4-iodoanisloe. This

could be an indication of catalyst heterogeneity, as the bigger molecule could not diffuse into the zeolite pores and react with imidazole.

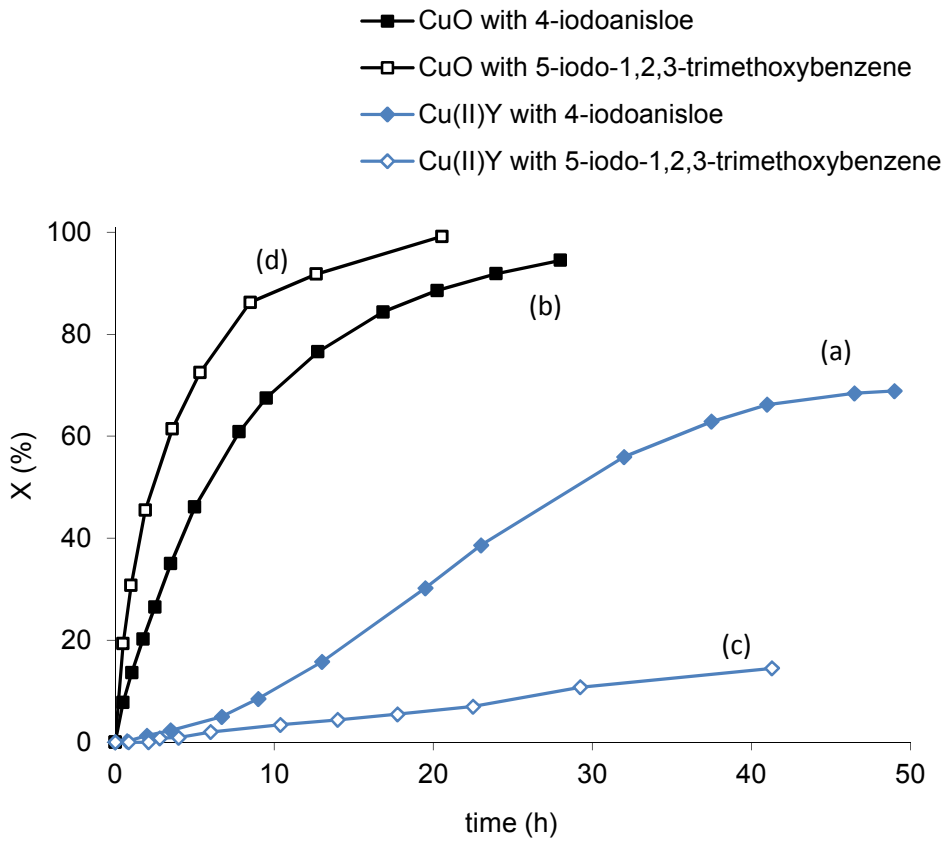

Figure 2.5 **Kinetic behavior of C-N cross coupling reaction between imidazole and 4-iodoanisole (a and b) or 5-iodo-1,2,3-trimethoxybenzene (c and d), using Cu(II)Y and K_2CO_3 (a and c) or CuO nanoparticles and t-BuOK (b and d), at 120 °C**

2.3.4 Stability of Copper Exchanged Zeolite

To be able to recycle and reuse a catalyst, it should be recoverable and stable. After the reaction was completed, the reaction mixture was centrifuged, and the solids were collected, washed with dichloromethane, then dried and sent for elemental analysis. Table 2.1 shows the copper and aluminum contents of the fresh and used catalyst. Comparing Cu/Al molar ratio before and after reaction, it can be said that the copper content is almost the same. Nevertheless, significant amount of potassium was found in the solid. The potassium is from the base used, K_2CO_3, which can be hardly separated from the zeolite, unless water is used to dissolve it. Using water might affect the copper content of zeolite, and this is why it was not used to wash the catalyst. Also, the copper content of the decanted reaction mixture was analyzed, and it was found that it contains 0.003 mmol copper per mL mixture. That is 10% of the starting concentration, which was 0.03 mmol copper per mL mixture. Although the copper content of the solid seemed to be the same, the presence of copper in the liquid mixture prevents the claiming of catalyst heterogeneity.

Table 2.1 Elemental analysis of Cu(II)Y before and after reaction using K_2CO_3 as a base

Sample	Al		Cu		K	
	wt %	Per mol Al	wt %	per mol Al	wt %	per mol Al
Fresh Cu(II)Y	10.0	1	6.01	0.255	-	-
Used Cu(II)Y	3.04	1	1.98	0.277	25.7	5.84

It is also important to assess the structural stability of the catalyst. PXRD patterns of fresh and used Cu(II)Y catalysts are shown in Figure 2.6. It is clear that the crystalline structure of the zeolite was not fully maintained, as many peaks disappeared or became much smaller. This instability along with the difficulty of separating the catalyst from the solid base makes it hard to consider Cu(II)Y as a recyclable catalyst.

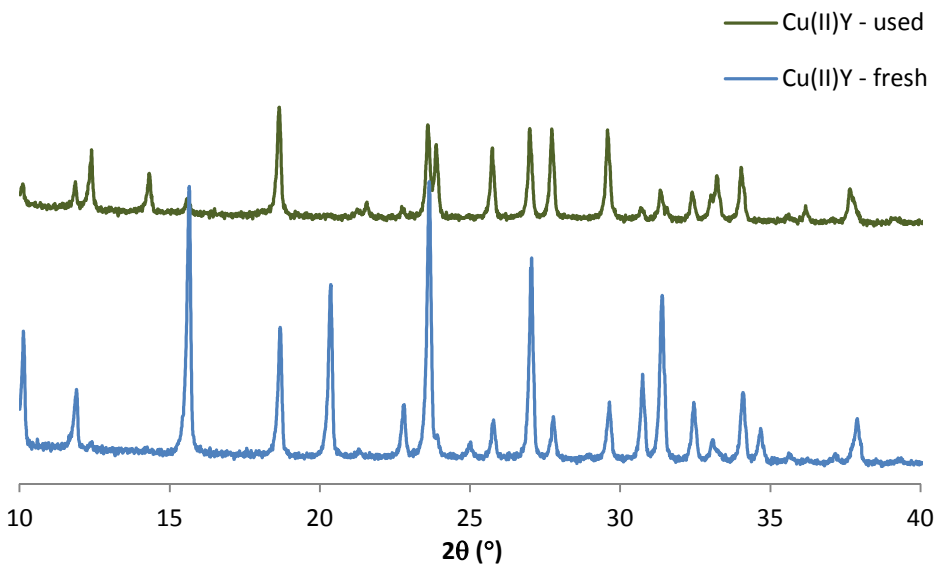

Figure 2.6 PXRD patterns of fresh and used Cu(II)Y catalyst when using K_2CO_3 as a base

Other bases were investigated as well. When using Cs_2CO_3 as base, 79% of the copper leached from the zeolite framework, Table 2.2. Also, the solid contained 22.5% Cs. As 2 mmol of Cs are needed to replace 1 mmol of Cu via ion-exchange, by doing simple calculations, it can be expected that this cesium most probably replaced copper in the zeolite framework cation exchange sites. Comparing the PXRD patterns of fresh and used

Cu(II)Y, Figure 2.7 shows that the destructive effect of Cs_2CO_3 on the crystallinity of the zeolite was similar if not worse than that of K_2CO_3. Organic bases, like triethylamine and 4-Dimethylaminopyridine, were also explored, but they were not useful, as the reaction did not proceed to any significant extent.

Table 2.2 Elemental analysis of Cu(II)Y before and after reaction using Cs_2CO_3 as a base

Sample	Si	Al		Cu		Cs	
	wt %	wt %	per mol Si	wt %	per mol Si	wt %	per mol Si
Fresh Cu(II)Y	29.3	10.7	0.381	9.14	0.138	-	-
Used Cu(II)Y	21.8	7.2	0.342	1.43	0.029	22.5	0.218

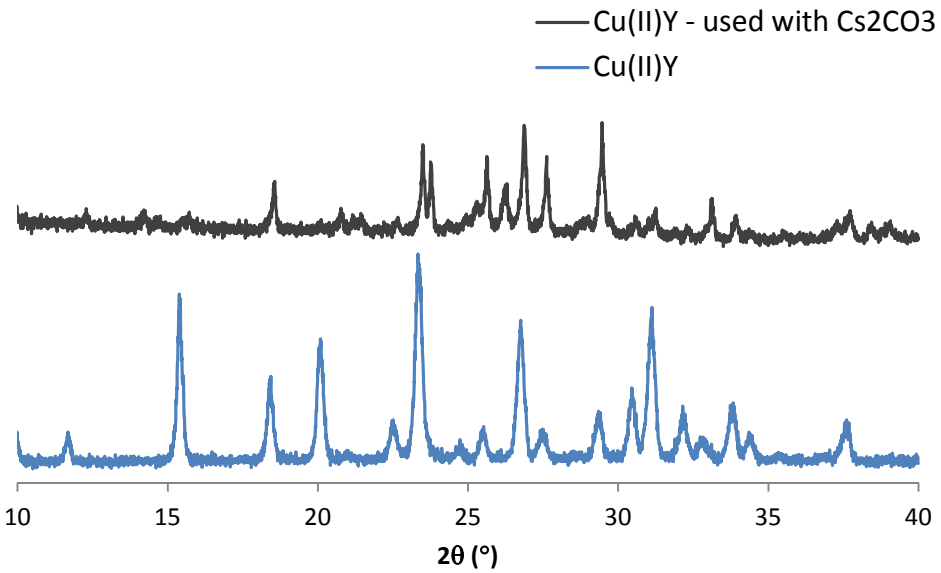

Figure 2.7 PXRD patterns of fresh and used Cu(II)Y catalyst when using Cs_2CO_3 as a base

2.4 Conclusions

Copper exchanged zeolite, Cu(II)Y, was investigated as a catalyst for the amination of aryl iodide with imidazole. It was found that the copper exchanged zeolite was a moderately active catalyst for the cross coupling reaction. Catalyst heterogeneity was assessed by conducting shape selectivity tests. It was found that a bulkier aryl-iodide, 5-iodo-1,2,3-trimethoxybenzene, that can actively react with imidazole when CuO nanoparticles were used as the catalyst, reacted to a very limited extent with imidazole when using Cu(II)Y as the catalyst. This might indicate that Cu(II)Y is a heterogeneous catalyst, as it had shape-selective properties, suggesting some catalytic turnover occurred within the zeolite pores. Nevertheless, since a base is needed for this type of reaction, retaining the zeolite crystallinity was a challenge. Different bases were tried, and they had two effects; the alkali (potassium or cesium) exchanged with copper, which helped it to leach more to the reaction mixture, and the crystallinity of the structure of zeolite was diminished. Therefore, it is important to support copper on a framework that is stable under the basic conditions required for this type of reaction if a heterogeneous, recyclable catalyst were to be achieved. Cerium oxide was chosen for this purpose, and the related work is presented in Chapter 3 of this thesis.

CHAPTER 3

COPPER OXIDE SUPPORTED ON MESOPOROUS CERIUM OXIDE AS A LIGAND-FREE CATALYST FOR N-ARYLATION OF IODOBENZENE WITH BENZYLAMINE – ACTIVITY AND HETEROGENEITY ASSESSMENT

3.1 Introduction

Aryl-nitrogen bonds are prevalent in many compounds that are of biological, materials, and pharmaceutical interest. Among the different methods used to form this aryl-nitrogen bond, N-arylation of aryl halides, the interest of this study, is usually carried out catalytically in polar solvent, with the aid of a base to help deprotonate the nucleophile.

In 2001, the Buchwald and Taillefer research groups[42,43] discovered efficient new copper/ligand systems for the formation of C-C, C-N, and C-O bonds, and since then many other research groups have focused their work in this area as well. [34–36,38,39,44–46] Along with the homogeneous catalytic systems that researchers initially developed, there were many trials to heterogenize copper by supporting it on different solids. [40,48–53]

As presented in Chapter 2 of this thesis, in a trial to study and investigate the heterogeneity of copper catalysis associated with a Cu(II)Y zeolite, it was concluded that it is important to support copper on a framework that is stable under the basic conditions required for typical aryl-nitrogen bond forming reactions.

Cerium oxide is known to have basic sites[54,55] and to be stable under basic conditions. Copper oxide supported on ceria ($CuO\text{-}CeO_2$) is known to be a highly effective catalyst in NO reduction, [56–67] CO and hydrocarbon oxidations,[58,67–70] the water-gas shift reaction,[71–75] and in many other reactions. This catalytic reactivity is generally ascribed to the synergistic interactions of CuO and CeO_2, which are related to their interdispersion, the facile creation of defects (e.g. oxygen vacancies) and redox interplay between copper and cerium redox couples (Cu^{2+}/Cu^{+} and Ce^{4+}/Ce^{3+}).[76,77]

The mechanism of the modified Ullmann reaction is still not totally unraveled, but most of the suggested mechanisms start with Cu^{+}.[78] The two main suggested mechanisms are a radical mechanism, as shown in Scheme 3.1, and oxidative addition/reductive elimination mechanism, as depicted in Scheme 3.2. Despite conflicting evidence, most authors agree that the reaction between the copper precursor complex and the nucleophile precedes the activation of the aryl halide.[78]

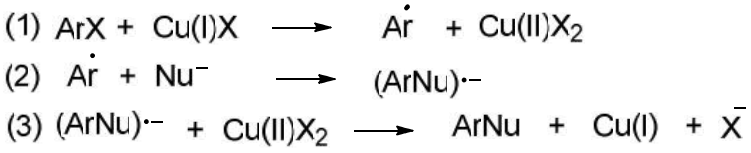

Scheme 3.1 General scheme for copper-catalyzed $S_{RN}1$-type mechanism for the Ullmann coupling. reaction[78]

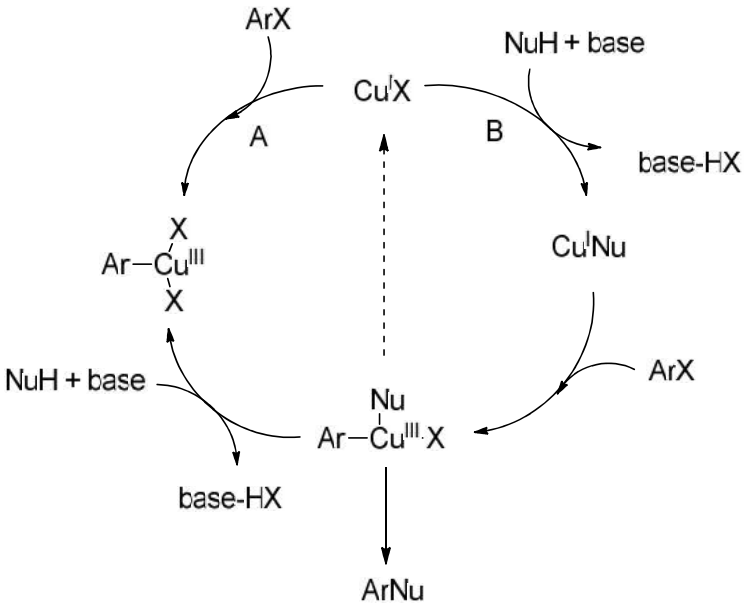

Scheme 3.2 Suggested oxidative addition/reductive elimination mechanism for C-N coupling reaction[62]

In this work, the basicity of CeO_2 encouraged us to choose it as a support for CuO domains, with the hope that C-N coupling reaction can be catalyzed without the need of added base. The reactivity of CuO supported on CeO_2 towards N-arylation of iodobenzene with benzylamine (Scheme 3.3) was assessed. The catalyst stability and heterogeneity were also studied and investigated. Finally, based on the effect of different bases on the catalyst reactivity, some mechanistic investigation was conducted.

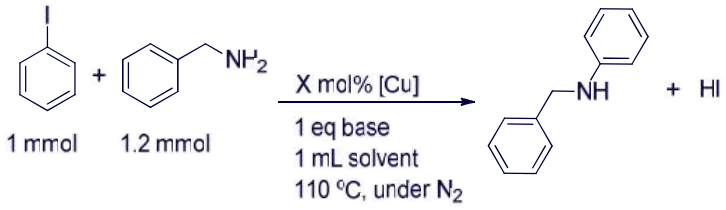

Scheme 3.3 N-arylation of iodobenzene with benzylamine to form N-benzylaniline

3.2 Experimental Details

3.2.1 Catalyst Preparation

3.2.1.1 Synthesis of Mesoporous CeO_2

To synthesize mesoporous cerium oxide (CeO_2), 12 g of 1-hexadecylamine (HDA) (Sigma-Aldrich, 98%) was dissolved in 70 mL of ethanol solution (50 wt% in water) at room temperature, then heated to 50 °C and stirred overnight. To this mixture, 32 g of cerium (III) acetate (1.5 hydrate) $Ce(CH_3COO)_2.xH_2O$ (Sigma-Aldrich, 99.99% trace metals basis) was added under vigorous stirring.

The above mixed suspension system (grey-purple) was stirred for 3 h at room temperature and transferred to an oven with a pre-set temperature of 60 °C, where it was statically aged for 48 h. The resultant solid material was harvested by centrifuged at 3000 rpm for 20 min and the sticky clear solution was decanted. The wet product was re-dispersed into 50 wt% ethanol solution again and the same centrifugation procedure was repeated twice.

The as-synthesized wet mesoporous ceria was dried under ambient atmosphere overnight and then it underwent a two-stage calcination as follows: The samples was transferred to a crucible in middle of an oven, where it was heated to 150 °C at ramp of 2 °C/min, hold on for 6 h, and then the temperature was increased to 400 °C at the same ramp for 4 h, followed by cooling the final product to about 40 °C.

3.2.1.2 Supporting CuO on Mesoporous CeO_2

A solution containing 1.69 g of copper nitrate tri-hydrate $Cu(NO_3)_2.3H_2O$ (Sigma-Aldrich, purity>99%) and 15 mL of absolute ethanol was added to 5 g of the above synthesized dry mesoporous ceria, to yield a 10 wt% ceria-supported copper oxide catalyst. The wet sample was dried under ambient atmosphere at 75 °C overnight. Then, the catalyst was heated to 500 °C at a ramp of 2 °C/min, and calcined in flowing air at 500 °C for 3 h.

Commercial CuO nanoparticles (Sigma-Aldrich, S_{BET} = 16 g/m^2) were used as received for comparison purposes.

3.2.2 Characterization

Powder X-ray diffraction (PXRD) was carried out with a PAnalytical X'Pert PRO diffractometer operating with Cu Kα radiation and an X'celerator RTMS detector. A step size of 0.002° 2θ and a scan rate of 10 s per step were used. Nitrogen adsorption isotherms were recorded at 77 K using a Micromeritics TriStar II 3020. BET (Brunauer-Emmett-Teller) surface areas were calculated using adsorption data. Average pore diameters were determined by BDB-FHH method (a simplified Broekhoff–de Boer method with a Frenkell–Halsey–Hill isotherm).[79] Elemental analysis by ICP-AES was carried out by ALS Environmental Division (Tucson, AZ).

3.2.3 Catalytic N-Arylation (C-N Cross Coupling Reaction)

In a typical reaction, the catalyst (0.05 eq. or 0.10 eq. Cu relative to iodobenzene), was added to a 25-mL two-neck round bottom flask containing 5 mmol iodobenzene (561 μL), 6 mmol benzylamine (655 μL, 1.2 eq.), 5 mmol base (either potassium hydroxide or potassium carbonate), 5 mL DMSO, and 2.5 mmol diethylene glycol dibutyl ether (0.5 eq., 618 μL) as an internal standard. The round bottom flask was attached to a condenser, evacuated and backfilled with nitrogen gas twice, and then immersed in a preheated oil bath, at 110 °C, to start the reaction. Samples of the reaction mixture were taken at specified times, filtered over silica gel column and diluted with dichloromethane, and the limiting reactant (iodobenzene) conversion was determined by GC-FID, and calculated by comparing the reactant to internal standard peaks area ratio to the ratio at the beginning of the reaction. The identity of the product was verified by GC-MS.

3.3 Results and Discussion

3.3.1 Catalyst Characterization

Elemental analysis of the prepared catalyst showed that it contains 9.0 wt% Cu with Cu/Ce ratio of 0.141 g/g or 0.311 mol/mol. Thus, the catalyst thereafter will be referred to as 9CuO-CeO_2. The PXRD pattern for the catalyst is shown in Figure 3.1, which shows the two characteristic peaks of crystalline CuO at $2\theta = 35.5°$ and 38.9°. For comparison, PXRD patterns of the bare mesoporous CeO_2 support and CuO commercial nanoparticles are also shown.

The porosity of the CeO_2 was characterized using nitrogen physisorption at 77 K. The bare support BET surface area was 128 m^2/g, which decreased to 73 m^2/g upon supporting CuO. The average pore diameter and the cumulative pore volume of the mesoporous CeO_2 were 35 nm and 0.21 cm^3/g respectively, and they slightly changed to 26 nm and 0.15 cm^3/g after supporting CuO. These results might indicate that there was some collapse of some large pores present in the bare mesoporous CeO_2, and that CuO is blocking some pores. A TEM image of supported CuO catalyst, Figure 3.2, shows that there were some large clusters on the support surface, which are most probably CuO clusters. The crystalline size of CuO domain was calculated by applying the Scherrer equation to the PXRD of 9CuO-CeO_2, at the angle of 35.5°, and found to be 25 nm, which is consistent with the size of the dark areas in the TEM image.

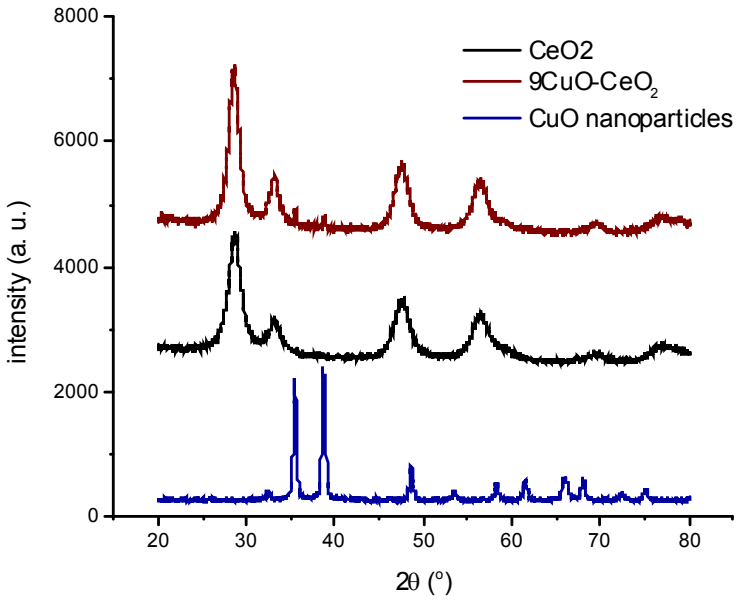

Figure 3.1 PXRD patterns for ceria-supported CuO catalyst (9CuO-CeO_2), bare mesoporous CeO_2 support and commercial CuO nanoparticles

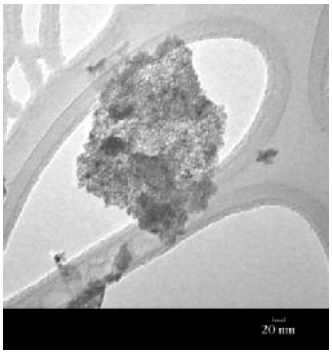

Figure 3.2 TEM image of ceria-supported CuO catalyst (9CuO-CeO_2)

3.3.2 Catalytic Reactivity

The carbon-nitrogen cross coupling reaction of iodobenzene and benzylamine to form N-benzylaniline (Scheme 3.3), was evaluated using different catalyst loadings and different bases.

Figure 3.3 shows the kinetic behavior of this C-N cross coupling reaction using 9CuO-CeO_2 as the catalyst under different reaction conditions.

3.3.2.1 Effect of Catalyst Loading

Figure 3.3 shows the kinetic behavior of C-N cross coupling reaction using 5 and 10 mol% copper. It can be noticed that increasing catalyst loading, using the same base, slightly increases the limiting reactant (iodobenzene) conversion, while it significantly increases the desired product (N-benzylaniline) yield, especially when using the weaker base, K_2CO_3.

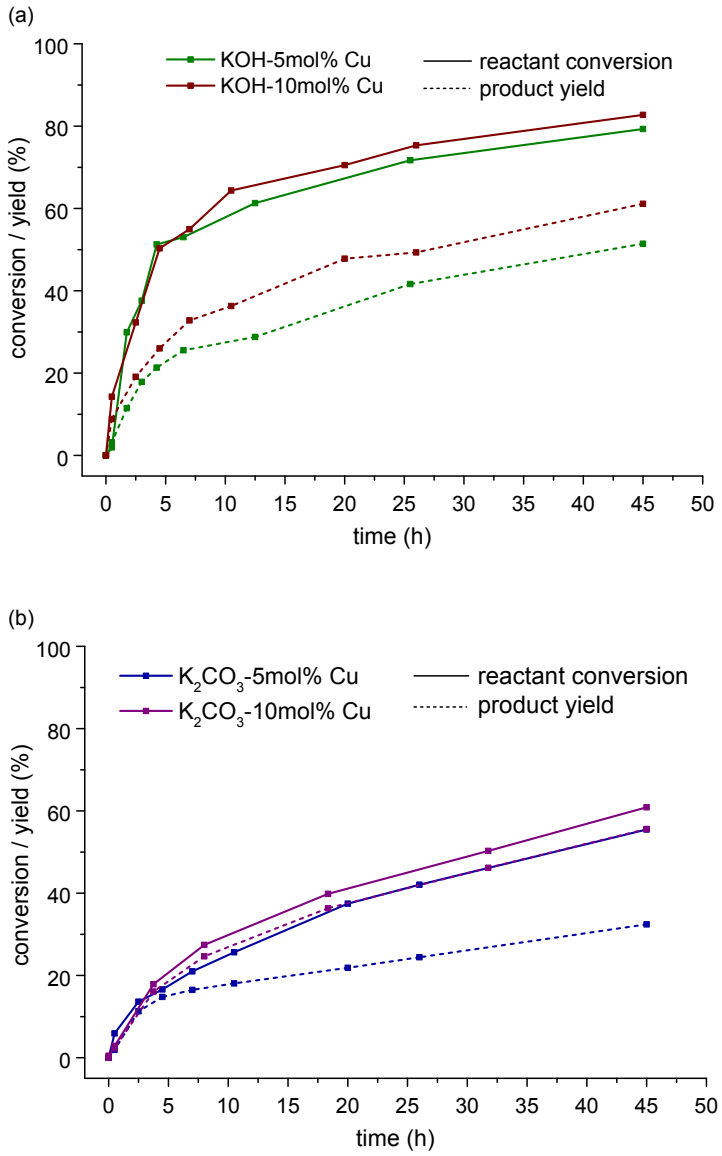

Figure 3.3 **Kinetic behavior of C-N cross coupling reaction between iodobenzene, benzylamine (1.2 eq.), in DMSO (1 mL per mmol iodobenzene), using 9CuO-CeO_2 (5 and 10 mol% copper) as a catalyst, and two different bases (KOH (a) and K_2CO_3 (b), 1 eq.) at 110 °C under N_2, to form N-benzylaniline.**

3.3.2.2 Effect of Added Base

Figure 3.3 also shows the kinetic behavior of C-N cross coupling reaction using two different bases; a strong base, KOH, and a weaker one, K_2CO_3. Although KOH led to higher reactant conversion, K_2CO_3 was more selective (65-90% selectivity) than KOH (40-50% selectivity) toward the desired product, N-benzylaniline, especially at the higher catalyst loading. The relatively low selectivity in both cases is thought to be due to the formation of some side products, the type of which depends on the used base.

In the case of potassium hydroxide, the main side products were phenol and diphenyl ether, as shown in Scheme 3.4. It is known in the literature that copper can catalyze the hydroxylation of aryl halides in the presence of potassium hydroxide under certain conditions.[80–84] A separate experiment was conducted to study the capability of 9CuO-CeO_2 in catalyzing this hydroxylation reaction.

Figure 3.4 shows the kinetic behavior of iodobenzene hydroxylation using potassium hydroxide. Under the standard reaction conditions used in C-N cross coupling experiments, this reaction yielded 33% phenol and 33% diphenylether. This competitive side reaction (Scheme 3.4) affected the performance of the supported copper catalyst toward producing the desired product (N-benzylaniline) when using KOH as a base, and thus reduced its yield.

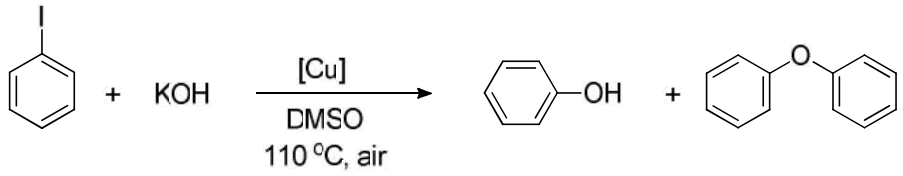

Scheme 0.1 **Formation of phenol and diphenylether as side products when using KOH as a base**

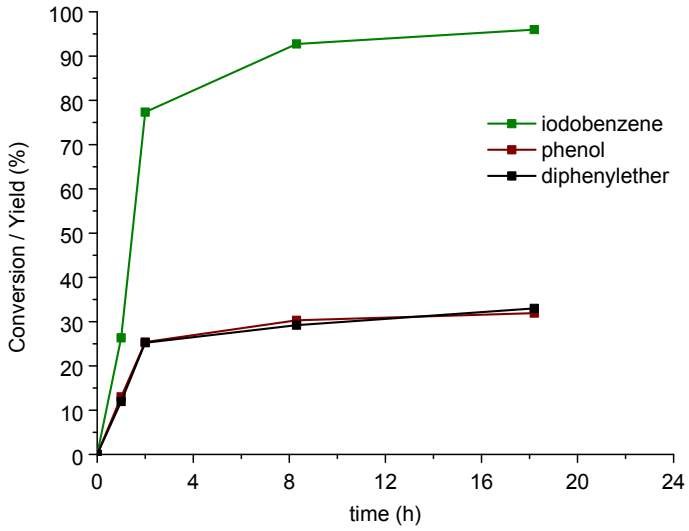

Figure 3.4 **Kinetic behavior of phenol and diphenylether formation using from iodobenzene and KOH (2 eq.), using 9CuO-CeO_2 (5mol% copper) as the catalyst, in DMSO (0.5 mL per mmol iodobenzene), at 130 °C under N_2.**

When using K_2CO_3 as a base, the main side product was noticed to be the N-benzylideneaniline, which can be formed either by coupling of benzaldehyde and aniline, both of which were also identified as side products, or by dehydrogenation of the final product, N-benzylaniline.

In both cases, there was also an amine oxidation side reaction, as shown in Scheme 3.5, forming N-benzylidenbenzylamine as another side product. This reaction does not need a base. The discovery of this side reaction here led to an entirely separate reaction pathway study of this oxidative coupling reaction. This reaction will be discussed in detail in Chapter 4.

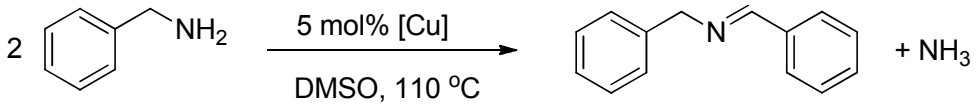

Scheme 0.2 Formation of N-benzylidenebenzylamine by benzylamine oxidative coupling reaction

In addition to the different side products that were formed when using different bases, analysis of the catalyst after reaction showed that the type of base affected the final oxidation state of copper. Figure 3.5 shows the PXRD patterns of the used 9CuO-CeO_2 catalyst after two reactions using different bases. When using KOH, the predominant copper oxidation state changed from (+2) to (+1), while it stayed (+2) when K_2CO_3 was used.

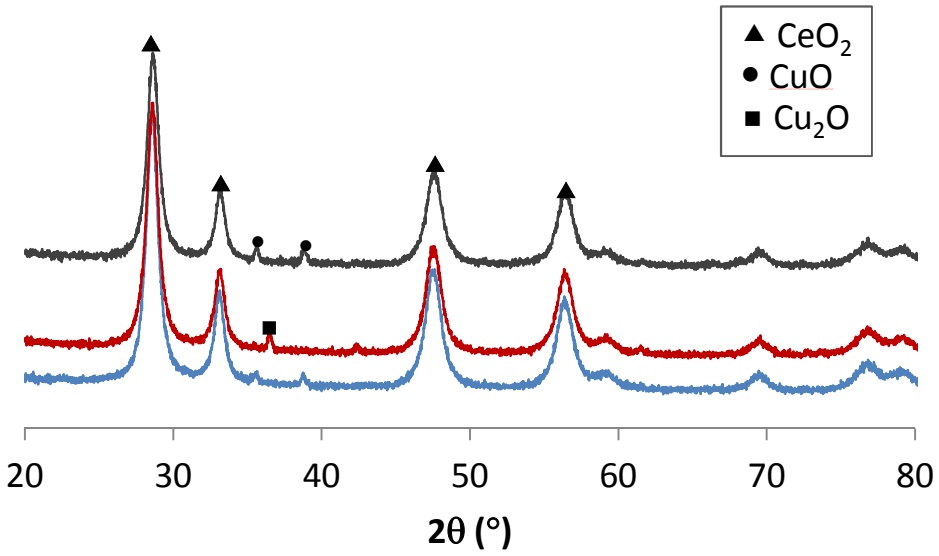

Figure 3.5 PXRD patterns for ceria-supported CuO catalyst (9CuO-CeO_2); fresh (gray), used with KOH (red), and used with K_2CO_3 (blue).

The first hypothesis regarding this observation was that when mixing KOH with DMSO, they *in situ* produced dimsyl potassium,[85] a strong reducing agent, and that potassium carbonate was not strong enough to produce this dimsyl anion. But the dimsyl anion is unstable and decomposes at temperatures higher than 40 °C, whereas the reactions were run at 110 °C. So, to understand the effect of the different bases on copper reduction, the catalyst 9CuO-CeO_2 was mixed with DMSO alone, with DMSO and KOH, and with DMSO and K_2CO_3. After mixing for 24 h at 110 °C, the catalyst was centrifuged and analyzed. Figure 3.6 shows a comparison between the PXRD patterns of the fresh and treated 9CuO-CeO_2 Neither DMSO by itself, nor DMSO with the base were able to reduce Cu(+2) to Cu(+1). This means that the reduction was a combined effect between DMSO, KOH, and the reagents. More related discussion will be presented in later.

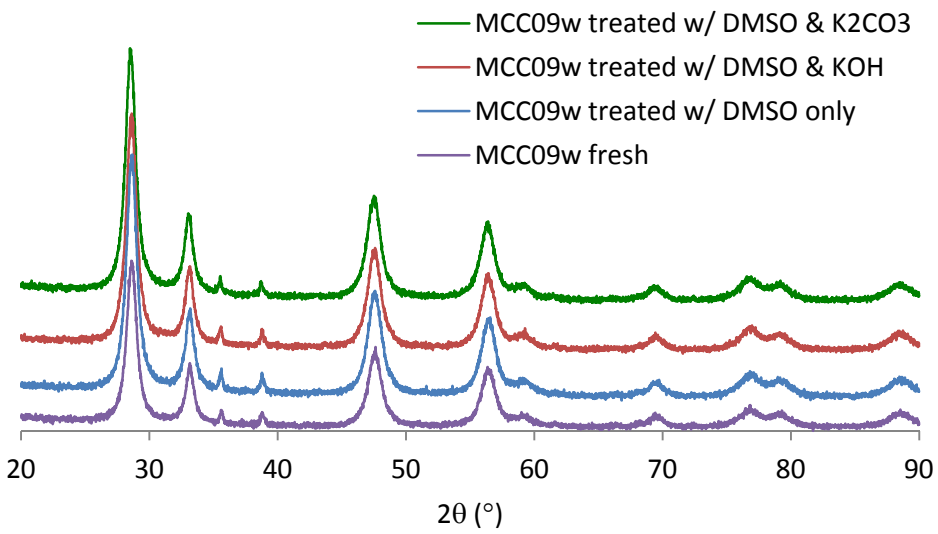

Figure 3.6 PXRD patterns for ceria-supported CuO catalyst (9CuO-CeO_2); fresh and after treatment with DMSO, DMSO with KOH, and DMSO with K_2CO_3.

3.3.2.3 Comparing the Catalytic Activity of Ceria-Supported CuO with CuO Nanoparticles

Figure 3.7 shows a comparison between the catalytic reactivity of CuO nanoparticles and 9CuO-CeO_2, where it can be noticed that both catalysts had almost the same behavior. This shows that supporting CuO did not really change its characteristics, and led to species that were as active as the unsupported CuO nanoparticles. This observation led to further investigation related to the nature of the active species. Whether the supported CuO stayed on the support and promoted the reaction as a solid entity or it leached into the solution and became active was an important question, as answering it can lead to an understanding of the nature of the active species and the heterogeneity (or homogeneity)

of this supported catalyst. A more detailed study of the catalyst heterogeneity is presented in the following section.

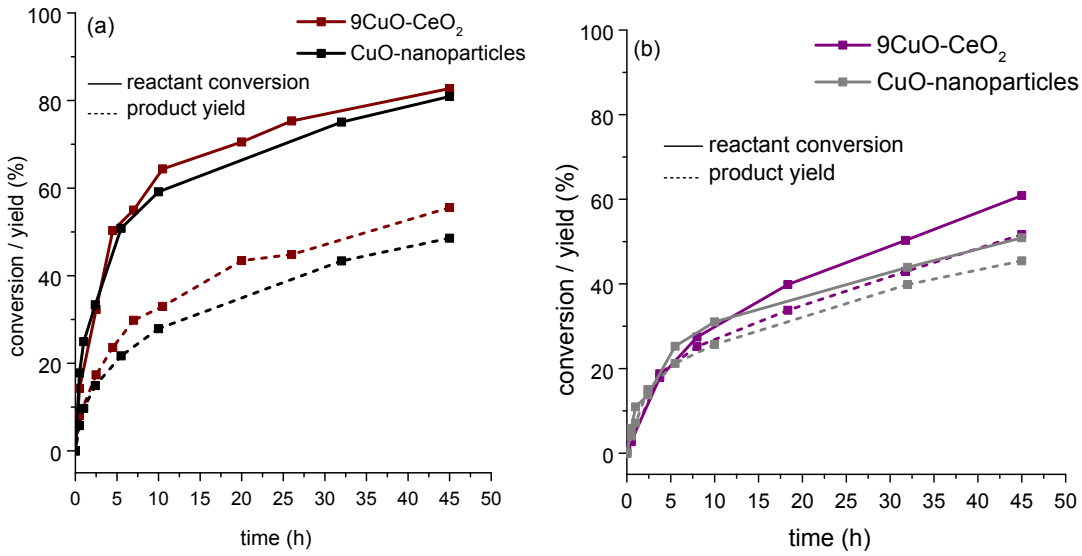

Figure 3.7 Kinetic behavior of C-N cross coupling reaction between iodobenzene and benzylamine (1.2 eq.), in DMSO (1 mL per mmol iodobenzene), using 9CuO-CeO_2 and CuO nanoparticles (10 mol% Cu) as catalysts, and two different bases (KOH (a) and K_2CO_3 (b), 1 eq.) at 110 °C under N_2, to form N-benzylaniline.

3.3.3 Catalyst Recyclability and Heterogeneity

3.3.3.1 Testing Copper Leaching

After running each of the four reactions shown in Figure 3.3, the catalysts were recovered by centrifugation, washed with de-ionized water and ethanol, dried, and then sent for

outside analysis. Table 3.1 shows the elemental analysis results for each of the recovered catalysts, in comparison with the fresh catalyst. It can be noticed that reactions run with K_2CO_3 caused more copper leaching than those run with KOH, but that the catalyst leached copper under all conditions. To further understand what exactly causes leaching, more experiments were conducted, as described below in Section 3.3.3.2.

Table 3.1 Elemental analysis of fresh and used 9CuO-CeO_2 catalyst

Experiment ID	Base used	Catalyst mol %	Cu wt %	Cu/Ce (g/g)	% Cu leaching
9CuO-CeO_2 (fresh)	-	-	9.0	0.141	-
9CuO-CeO_2/KOH/5	KOH	5	5.9	0.106	25%
9CuO-CeO_2/KOH/10	KOH	10	6.3	0.103	27%
9CuO-CeO_2/K_2CO_3/5	K_2CO_3	5	5.1	0.084	41%
9CuO-CeO_2/K_2CO_3/10	K_2CO_3	10	6.0	0.083	41%

3.3.3.2 Why Does Copper Leach?

To better understand the system and help design a better catalyst, it is useful to know which reactant/reagent has the main role in leaching copper from its support. Looking at the results in Table 3.1, one might hypothesize that K_2CO_3 by itself causes more leaching than KOH. To test this hypothesis, the following experiment was performed. In 5 different flasks, the catalyst was mixed with only DMSO, and with DMSO plus only one of the reagents/reactants used in the reaction at the same reaction temperature, 110 °C.

After 24 h, the mixture was centrifuged and the catalyst was recovered, washed, dried, and then sent for elemental analysis. The results are shown in Table 3.2.

Table 3.2 Leaching test and effect of different reactants/reagents

Catalyst mixed with	Cu wt %	Ce wt %	Cu/Ce g/g	Cu leaching %	Leaching because of reactant/reagent only
DMSO	7.35	57.60	0.128	10%	N/A
DMSO and KOH	6.25	54.39	0.115	19%	9%
DMSO and K_2CO_3	6.09	54.47	0.112	21%	11%
DMSO and iodobenzene	5.76	62.31	0.092	34%	24%
DMSO and benzylamine	6.63	59.82	0.111	21%	11%

The results in Table 3.2 show that every single reactant and reagent in this system has its own role in leaching copper from its support, with iodobenzene having the most effect. Interestingly, if KOH and K_2CO_3 are the only reagents in the mixture, the amount of copper leaching is almost the same (9% and 11% respectively). This contradicts the hypothesis stated above that resulted from the Table 3.1 results; K_2CO_3 caused more leaching than KOH. A look back to the suggested mechanisms in the literature might help explain these two contradicting results.

As mentioned earlier, the mechanism of modified Ullmann reaction is still not totally unraveled. The base is needed to initiate the reaction by activating and deprotonating the nucleophile. Deprotonation with KOH yields water, whereby its coexistence with KOH and CuO forms the soluble complex $[Cu(OH)_4]^{2-}$. This complex can decompose and form $Cu(OH)_2$, which in turn is thought to react with the product, N-benzylaniline, and become

reduced to Cu_2O,[86] with the formation of N-benzylideneaniline, according to Scheme 3.6. Although it cannot be considered to be definitive evidence, the formation of small amount of N-benzylideneaniline was detected by GCMS, and this supports the suggested mechanism of CuO reduction to Cu_2O. The suggested need of coexistence of the base and the amine for CuO dissolution to occur might explain why the conclusion made by Jammi et al about heterogeneous catalysis by CuO nanoparticles might not be considered definitive.[41] In their heterogeneity assessment, they mixed CuO nanoparticles with DMSO in the presence and absence of KOH, at 110 °C for 24 h. They centrifuged the nanoparticles and used the liquid to run the reaction in the presence of KOH under N_2, and noticed no activity. This can be true but does not mean that the reaction is occurring heterogeneously because Cu^{2+} dissolution from CuO nanoparticles needs H_2O that is produced from nucleophile deprotonation.

$$CuO + 2\ KOH + H_2O \longrightarrow K_2[Cu(OH)_4] \longrightarrow 2\ KOH + Cu(OH)_2$$

$$Cu(OH)_2 + \frac{1}{2}\ Ph\text{-}CH_2\text{-}NH\text{-}Ph \longrightarrow \frac{1}{2}\ Cu_2O + \frac{3}{2}\ H_2O + \frac{1}{2}\ Ph\text{-}CH{=}N\text{-}Ph$$

Scheme 3.6 Proposed mechanism for the reduction of CuO to Cu_2O.

On the other hand, deprotonation with K_2CO_3 yields the bicarbonate anion. The coexistence of the Cu^{2+} cation and HCO^{3-} anion produces copper carbonate, $CuCO_3$, and the H^+ cation as shown in Scheme 3.7.[87] The free proton reacts with CuO, and helps

leaching more copper from the support, according to Scheme 3.8.[88] Also, the formation of solid copper carbonate, which is insoluble in DMSO, drives the equilibrium, Scheme 3.7, to the right, producing more H^+ and consuming more Cu^{2+}. The formation of soluble active $[Cu(OH)_4]^{2-}$ when using KOH versus the precipitation of the inactive $CuCO_3$ might explain the reason behind the KOH-system being more active than the K_2CO_3-system, although it leaches less copper. The formation of $CuCO_3$ was verified by XRD analysis of CuO nanoparticles used in running the same reaction (Scheme 3.3) with K_2CO_3, as the base as shown in Figure 3.7. When taking the PXRD pattern of CuO nanoparticles after reaction (Figure 3.8), $CuCO_3$ characteristic peaks at 31.6° and 52.1° were identified. It was hard to identify those peaks in the 9CuO-CeO_2 pattern, as they are expected to be much smaller in size than CeO_2 peaks and covered by the pattern noise. Similar to the 9CuO-CeO_2 results, most of the CuO nanoparticles were reduced to Cu_2O when KOH was used as a base.

$$Cu^{2+} + HCO_3^- \leftrightarrow CuCO_3 + H^+$$

Scheme 3.7 Formation of $CuCO_3$[87]

$$CuO + 2H^+ \rightarrow Cu^{2+} + H_2O$$

Scheme 3.8 Copper dissolution in the presence of acidic proton[88]

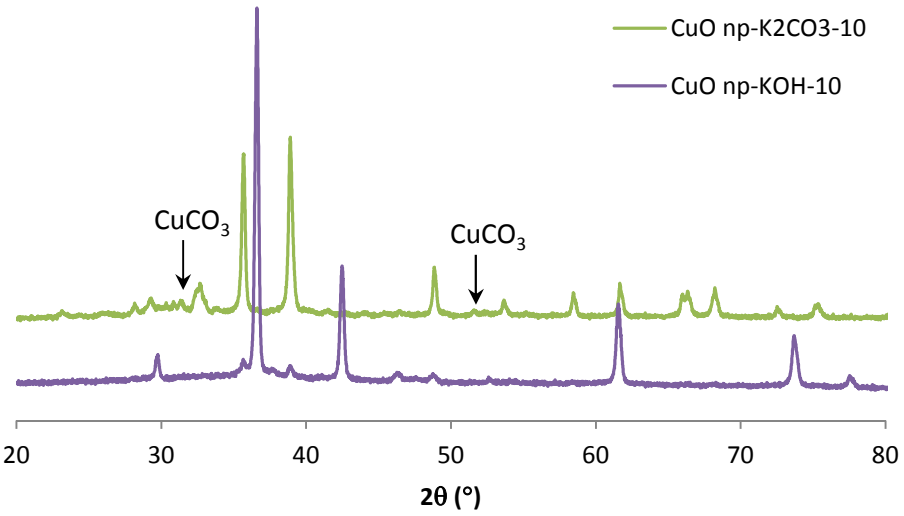

Figure 3.8 PXRD pattern of CuO nanoparticles after running C-N cross coupling reaction using KOH (purple) or K_2CO_3 (green) as a base

Finally, the effect of copper coordination with iodobenzene cannot be ignored. It is shown in Table 3.2 that when iodobenzene and DMSO were solely mixed with 9CuO-CeO_2, there was 34% copper leaching, 24% of which could be assigned to iodobenzene. The coordination between copper and iodobenzene might have an added role in solubilizing and thus leaching copper from the ceria support.

3.3.3.3 Hot Filtration Test

Hot filtration tests are usually used to assess the heterogeneity of solid catalysts. As shown in Table 3.1, in these reactions, 25-40% of the copper leached from the supported catalyst, 9CuO-CeO_2. Whether the leached copper or the copper left on the support is the active species in the catalytic reaction can be assessed by running a hot filtration test.

After running the reaction for 2 h, the reaction mixture was filtered while still hot, the filtrate was received in an evacuated clean pre-heated flask, filled with nitrogen, and the reaction was continued without the solid catalyst in this second flask. The progress of the reaction was monitored over time. Figure 3.9 (a) shows the results of this test, and as can be seen in the figure, although the conversion of the limiting reactant continued, the formation of the desired C-N coupling product stopped. These data lead to a conclusion that the C-N cross coupling reaction is possibly occurring on the surface of the solid CuO species, and that the leaching copper is not the active catalytic species that yields the desired product, N-benzylaniline, in this case.

However, in considering this specific catalytic reaction, it was determined that reaction conditions were not strictly the same before and after filtration. The used base, KOH, has very low solubility in the organic solvent (DMSO), and thus it was also filtered out with the solid catalyst. Therefore, the same test was repeated with fresh base being added to the filtrate receiving flask, and the result was totally different. Figure 3.9 (b) shows that when adding the base (KOH in this case) to the filtrate receiving flask, the reaction continued to form the desired product with even higher yield. This means that this reaction runs primarily or exclusively homogeneously, and the leached copper is the active species.

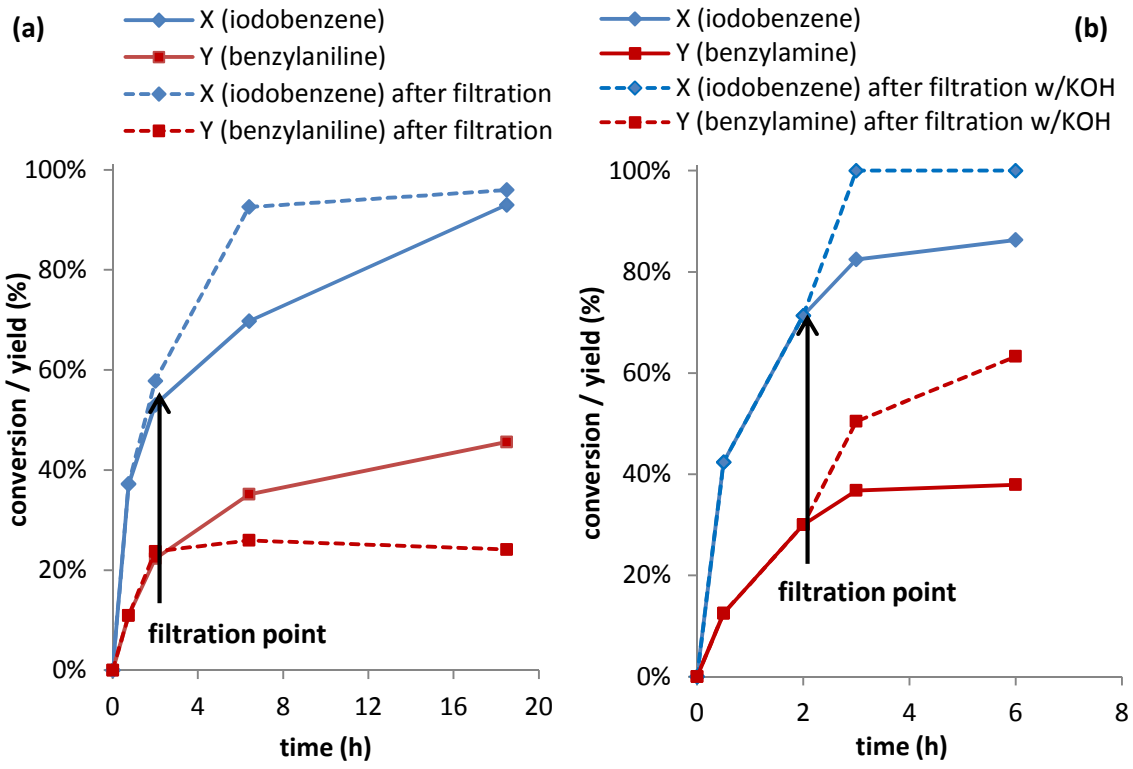

Figure 3.9 **Hot filtration test (a) without and (b) with adding KOH to the filtrate receiving flask**

3.3.3.4 Recyclability Test

The recyclability of the 9CuO-CeO_2 catalyst was also evaluated. After completion of a reaction, the catalyst was recovered by centrifugation, washed with de-ionized water and ethanol, dried at 100 °C overnight, and used in subsequent cycle. Assuming no loss of copper from the used catalyst, the same catalyst loading was used in the following cycle. Figure 3.10 shows the results of this recyclability test. The catalyst lost part of its activity from cycle 1 to 2 to 3, yielding less product after each cycle. The catalyst recovered from the third cycle was regenerated by calcination at 400 °C for 3 h. After regeneration, the

catalyst recovered part of its activity. Therefore, the loss of catalyst activity could be partially due to organic species depositing on its surface. Also, since this experiment was run assuming no copper leaching, the reduced activity could be assigned to the reduced amount of copper added to the system after each cycle. Part of the catalyst recovered from the second cycle was sent for elemental analysis. Considering the actual amount of copper added in each cycle, the TOF of the first cycle calculated over the first hour was 2.5 mmol product/(mmol Cu.h), while for the third cycle it was 3.3 mmol product/(mmol Cu.h). So despite the fact that copper leached from the support, it stayed capable of catalyzing the reaction at even better rate, perhaps due to more efficient leaching in subsequent runs. Nevertheless, the TON of the third cycle was about 30% less than that of the first cycle; 680 mmol product/mmol Cu for the third cycle compared to 940 mmol product/mmol Cu for the first cycle. In conclusion, it can be said that this catalyst acts as a reservoir for soluble copper species and needs regeneration after each cycle to remove any organic species depositing on its surface, as evidenced by the recovery of some activity after calcination.

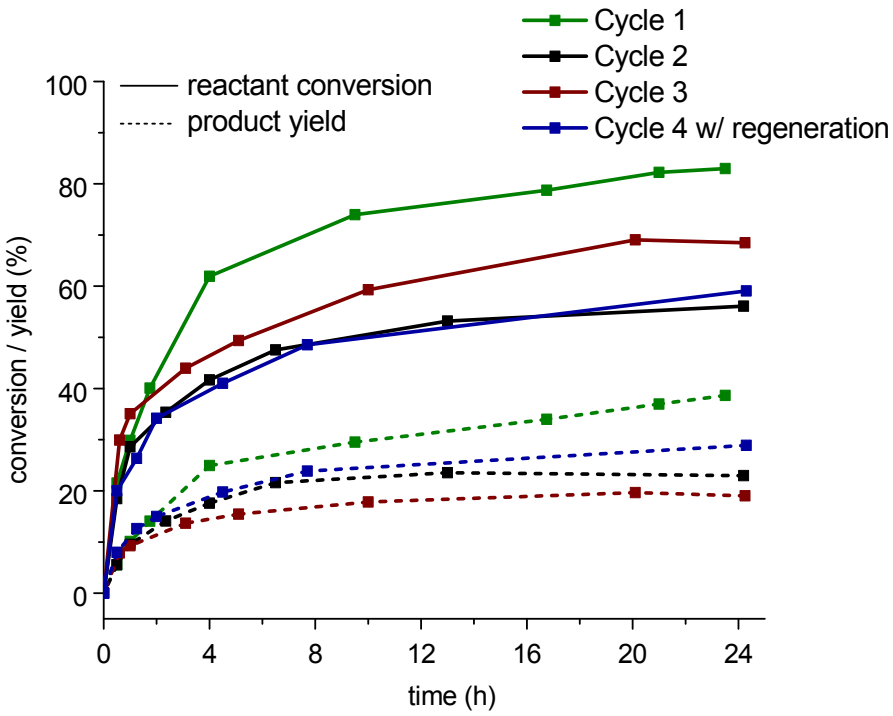

Figure 3.10 Recyclability of 9Cu-CeO_2 catalyst with and without regeneration, using 5 mol% copper and KOH as a base, at 110 °C under N_2

3.4 Conclusions

Copper oxide supported on cerium oxide was investigated as a catalyst for C-N coupling reaction between iodobenzene and benzylamine. It was found that copper leached from the support and it was demonstrated through hot filtration tests that the leached copper species was the main active catalyst. Leaching was caused by the solvent (DMSO) as well as the used reactants and the base. The base is needed to deprotonate and activate the N-nucleophile, but this deprotonation step might significantly contribute to copper leaching as well. Also, the coexistence of base, reactant and solvent caused much more leaching than if each reagent/reactant was solely mixed with the catalyst. These findings mean that designing a truly heterogeneous catalyst for his reaction that is capable of

keeping the copper on the support under these harsh conditions is a challenging task. This catalyst can be recycled but only as a reservoir to produce the soluble active copper species. The catalyst needs regeneration before recycling to remove deposited organic substances and partially recover its activity.

CHAPTER 4

REACTION PATHWAYS OVER COPPER AND CERIUM OXIDE CATALYSTS FOR DIRECT SYNTHESIS OF IMINES FROM AMINES UNDER AEROBIC CONDITIONS

4.1 Introduction

Imines are important intermediates in the synthesis of various biologically active nitrogen-containing compounds. Imines are traditionally synthesized by several methods, including direct synthesis from amines and alcohols in the presence of catalyst and base,[89–96], self-condensation of primary amines with oxidants,[94,97–102], and via oxidation of secondary amines.[100,103–108] In the last several years, it has been demonstrated that imines can be synthesized by conversion of two moles of the parent primary amine under oxidative conditions in the presence of a variety of suitable catalysts.[94,97,98,101,106,109–121] A prototypical reaction of this type is benzylamine oxidative homocoupling to form N-benzylidenebenzylamine. This reaction has been reported to be catalyzed by homogeneous copper (I) chloride under mild aerobic conditions,[101] a copper (II) complex,[121] bulk gold powder,[106] supported gold nanoparticles,[115,119,122] ruthenium N-heterocyclic carbene (NHC) catalysts,[109] V_2O_5 catalysts with aqueous hydrogen peroxide,[97] and by a molecular vanadium complex catalyst, $VO(Hhpic)_2$[120] among others.

As mentioned in Chapter 3, while exploring copper oxide supported on mesoporous ceria ($CuO\text{-}CeO_2$) as a catalyst for C-N coupling reaction between iodobenzene and benzylamine, we serendipitously discovered it to be highly efficient in the aerobic oxidation of benzylamine to form N-benzylidenebenzylamine, Scheme 4.1. Following this initial observation, we carried out a systematic study of the conversion of benzylamine in the title reaction, establishing the role of the copper species and ceria support on the reaction. The heterogeneity, recyclability, and the relation between copper leaching from the support and catalyst activity were also studied and investigated.

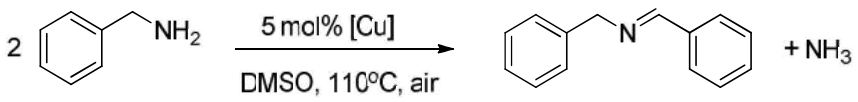

Scheme 4.1 Oxidative coupling of benzylamine to N-benzylidenebenzylamine

4.2 Experimental Details

4.2.1 Catalyst Preparation

A commercial mesoporous CeO_2 (Rhodia, S_{BET} = 211 m^2/g, average pore diameter = 3.2 nm, V_{pore} = 0.130 cm^3/g, 4-5 μm particle diameter) was used as received. The $CuO\text{-}CeO_2$ catalyst was prepared by wetness impregnation. First, 5 g of CeO_2 was added to 0.75 mL of 2.57 g/mL aqueous solution of $Cu(NO_3)_2.3H_2O$ (Sigma-Aldrich, purity>99%) as a precursor, to yield a 9 wt % ceria-supported copper catalyst. The catalyst was then heated

at ramp of 3 °C/min in an air flow to 120 °C and dried for 3 h. Then it was further heated to 500 °C at ramp of 3 °C/min, and calcined in flowing air at 500 °C for another 3 h. Elemental analysis established the copper content in this CuO-CeO_2 catalyst as 9.2 wt %, and thus it is referred to as CeCu(II)09. Two additional catalysts with lower copper oxide loadings were prepared similarly, using the appropriate $Cu(NO_3)_2.3H_2O$ concentration to yield 1 wt % copper, CeCu(II)01, and 5 wt % copper, CeCu(II)05, catalysts.

Commercial CuO nanoparticles (Sigma-Aldrich, S_{BET} = 12 m^2/g) were used as received for comparison purposes.

4.2.2 Characterization

Powder X-ray diffraction (PXRD) was carried out with a PAnalytical X'Pert PRO diffractometer operating with Cu Kα radiation and an X'celerator RTMS detector. A step size of 0.002° 2θ and a scan rate of 10 s per step were used. Nitrogen adsorption isotherms were recorded at 77 K using a Micromeritics TriStar II 3020. BET (Brunauer-Emmett-Teller) surface areas were calculated using adsorption data. Average pore diameters were determined by BDB-FHH method (a simplified Broekhoff–de Boer method with a Frenkell–Halsey–Hill isotherm).[79] Elemental analysis by ICP-AES was carried out by Columbia Analytics (Tucson, AZ). Scanning Electron Microscopy (SEM) images and electron-dispersive X-ray (EDX) analysis were obtained on a JEOL LEO-1530 at a landing energy of 15 kV using the 'In Lens' mode detector. Hydrogen-temperature programmed reduction (H_2-TPR) was measured using approximately 150 mg of fresh catalysts in a Micromeritics AutoChem II 2920. The samples were placed in a U-

shaped tube and first oxidized in 10% O_2-He flow of 60 mL/min while heating from room temperature to 600 °C at 10 °C/min, then passivated under helium and returned to room temperature. The TPR spectrum was then recorded by heating the samples from room temperature to 400 °C at 10 °C/min, under 60 mL/min flow of 10% H_2-Ar mixture.

4.2.3 Catalytic Conversion of Benzylamine to N-Benzylidenebenzylamine

The catalyst, generically coded as CeCu(X)YY (0.05 eq. Cu relative to the amine), was added to a 25-mL two-neck round bottom flask containing 3 mmol benzylamine (327 μL), 3 mL DMSO, and 1.5 mmol diphenyl ether (0.5 eq., 238 μL) as an internal standard. The round bottom flask was attached to a condenser, and immersed in a preheated oil bath, at 110 °C, in an air atmosphere, to start the reaction. Samples of the reaction mixture were taken by a needle and a syringe through rubber septum at specified times, filtered over silica gel column and diluted with ethyl acetate, and the product yield was determined by GC-FID. The identity of the product was verified by GC-MS. The product yield is calculated by dividing the product concentration by the initial concentration of the reactant, benzylamine, after calibrating the GC-FID peak in reference to the internal standard, diphenylether.

4.3 Results and Discussion

4.3.1 Catalyst Characterization

Table 4.1 shows the copper and cerium content of the synthesized catalysts. The results are close to the theoretical values. PXRD patterns for the catalysts are shown in Figure 4.1. Using these patterns and the Scherrer equation, the crystallite sizes of the copper and cerium domains are estimated and listed in Table 4.1. The PXRD patterns of CeCu(II)01 and CeCu(II)05 (not shown) are very similar to that of pure mesoporous CeO_2, with no detectable crystalline CuO peaks (e.g. at $2\theta = 35.5°$ and 38.8°), suggesting high dispersion of CuO on the ceria support.

Table 4.1 Physical properties of the composite CuO-CeO_2 catalysts, CuO nanoparticles, and CeO_2 support

Catalyst	Cu (wt %)	Cu/Ce (mol/mol)	S_{BET} (m^2/g)	Average pore diameter(s)[1] (nm)	Cumulative pore volume[1] (cm^3/g)	[Cu] Crystallite size[2] (nm)	[Ce] Crystallite size[2] (nm)
CeO_2	-	-	211	2.6, 4.5	0.130	-	5.0
calcined[4]-CeO_2	-	-	153	4.0	0.161	-	6.0
CuO	-	-	12	-	-	19	-
CeCu(II)01	1.1	0.031	127	3.6, 5.0	0.141	-	6.5
CeCu(II)05	5.3	0.153	105	3.4, 5.3	0.114	-	6.7
CeCu(II)09	9.2	0.269	105	3.7, 7.3	0.120	28	6.1

[1] Calculated from nitrogen-adsorption isotherms at 77 K, using t-plot for micropore area, and BDB-FHH method for average pore diameter and cumulative pore volume

[2] Estimated using the Scherrer equation, from X-ray line-broadening at $2\theta = 35.5°$ for CuO and at $2\theta = 28.5°$ for CeO_2

[4] After calcination at 500 °C

Crystalline CuO peaks are clearly detected in the CeCu(II)09 material, and the crystallite size of the largest particles was estimated using the Scherrer equation to be 28 nm, as shown in Table 4.1. Knowing that the mesoporous CeO_2 average pore diameter was around 4 nm, based on the nitrogen physisorption isotherms (see below), and that the support particle size is 4-5 μm, Figure 4.2, it appears that the large, crystalline CuO domains were on the outer surface of CeO_2 crystallites, but may be also be contained within the CeO_2 particles. In addition, there were some unsupported CuO particles, which were estimated by H_2-TPR (below) to represent 35% of the total CuO present in the sample.

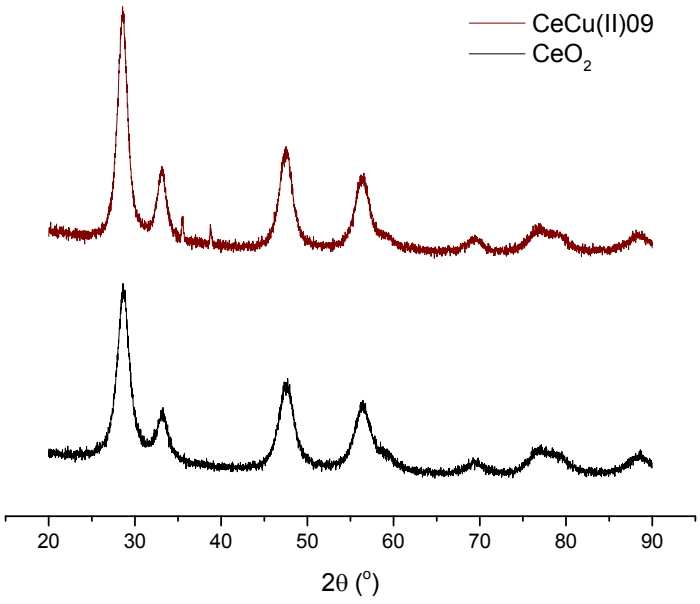

Figure 4.1 Powder XRD patterns for bare CeO_2 and CeCu(II)09 catalyst

The porosity of the CeO_2 was characterized using nitrogen physisorption at 77 K. The material had a relatively high BET surface area, 211 m^2/g, which decreased to 153 m^2/g upon calcination at 500 °C. The average pore diameter and the cumulative pore volume of the as received mesoporous CeO_2 were 3.2 nm and 0.13 cm^3/g respectively, and they changed to 4.0 nm and 0.16 cm^3/g upon calcination. The crystallite size of CeO_2 also increased from 5.0 nm to 6.0 nm after calcination. Figure 4.3 shows the pore size distribution of the ceria support and the synthesized catalysts. It can be noted that upon calcination of the CeO_2, the pore size distribution changed from bimodal with 2.6 and 4.5 nm average pore diameters to a mono-modal distribution with 4.0 nm average pore diameter. The pore diameter of 3.8 nm was unchanged upon incorporation of copper onto the solid.

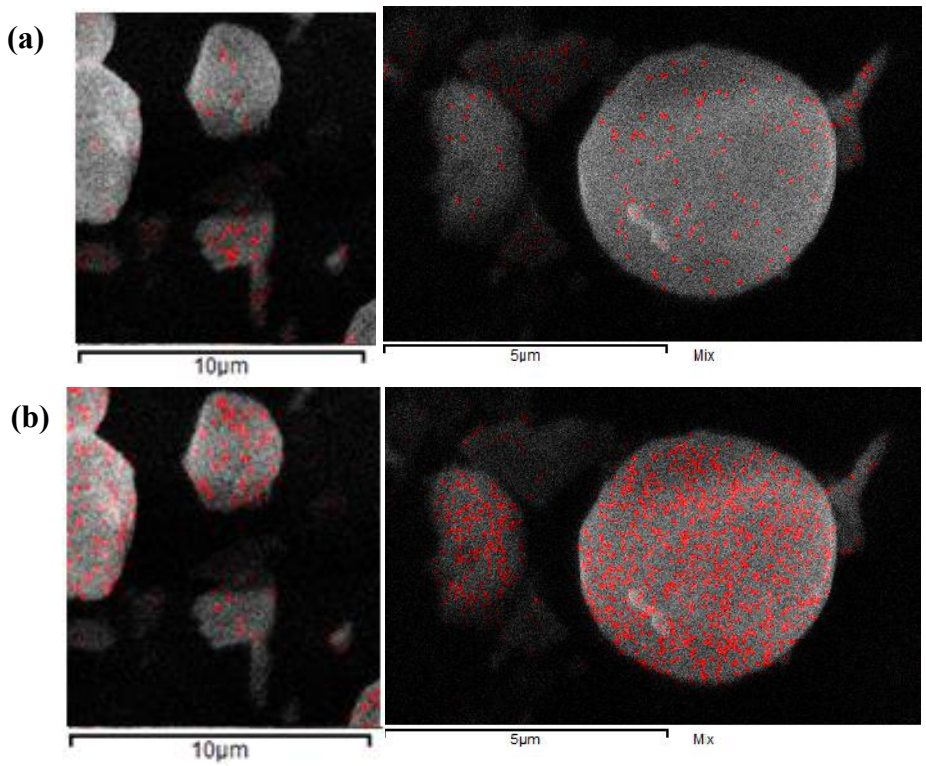

Figure 4.2 SEM images with (a) Cu mapping, and (b) Ce mapping of CeCu(II)09 catalyst

Supporting CuO on CeO_2 and progressively increasing the CuO loading reduced the BET surface area and changed the pore size distribution from mono-modal to bimodal. This may suggest that copper oxide interacts with CeO_2 particles in such a way as to create the new, larger pores seen in the pore size distribution curves in the range from 5 to 8 nm, Figure 4.3. Nonetheless, these pore size changes are subtle and significant changes in porosity upon copper addition are not evident.

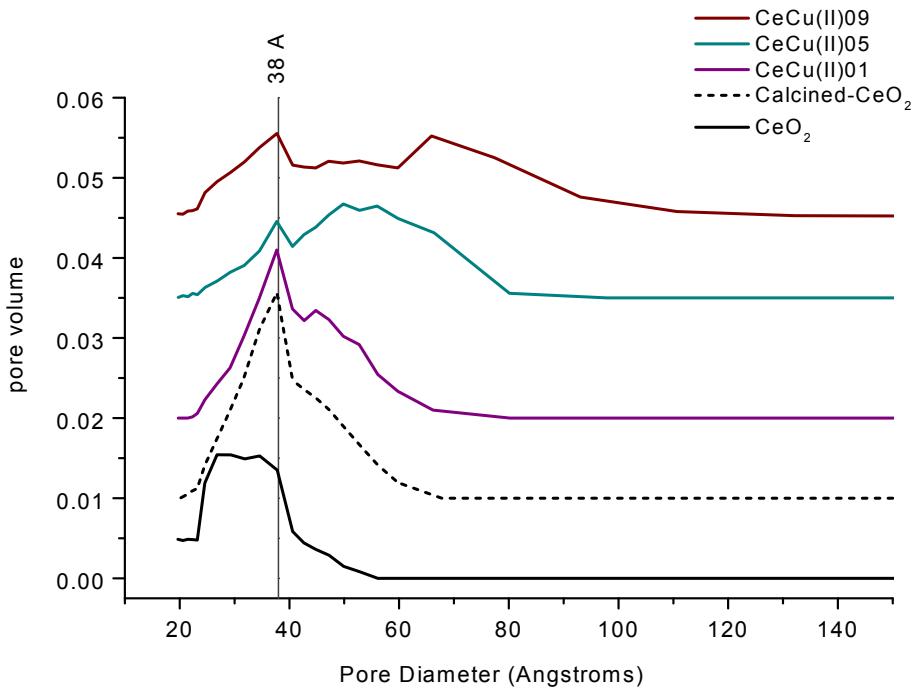

Figure 4.3 Pore size distribution of CeO_2 support and the synthesized CuO/CeO_2 catalysts calculated by the BDB-FHH method from nitrogen physisorption data at 77 K

Table 4.2 and Figure 4.4 show and summarize H_2-TPR patterns for the three supported CuO-CeO_2 catalysts, specifically CeCu(II)01, CeCu(II)05, CeCu(II)09, and for unsupported CuO nanoparticles, as a reference. It is known that CeO_2 has two reduction peaks at about 430 °C and 900 °C, which are ascribed to the reduction of surface and bulk oxygen of CeO_2, respectively.[123] Although bulk CuO has been shown to reduce at 300-400 °C,[124–126], the H_2-TPR pattern of unsupported CuO nanoparticles shown in Figure 4.4 starts reduction at a much lower temperature, 100 °C, and has one main peak at 229 °C, with a leading shoulder at 185 °C. This lower reduction temperature may be associated with the nanoparticle nature of the CuO sample, as it has been shown that

when the particle size of CuO was decreased, the materials is more easily reduced.[127] Also, it has been shown in the literature that the shape and position of the H_2-TPR peaks of CuO-CeO_2 system depend on the copper content, the type of copper species, the interaction between CuO and CeO_2, and on the surface area of the support.[124–126,128,129] The CeCu(II)01 material contained minimal reducible material, as expected from the low CuO loading, and showed a broad peak centered at 159 °C and another weaker broad peak at 288 °C. The total H_2 consumption was 640 μmol/g. Theoretically, for a 1 wt% Cu sample, 167 μmol H_2/g was required to completely reduce all the CuO to metallic copper. The difference, 473 μmol H_2/g, was expected to be associated with reduction of the ceria support. Since the CuO in CeCu(II)01 was highly dispersed, as indicated by PXRD, the H_2-TPR reduction peak at 159 °C can be related to highly dispersed CuO particles and/or Cu^{2+} isolated species, while the high temperature peaks, 217 °C and 288 °C may be associated with the reduction of surface ceria.[124–126]

The reduction profile for the CeCu(II)05 material included a sharp peak at 86 °C with a shoulder at 95 °C, and another smaller peak at 129 °C, with a total H_2 consumption of 1340 μmol H_2/g. As suggested by Ayastuy,[125] the former peak may be related to reduction of highly dispersed CuO domains that are not strongly interacting with the CeO_2 support, whereas the latter peak was likely associated with the simultaneous reduction of ceria and the CuO species that were directly interacting with CeO_2 support, as in the case of CeCu(II)01. Comparing the theoretical amount of H_2 required for complete reduction of CuO in CeCu(II)05, 836 μmol/g, with actual amount, about 500 μmol H_2/g were consumed to reduce the CeO_2 support. This value was

approximately similar to the amount assigned to ceria reduction in the CeCu(II)01 sample.

The total H_2 consumption during TPR of the CeCu(II)09 material was 1890 μmol H_2/g, and the reduction profile was similar to CeCu(II)05 sample, with a sharp peak at lower temperature, 76 °C, and a broader one at higher temperature, 128 °C. There was also an additional peak at 140 °C. Theoretically, 1454 μmol H_2/g was needed for complete CuO reduction of the copper in CeCu(II)09 and thus about 440 μmol H_2/g was associated with reduction of the ceria support. Comparing CeCu(II)05, CeCu(II)09, and as suggested by Ayastuy,[125] it was hypothesized that the peak at 76 °C was related to reduction of highly dispersed CuO species not in strong contact with CeO_2, and the peaks at 128 °C might be related to simultaneous reduction of ceria and CuO species in direct contact with CeO_2. The peak at 140 °C is suggested to be associated with reduction of larger domains of crystalline/bulk CuO species. In all 3 cases, only 16-18% of the total CeO_2 was reduced. The collected TPR data coupled with PXRD data demonstrate that the CuO domains in the three supported samples are clearly different, being highly dispersed and non-crystalline in the low loading sample, and with the highest loading sample having some larger, crystalline CuO domains, some of which may be unsupported.

Table 4.2 **H_2-TPR analysis results of for three supported CuO catalysts, CeCu(II)01, CeCu(II)05, CeCu(II)09, and CuO nanoparticles**

CeCu(II)01		CeCu(II)05		CeCu(II)09		CuO nanoparticles	
T (^oC)	H_2 consumption (µmol/g)	T (^oC)	H_2 consumption (µmol/g)	T (^oC)	H_2 consumption (µmol/g)	T (^oC)	H_2 consumption (µmol/g)
159	190	86	490	76	650	185	2723
217	240	95	360	105	240	229	7170
288	210	110	300	128	540		
		129	190	140	460		
Total	640	**Total**	1340	**Total**	1890	**Total**	9893
Theoretical	167	**Theoretical**	836	**Theoretical**	1454	**Theoretical**	12572
Reduction of CeO_2	473 (74% of H_2)	**Reduction of CeO_2**	504 (38% of H_2)	**Reduction of CeO_2**	436 (23% of H_2)		

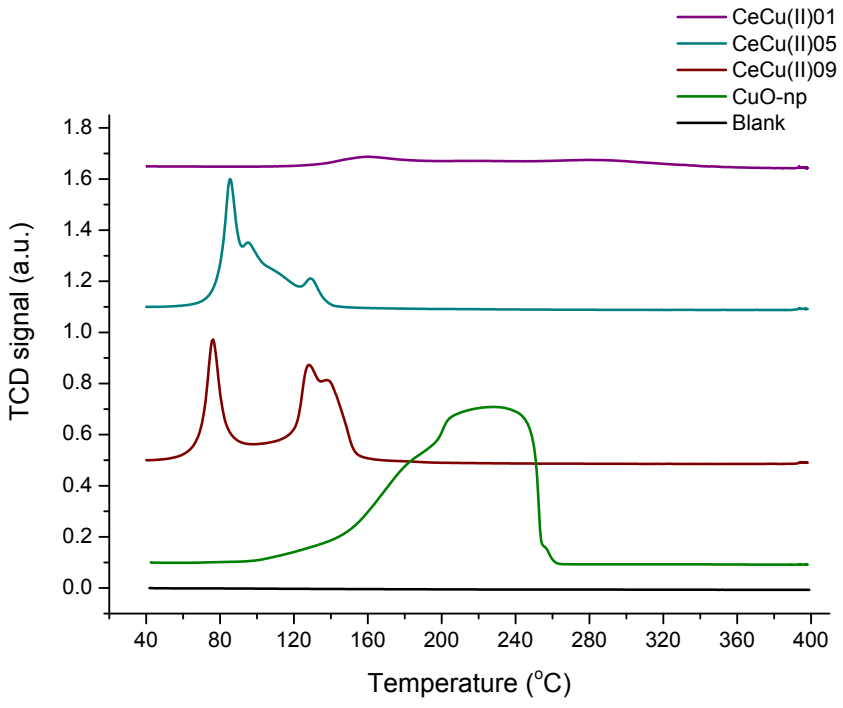

Figure 4.4 **H_2-TPR profiles of catalysts CeCu(II)01, CeCu(II)05, CeCu(II)09, and CuO nanoparticles**

4.3.2 Catalytic Reactivity

The oxidative coupling of benzylamine to form N-benzylidenebenzylamine in DMSO, Scheme 4.1, was evaluated over the series of copper oxide–ceria catalysts along with CeO_2 and CuO as controls. As this catalytic conversion was discovered serendipitously while using dimethylsulfoxide (DMSO) as the solvent for C-N coupling reaction, we continued to work with DMSO as the main solvent. Other solvents, such as toluene, were tried, but these solvents were found to be far less effective. The initial rate with toluene was one third the initial rate with DMSO. Also, after 24 h, the product yield with toluene was one third that using DMSO.

Figure 4.5 shows the kinetic behavior of the benzylamine oxidative coupling reaction using CeCu(II)09 as the catalyst. After an induction period of 8 h, with an initial benzylamine conversion rate of 0.36 mmol/(g cat.h) (3.85 mmol/(g Cu.h) or 3.39 μmol/(m^2 cat.hr)), the rate increased to 2.41 mmol/(g cat.h) (26.1 mmol/(g Cu.h) or 22.9 μmol/(m^2 cat.h)), and 85% product yield was obtained after 22 h. The product yield decreased after this point due to the decomposition of the product, N-benzylidenebenzylamine, to benzaldehyde, as verified by GC-MS analysis. The formation of benzaldehyde at extended reaction times was promoted by the presence of H_2O produced from the dehydrogenation of benzylamine to benzylimine, Scheme 4.2. This was verified by running a reaction under the same conditions, starting with N-benzylidenebenzylamine and 1 equivalent H_2O. It was found that N-benzylidenebenzylamine decomposed linearly at a rate of 0.055 mmol/(g cat.h) (0.60 mmol/(g Cu.h) or 0.524 μmol/(m^2.h)), with benzaldehyde being formed at a rate of 0.105

mmol/(g cat.h) (1.14 mmol/(g Cu.h) or (1.0 μmol/(m^2.h)), which was stoichiometrically correct.

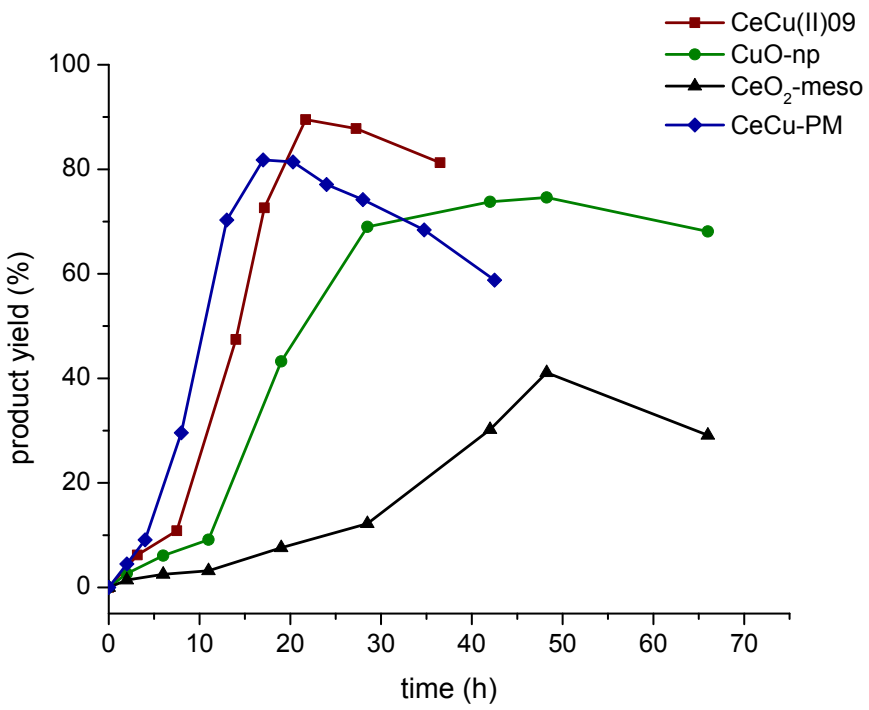

Figure 4.5 **Kinetic profiles for the oxidative coupling of benzylamine using the bare ceria support (CeO_2-meso), unsupported CuO nanoparticles (CuO-np), a physical mixture of CuO nanoparticles and ceria (CeCu-PM), and the CeCu(II)09 material, as catalysts. Conditions: benzylamine (3 mmol), catalyst (5 mol% Cu), DMSO (3 ml), 110 °C, air.**

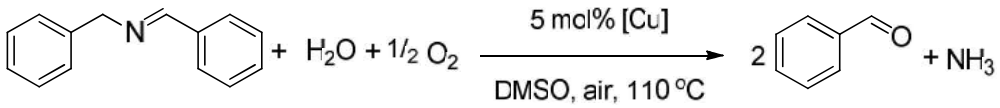

Scheme 4.2 **N-Benzylidenebenzylamine decomposition to benzaldehyde**

Given the complex shape of the kinetic profile for the CeCu(II)09 catalyst, the ceria support, unsupported CuO nanoparticles and a physical mixture of the two oxides were evaluated in an attempt to gain further insight into the reactivity. Figure 4.5 shows that the CeO_2 alone had moderate activity for the amine oxidation. A maximum yield of 41% was reached after 48 h. The shape of the kinetic profile was similar to that of the CeCu(II)09 catalyst, but as noted in Table 4.3, the rates in each stage were lower, and the induction period was somewhat prolonged. When using unsupported CuO nanoparticles as the catalyst (referred to as CuO), an induction period of 11 h was observed, after which a maximum product yield of 75% was reached after 48 h. Interestingly, when a physical mixture of CuO and CeO_2 (referred to as CeCu-PM) was used as a catalyst, the initial rate was significantly higher than those of the individual oxides, with a significantly reduced induction period. After the first hour, the rate of reaction was almost the same as that of CeCu(II)09, after its induction period, as well as that of ceria-free CuO in its first 8 h, after its induction period. A maximum product yield of 84% was reached in 17 h. The initial and maximum observed rates in each case are given in Table 4.3. It is also important to note that the formation of benzaldehyde at extended reaction times was mostly promoted by CeO_2, as the rate of product decomposition in the case of CuO was much less than the rates in the other 3 experiments that have CeO_2 in the catalytic system.

Table 4.3 Rates of reaction over the various catalysts*

Catalyst	CeCu(II)09	CeO_2	CuO	CeCu-PM
Initial amine conversion rate (in first 2 hours)				
mmol/(g cat.h)	0.36	0.29	2.97	0.64
mmol/(g Cu.h)	3.85	N/A	3.71	7.08
μmol/(m^2.h)	3.39	1.38	247.2	N/A
mmol/(g Ce.h)	0.50	0.36	N/A	0.86
Highest observed amine conversion rate,				
mmol/(g cat.h)	2.41	0.58	10.7	2.37
mmol/(g Cu.h)	26.1	N/A	13.3	26.4
μmol/(m^2.h)	22.9	2.74	888.4	N/A
mmol/(g Ce.h)	3.35	0.72	N/A	3.20

* Copper loading in case of CeCu(II)09, CuO, and CeCu-PM is 0.05 mole per mole of reactant. Cerium loading in case of CeO_2, CeCu(II)09, and CeCu-PM is 0.18 mole per mole reactant.

The shape of the kinetic profiles may be used to gain insights into the roles of CuO and CeO_2 phases in the oxidative coupling reaction. CuO catalyst had a longer induction period than CeCu(II)09 catalyst, and the physical mixture of oxides (CeCu-PM) had a severely reduced induction period. Furthermore, the initial rate of the CeCu-PM catalyst was approximately the sum of the initial rates of individual oxide catalysts, CuO and CeO_2. The first step of this reaction is believed to be the dehydrogenation of benzylamine to benzylimine (Scheme 4.3),[106] and in this regard, it has been reported by Tamura[130] that the N-H group of amines adsorbs on CeO_2 via the surface Lewis acid

sites (Ce^{4+}) of CeO_2, and the strongly basic oxygen atom adjacent to the Ce^{4+} cation (Scheme 4.4), and this may play a role in activating the N-H group in benzylamine. However, ceria alone appears inefficient in catalyzing the overall reaction, as observed in Figure 4.5, with it showing the slowest initial and maximum observed rates, Table 4.3. On the other hand, if one compares the copper-containing catalysts CeCu(II)09, CuO, and CeCu-PM, and excludes the induction periods, it is apparent that all these catalysts have a similar rate of reaction. This observation suggests that CuO species are the main catalysts for the overall process, ultimately producing the final product, N-benzylidenebenzylamine. The CeO_2, when present, may play a role of providing additional sites to promote the first step of the reaction. This will be discussed in more detail below.

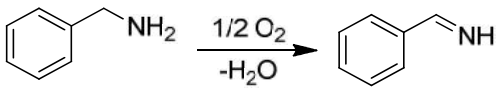

Scheme 4.3 Oxidative dehydrogenation of benzylamine to benzylimine

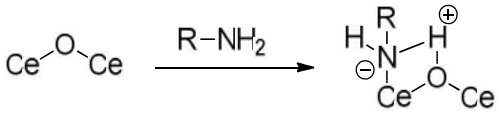

Scheme 4.4 N-H group activation by CeO_2 [130]

The stability of the CeCu(II)09 catalyst was evaluated. After completing the reaction, the catalyst was recovered by centrifugation, washed with de-ionized water, and re-calcined at 500 °C. Elemental analyses of fresh and used catalysts show that the fresh catalyst had 9.2 wt % copper, with Cu/Ce molar ratio of 0.269, and that the re-calcined, used catalyst had 8.6 wt% copper, with a 0.240 Cu/Ce molar ratio. Accordingly, 11% of copper was lost from the CeCu(II)09 catalyst after the first cycle.

Knowing that there was 11% copper leaching from the support in the first cycle, it became necessary to test the effect of that leached copper on the reactivity of the system. Running the same reaction under the same conditions (Scheme 4.1), in a second experiment, the catalyst was filtered off (hot filtration) when the product yield reached 30%. The solid-free reaction solution was allowed to continue to react and the product yield was monitored. The reaction continued to proceed with a similar rate as before the filtration, suggesting that the leached copper species were largely responsible for the catalytic conversion when the reaction rate was highest, at moderate conversions. This supports the hypothesis that copper species were the main catalyst for the formation of the final product and suggests another cause, beyond generation of the initial imine intermediate, may contribute to the observed induction period, copper leaching.

To further clarify the role of ceria vs. copper in this reaction, and to test whether the induction period was related to copper leaching, an additional experiment was conducted. The reaction, shown in Scheme 4.1, was started with only CeO_2 as catalyst, and after 20 h, CuO was added to the reaction. As shown in Figure 4.6, with CeO_2 alone, the rate of product formation was low, and once the CuO catalyst was added, the rate increased significantly, from 0.15 to 2.4 mmol/(g cat.h). This experiment further demonstrates that

CuO species most efficiently promote the overall reaction, and that the presence of CeO_2 primarily helps in shortening the induction period associated with the first step compared to using CuO alone.

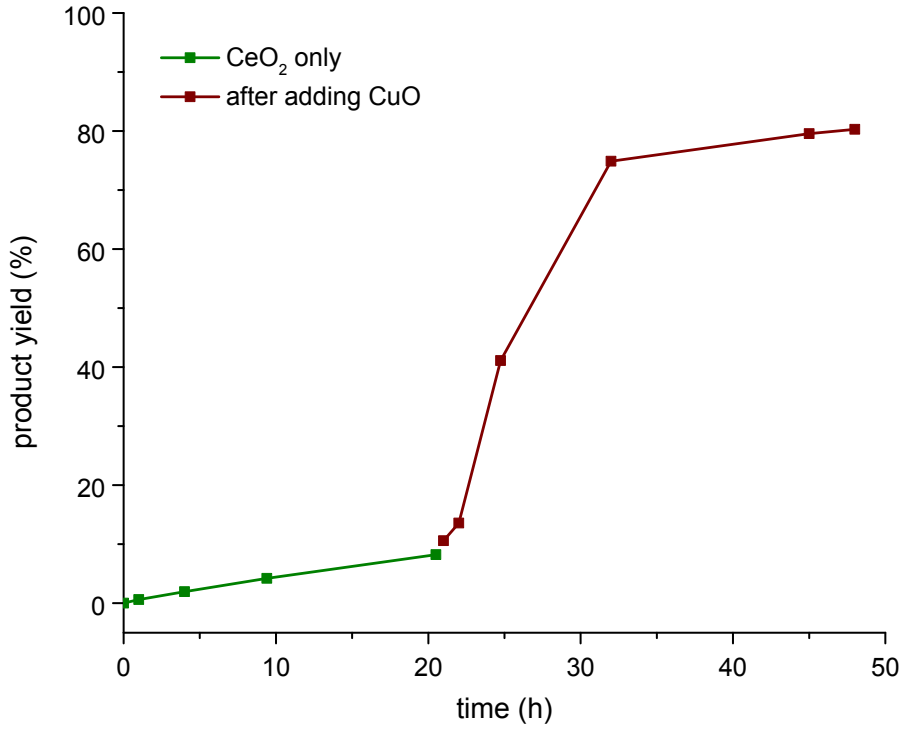

Figure 4.6 **Kinetic profiles for the oxidative coupling of benzylamine using the bare ceria support, followed by addition of unsupported CuO nanoparticles after 20 h. Reaction carried at 110°C under aerobic atmosphere.**

To further resolve this issue, the same reaction starting with CeO_2 alone was run in parallel in three separate flasks for 5.5 h, after which solid CuO nanoparticles were added to two flasks (0.25 mol% and 1.25 mol%), and pre-dissolved, soluble CuO species (also

at 0.25 mol%), were added to the third flask.[1] The initial kinetic profiles for these experiments are shown in Figure 4.7. As shown in the figure, adding 1.25 mol% solid CuO nanoparticles increased the rate 5 fold compared to addition of 0.25 mol% solid CuO nanoparticles. On the other hand, when adding "soluble" and "solid" CuO nanoparticles at the same loading (0.25 mol%), there was almost no difference in the rate. Because pre-dissolved and solid CuO nanoparticles gave similar rates, one may view that these experiments support the hypothesis that the induction period might not be due to the time needed to solvate copper species, but instead may be due to the time needed to build sufficient amount of the intermediate, benzylimine, which is effectively promoted by both CeO_2 and copper species.

[1] Soluble CuO species were produced by stirring CuO nanoparticles at reaction temperature in DMSO for 15 h, then quickly centrifuging the mixture, and pipetting off the supernatant containing dissolved copper species while the solution was still warm. The residual CuO nanoparticles were dried and weighed, and this weight was used to estimate the amount of dissolved CuO species for comparison with solid addition.

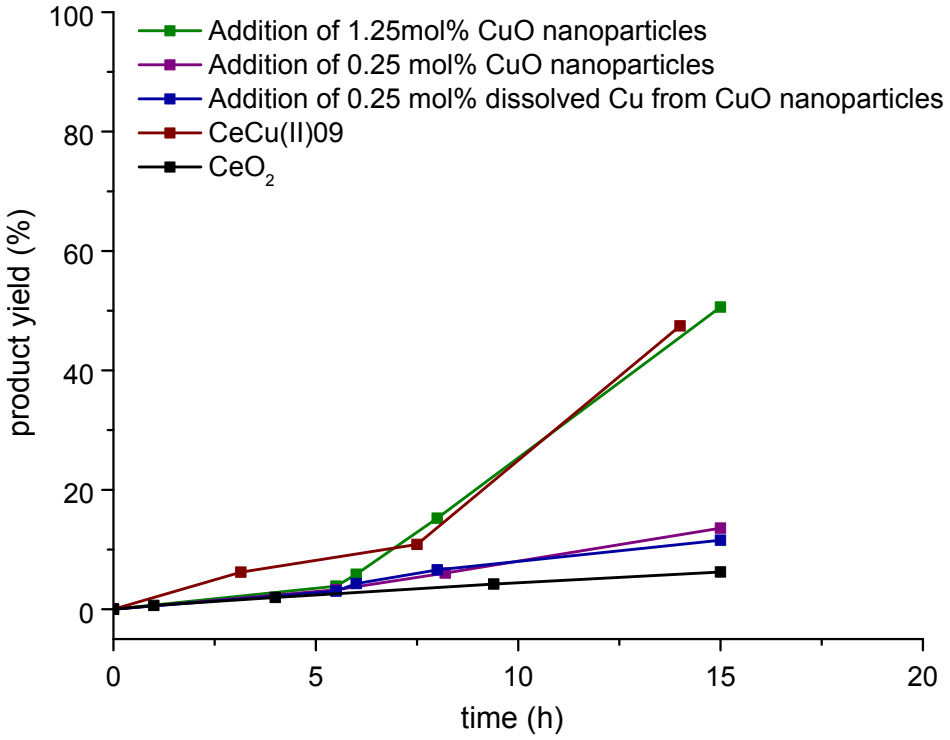

Figure 4.7 **Kinetic profiles for the oxidative coupling of benzylamine using the bare ceria support, followed by addition of "solid" and "soluble" copper species derived from CuO nanoparticles after 5.5 h. Reaction carried at 110 °C under aerobic atmosphere.**

Nonetheless, additional tests were done to evaluate the relation between copper leaching and the production rate of the final coupled product, the dissolved copper concentration was measured in another experiment (similar to that in Figure 4.5 using CeCu(II)09) as a function of time and related to product yield, as shown in Figure 4.8. It is apparent that the rate increases in proportion to the amount of copper dissolved in the reaction mixture. In this experiment, samples were withdrawn at specified times, and solid catalyst was removed by centrifugation, and the clear solution was sent for elemental analysis. As the copper concentration increased from 9 ppm to 95 ppm, the product yield increased

accordingly from 8% to 85%. In contrast to the above paragraph, these experiments support the idea that CuO species dissolved in the reaction mixture are primarily responsible for the overall reaction, and contribute to the observed induction period.

Figure 4.9 shows the kinetic profiles of supported catalysts with different copper loadings, CeCu(II)01, CeCu(II)05, and CeCu(II)09. It is clear that the induction period increased with increasing copper loading on the support, from approximately 0 h to 5 h to 8 h, while the maximum product yield increased with increasing copper loading, from 49% to 70% to 85% (note: reactions were conducted with fixed copper loading in the reactor, and therefore with varied ceria content). This supports the hypothesis that a key role of CeO_2 may be reducing the induction period by catalyzing the first step of the reaction, as more CeO_2 is available in the case of CeCu(II)01 than in CeCu(II)05 and CeCu(II)09. An alternate explanation is that highly dispersed copper domains more slowly leach into solution, if one argues that copper dissolution is the main cause of the induction period. The reduction of product yield may be related to the amount of ceria in the reactor, since the ceria promotes product decomposition to benzaldehyde, as mentioned earlier.

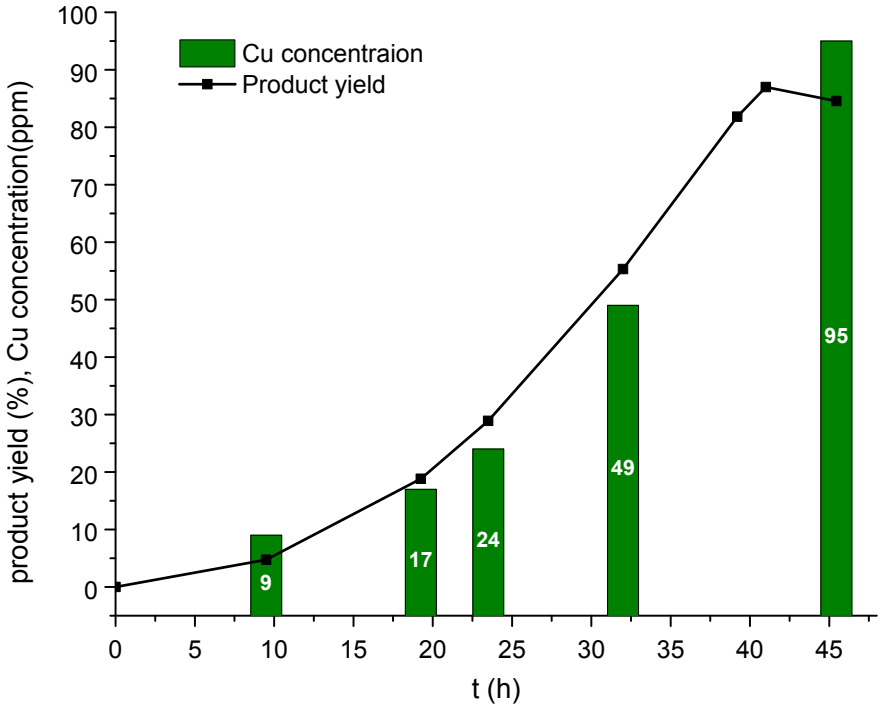

Figure 4.8 **Kinetic profiles for the oxidative coupling of benzylamine using CeCu(II)09 catalysts and the effect of Cu concentration in the solution on the product yield. Conditions: benzylamine (3 mmol), catalyst (5 mol% Cu), DMSO (3 ml), 110 °C, air.**

To further understand the reduction of the induction period in the CeCu(II)01 experiment, the amount of CeO_2 in CeCu(II)01 was calculated, found to be 172 mol% based on reactant, and this amount of CeO_2 was used in a new experiment. In this experiment, shown in Figure 4.10, the initial rate was almost four times the one with CeCu(II)01, and the product decomposition rate was about 3 times the rate observed CeCu(II)01. Keeping in mind that in the case of the CeO_2 experiment, though the CeO_2 loading was similar to the CeCu(II)01 catalyst, many more CeO_2 sites were available in this case, as the highly dispersed CuO species block access to CeO_2 sites. The observations support the

hypotheses that CeO_2 promotes the decomposition of N-benzylidenebenzylamine to benzaldehyde, and that the induction period can be reduced or eliminated (see Figure 4.10) by adding CeO_2 to the reactor. This suggests that the initial slow step in the process, generating the imine intermediate, can be accelerated with CeO_2 domains, as shown in Scheme 4.3.

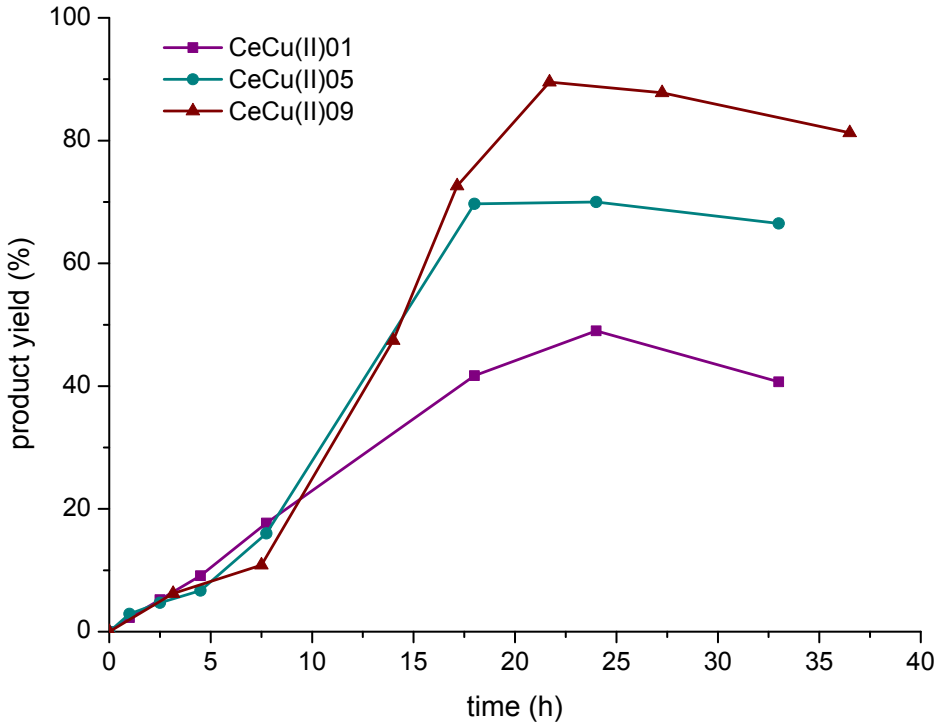

Figure 4.9 **Kinetic profiles for the oxidative coupling of benzylamine using ceria-supported catalysts with different Cu(II) loadings: CeCu(II)01, CeCu(II)05 and CeCu(II)09. Conditions: benzylamine (3 mmol), catalyst (5 mol% Cu), DMSO (3 ml), 110 °C, air.**

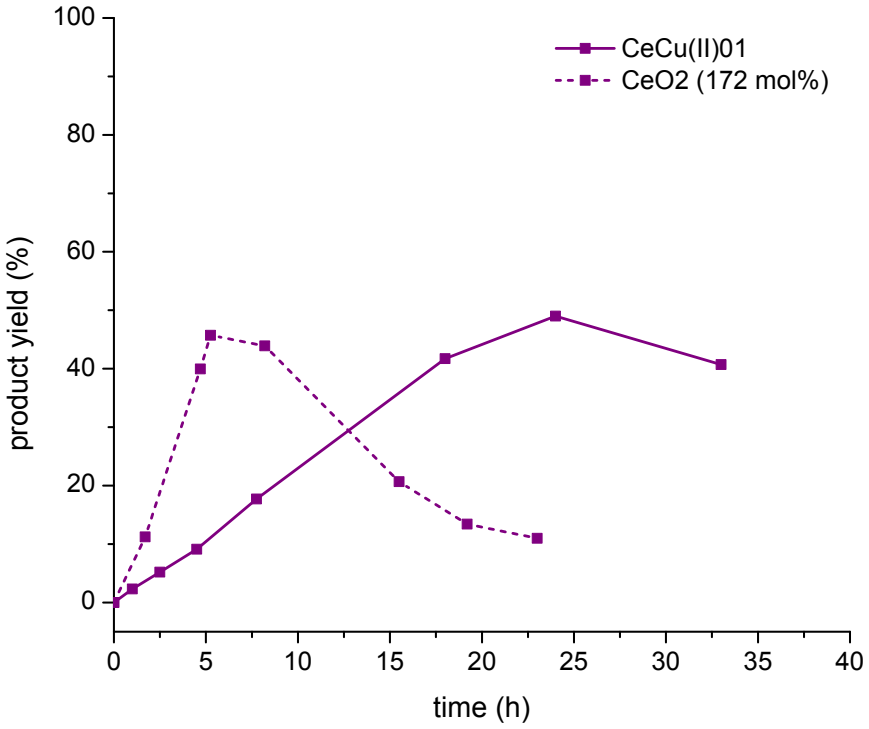

Figure 4.10 Comparison between mesoporous CeO_2 (172 mol%) and CeCu(II)01 as catalysts, and their effect on the kinetic profiles of the oxidative coupling of benzylamine. Reaction carried at 110 °C under aerobic atmosphere.

The collected data above argue for both copper and ceria species playing a role in the catalysis. The induction period is caused by multiple factors, an important one is copper dissolution, and a second one is the presence or absence of CeO_2, with CeO_2 shortening the induction period. Dissolved copper species appear to be the most effective catalysts for this reaction, and these species do not contribute appreciably to product decomposition, whereas CeO_2 domains lead to significant product decomposition and reduction in overall yield.

Scheme 4.5 depicts two hypothetical reaction pathways for the target aerobic oxidative benzylamine homocoupling reaction.[106,131] As noted above in Table 4.3, CuO catalyst gave a much higher initial reaction rate (per gram catalyst) compared to CeO_2, however, addition of ceria to the CuO catalyst substantially shortened the induction period, as shown in Figure 4.6. Since the first step of the coupling reaction, the dehydrogenation of amine to imine, produces water, and since CeO_2 has the ability to adsorb water, it was hypothesized that CeO_2 reduced the induction period not only by potentially activating the N-H group (kinetic effect), but also by adsorbing water (thermodynamic effect, shifting an equilibrium), and hence favoring the production of the intermediate benzylimine (Scheme 4.3). To test this hypothesis, CeO_2 was dried at 200 °C under vacuum overnight, and this dried CeO_2 was used in the same reaction. Figure 4.11 compares the rates of this experiment with the experiment that used CeO_2 without drying. The data show dry CeO_2 was more active than the one stored under atmospheric conditions. The productivity of dry CeO_2 was almost double that of wet CeO_2 after twenty-four hours of reaction. These results suggest that CeO_2 may promote this reaction by both activating the amine N-H and adsorbing the water produced from the first step of this oxidative coupling reaction (Scheme 4.3).

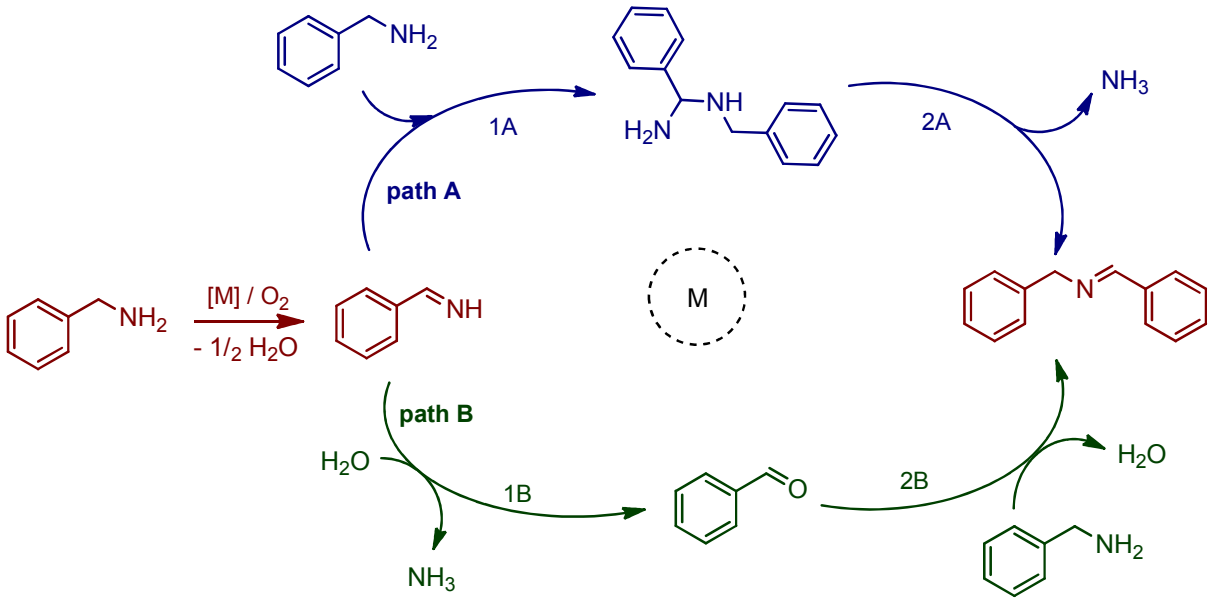

Scheme 4.5 **Proposed reaction pathways for aerobic oxidation of benzylamine to benzylamine**

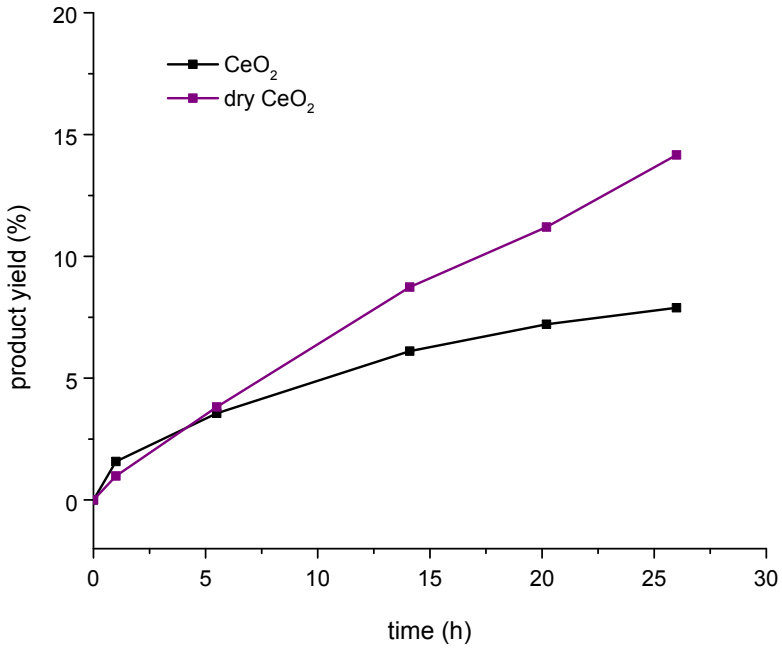

Figure 4.11 **Comparison between bare CeO_2, and dry bare CeO_2 as catalysts, and their effect on the initial rate of amine oxidative coupling reaction.**

The reusability of the CeCu(II)09 catalyst in a subsequent catalytic reaction was evaluated . As mentioned earlier, after completing the reaction, the catalyst was recovered by centrifugation, washed with de-ionized water, and re-calcined at 500 °C, before use in a second cycle. Elemental analyses of fresh and used catalysts show that 11% of copper was lost from the CeCu(II)09 catalyst after the first cycle. Before use in a second cycle, this loss was taken into consideration so that 5 mol% Cu was added to the reaction in both cases.

Figure 4.12 shows the kinetic curve of the first cycle, using the fresh catalyst, and the second cycle, with the recovered, calcined catalyst. In the second cycle, the induction period decreased from 8 to 3 h, and the overall product yield was 90% of the first cycle. After the induction periods, the rates of reaction were almost the same in both cases, 1.54±0.1 mmol/(g cat.h). Since the catalyst was re-calcined before recycling, carbon-desposition was excluded as the cause of the loss in yield. The reduction in the induction period may be associated with the presence of less CuO on the CeO_2 surface due to copper leaching, exposing more of the ceria surface, which is hypothesized to enhance the first dehydrogenative step of the reaction (see above). From PXRD (as shown in Figure 4.13) using the Scherrer equation, the crystallite sizes of CuO and CeO_2 in the used catalyst were estimated to be 38 nm and 6.6 nm, respectively. Comparing these values with those of the fresh catalyst, 28 nm and 6.1 nm, it seems that some copper agglomeration occurred after using the fresh catalyst. Given that in the work using different CuO loadings described above, the induction period was longest with the highest CuO loading and largest CuO domain size, the observation that the CuO domains were larger in the recycled catalyst but a shorter induction period was observed suggests

that the nature of the copper species did not have a dominant effect on the induction period. Rather, the induction period was likely shorter in the recycled catalysts due to greater exposed CeO_2 surface area. Also, as mentioned earlier, having more CeO_2 in the system means more decomposition of the final product to benzaldehyde, which may be another cause for the lower product yield.

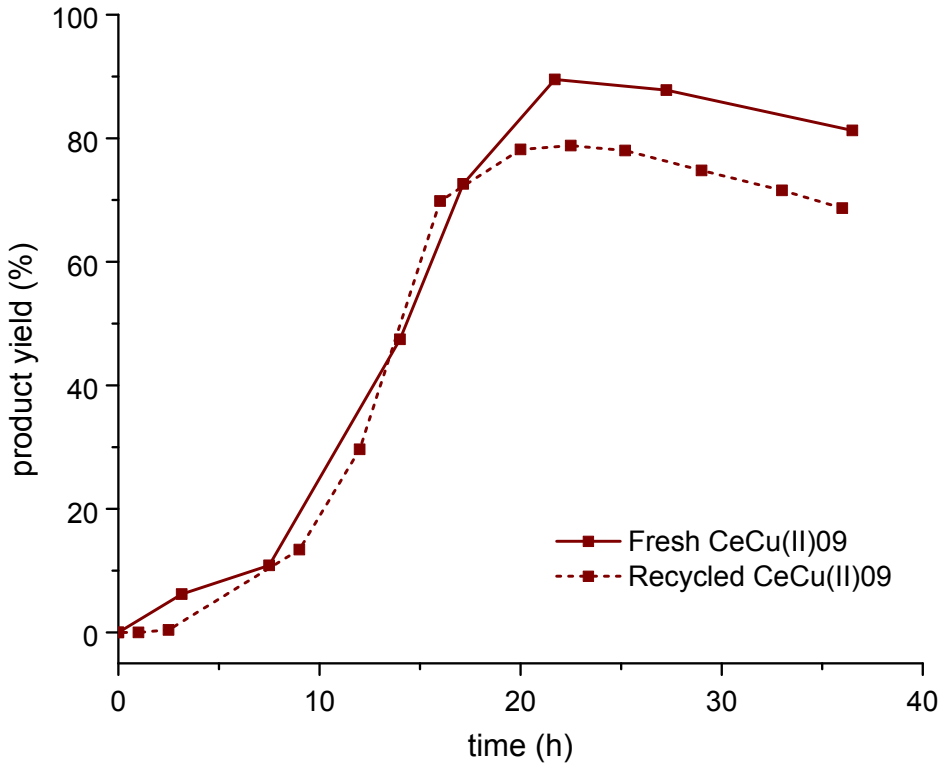

Figure 4.12 Kinetic profiles for the oxidative coupling of benzylamine over two cycles using the CeCu(II)09 catalyst. Conditions: benzylamine (3 mmol), catalyst (5 mol% Cu), DMSO (3 ml), 110 °C, air.

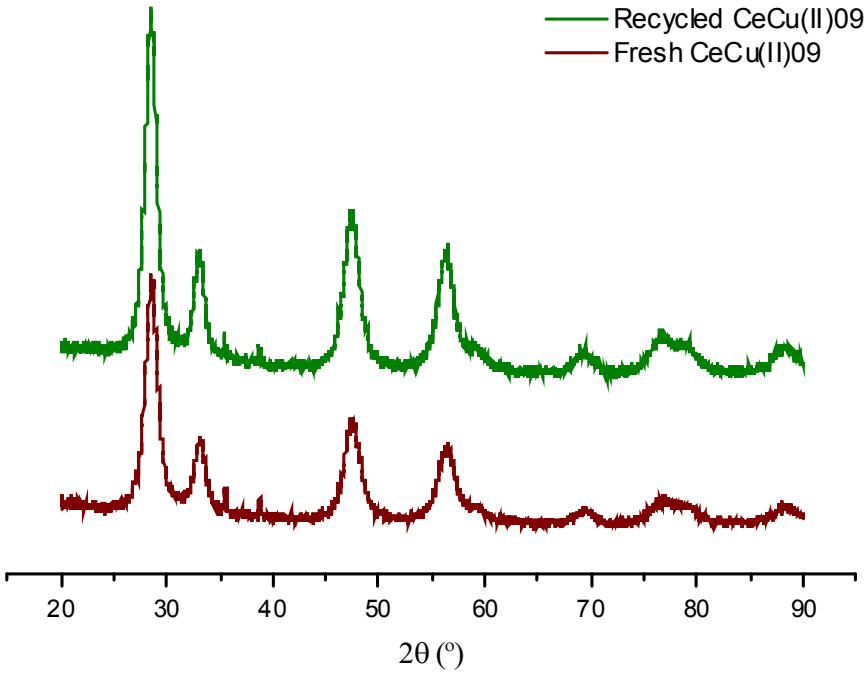

Figure 4.13 Powder XRD patterns of fresh and used CeCu(II)09 catalysts

4.3.3 Proposed Reaction Pathway

In the literature, two mechanisms have been proposed for the oxidation of primary amines to a dimeric imine product[106] as shown in Scheme 4.5. Both mechanisms proceed by way of an initial oxidative dehydrogenation of the amine to the imine intermediate, RCH=NH. For benzylamine, this intermediate is unstable and difficult to detect by routine spectroscopic techniques. In path A, the imine intermediate is then attacked by a second molecule of the primary amine, giving an aminal, which loses NH_3 to give the coupled imine product $RCH=NCH_2R$. In path B, the initially formed imine intermediate reacts with trace amounts of H_2O to give the aldehyde RCH=O and NH_3,

with the aldehyde subsequently reacting with a second molecule of the amine to give the imine product. The last step, 2B, is accomplished in minutes under these reaction conditions; when benzylamine was added to benzaldehyde, with 5 mol% Cu from CeCu(II)09 in DMSO, the N-benzylidenebenzylamine yield was 95% immediately upon immersing the reaction flask in the 110 °C preheated oil bath.

To gain further insight into the reaction pathway, a control experiment was run under the exact same conditions, Scheme 4.1, but without any catalyst. It was found that the initial rate was almost half of that observed in the experiment with CeO_2 alone. Other experiments were run under the same reaction conditions, but with the addition of 0.5 equivalents of water.

Figure 4.14 shows the kinetic profiles of the reactions with and without added water. Adding water to the CeCu(II)09 catalyst and the CuO catalyst significantly increased the induction periods in both cases, decreased the maximum observed rates by 50%, and decreased the maximum yield in the case of CeCu(II)09. On the contrary, adding H_2O to CeO_2 alone increased its initial and maximum observed rates and led to higher maximum yield. These observations might suggest that CuO catalysis primarily follows path A, as added water shifts the formation of imine intermediate to the left and slows the overall reaction rate, while CeO_2 catalysis primarily follows path B, as excess H_2O helps accelerate the hydrolysis of intermediate imine to the aldehyde, step 1B. This may be why CeCu(II)09 is more active than individual CuO and CeO_2, as it combines both pathways.

To further test this hypothesis, several other experiments were run, to study the relative rates of steps 1A and 1B using CuO and CeO_2 as catalysts. In these experiments, N-benzylidenemethylamine was used as a substrate because it is more stable than benzylimine and can be quantified using GC-FID. To study step 1A, benzylamine was added to 1 equivalent N-benzylidenemethylamine, with 5 mol% Cu from CuO in DMSO (Scheme 4.6). This reaction yielded 75% N-benzylidenebenzylamine immediately upon immersing the reaction flask in the 110°C preheated oil bath. This observation strongly supports the hypothesis that copper mediated reactions proceed via path A. Running the same reaction, Scheme 4.6, with CeO_2 formed a minimal amount of desired product. To study step 1B, N-benzylidenemethylamine was added to 1 equivalent of H_2O, with 5 mol% Cu from CuO in DMSO. In this reaction, 12% benzaldehyde was formed in 12 hours. When running the same reaction, 1B, using CeO_2 instead of CuO, 22% benzaldehyde was formed in 12 hours. These data suggest that it is unlikely that CuO-based catalysts proceed via path B with significant rates under the conditions used here. In addition, when running the reaction starting with N-benzylmethylamine, it was noticed the rate of N-benzylidenemethylamine formation using CuO was double the rate observed using CeO_2, supporting the hypothesis mentioned earlier (in Section 4.3.2) that CuO domains may be the main catalysts for the overall process. It is also noteworthy that with CeO_2, more benzonitrile was formed than in the case with the CuO catalyst, which might explain the limited ability of CeO_2 to produce the desired final product, N-benzylidenebenzylamine, as intermediate was siphoned off into side-products.

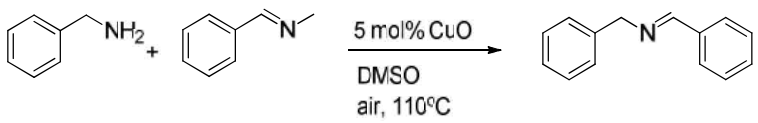

Scheme 4.6 **Studying step 1A of proposed mechanism, adding benzylamine to 1 equivalent N-benzylidenemethylamine**

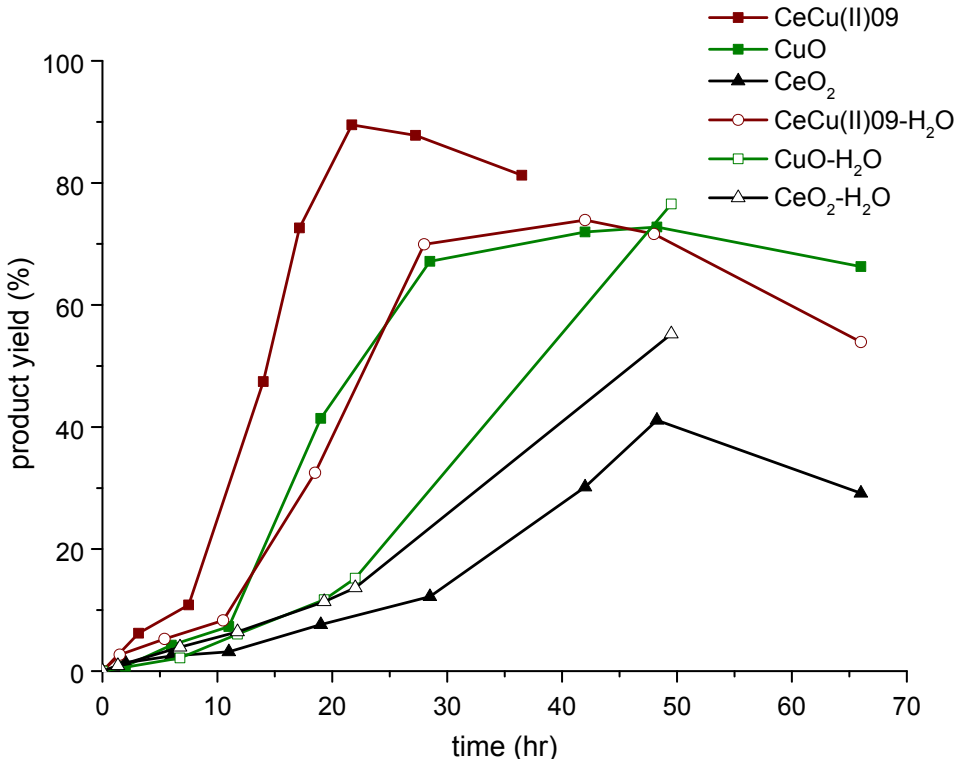

Figure 4.14 **Effect of adding 0.5 equivalents of water on the kinetic profiles of oxidative coupling of benzylamine using CuO, CeO_2, and CeCu(II)09 as catalysts. Reaction carried at 110°C under aerobic atmosphere.**

After running this comprehensive set of experiments, it is proposed that the overall coupling reaction runs according to the following pathway: benzylamine is oxidatively dehydrogenated to the benzylimine intermediate by copper species, and this step is enhanced by the existence of CeO_2, which absorbs water molecules formed by this dehydrogenation, and thus shifts the reaction to the right. CeO_2 may participate, in parallel, in the catalytic dehydrogenation reaction. Once the benzylimine intermediate is formed, copper species catalyze the coupling with a second molecule of benzylamine, causing the fast formation of the final product, N-benzylidenebenzylamine, and the loss of NH_3 (path A). On the other hand, CeO_2 can competitively convert the benzylimine intermediate to benzaldehyde, at a slower rate, and once the benzaldehyde is formed, it spontaneously reacts with a second molecule of the benzylamine to give the final imine product, N-benzylidenebenzylamine (path B). Based on the reaction rates observed, this pathway is less important under the conditions used here.

4.4 Conclusions

Copper oxide supported on ceria (CuO-CeO_2) was shown to be an effective, somewhat stable, and recyclable catalyst for the direct synthesis of imines from amines under aerobic conditions. Copper(II) oxide and ceria alone also promoted the conversion, but not as efficiently as the combined catalyst. Varying the loading of the copper(II) oxide on the ceria support affected the overall product yield, as well as the induction period; catalysts with higher copper loading gave higher yield of N-benzylidenebenzylamine due to the higher rate of product formation over copper oxide domains and the reduced ceria

content in the reactor, as the ceria promoted product decomposition. Leaching studies demonstrated that the majority of the copper catalysis occurred in solution.

A series of experiments demonstrated that ceria and copper domains promote the reaction primarily via two distinct pathways. Both pathways begin with an initial oxidative dehydrogenation of the amine to form an imine. Subsequently, copper(II) oxide domains appeared to primarily promote product formation via path A, involving the coupling of benzylimine with a second molecular of benzylamine, with liberation of ammonia. In contrast, ceria produced the N-benzylidenebenzylamine product more slowly, primarily via path B, involving hydrolysis of the benzylimine to form benzaldehyde, which was quickly coupled with benzylamine to form the N-benzylidenebenzylamine product.

This CuO-CeO_2 catalytic system has the advantages of being both easily separated from the reaction media and more active than unsupported CuO nanoparticles at similar copper loadings, because of the added efficiency of CeO_2 domains. However, the catalyst is not fully recyclable, as the copper catalysis occurs in solution, and thus the catalyst may only be reused to good effect until the copper reservoir is depleted.

CHAPTER 5

AN INVESTIGATION OF THE EFFECT OF SUPPORT, TEMPERATURE, AND SOLVENT ON THE HOMOGENEITY/ HETEROGENEITY OF SOLID COPPER CATALYSIS

5.1 Introduction

Copper oxide nanoparticles[41,47,132] and supported copper[2,28,133–135] catalysts are widely studied and used as heterogeneous catalysts (or perhaps precatalysts, as this work will detail) in a variety of homo- and cross-coupling reactions in organic synthesis. Heterogeneous catalysts are of course of interest because they are easy to separate from the reactants and products, to recover, and potentially to recycle, thus reducing waste. However, in many cases whereby solid palladium [9] and copper precatalysts were used in liquid phase coupling reactions, the nature of the active species remained ambiguous, with some authors asserting heterogeneous catalysis occurs at the solid Cu or Pd surface, while other studies demonstrating that metal species leached into solution could account for some or the entire catalytic turnover. Often claims of heterogeneity are supported with limited definitive data on the nature of the active species, with simple catalyst recyclability tests often used as a way to suggest the catalysts' heterogeneity. [41,47,132] Thus, in most cases, a rigorous assessment of catalyst heterogeneity is not completed.

Having worked extensively on the elucidation of the heterogeneity/homogeneity of supported Pd catalysts in Heck and Suzuki coupling reactions, we became interested in the heterogeneity/homogeneity question as it relates to supported copper oxide catalysts

in liquid phase coupling reactions. This literature is substantially sparser than the related palladium literature, though there is an array of studies of catalyst leaching and heterogeneity in selected coupling reactions. For example, He and Cai[28] showed that their Amberlyst A-21 polymer-supported copper iodide catalyst, used for terminal alkyne homocoupling under solvent-free conditions, was recyclable with insignificant copper leaching from the support. On the other hand, Biffis et al[2] showed that despite the observed high activity for Sonogashira coupling, an alumina supported CuO precatalyst significantly leached copper and the catalyst was not fully recoverable. Oishi et al[133] claimed their TiO_2 supported $Cu(OH)_x$ catalyst to be truly heterogeneous catalyst for the oxidative alkyne-alkyne homocoupling reaction, and supported their conclusions with hot filtration and recyclability tests. They also successfully synthesized supported copper hydroxide catalyst on manganese oxide-based octahedral molecular sieve OMS-2 ($Cu(OH)_x$/OMS-2)[136] and used it as a heterogeneous catalyst for terminal alkyne homocoupling. This catalyst was reused 13 times, with a total TON of 666. In another study, Ma et al[134] showed that copper (I) leached significantly from a N,N,N′,N′-tetraethylenetriamine (TEDETA)-modified SBA-15 silica support when used for the oxidative homocoupling of terminal alkynes without added free base, and that this leaching affected the recyclability of the catalyst. Previously, we studied the oxidative homocoupling of benzylamine using the CuO supported on mesoporous CeO_2 (CuO/CeO_2)[135] and showed that the concentration of leached copper in the solution correlated with the rate of reaction. Thus, the literature contains an array of reports describing the heterogeneity of supported copper precatalysts in liquid phase coupling reactions with varied conclusions with regard to catalyst stability and heterogeneity.

In this study, by performing comprehensive set of tests, we will try to show evidence that copper leaches from almost any support when it is utilized under basic conditions.

In Chapter 2, where C-N coupling of 4-iodoanisole with imidazole was studied using copper exchanged NaY zeolite catalysts; it was shown that the strongly basic reaction conditions destroyed the crystalline structure of the NaY zeolite. Although the shape selectivity tests suggested that the reaction might be occurring inside the zeolite pores, the basic environment prevented the recycling of the catalyst, due to catalyst degradation.

In Chapter 3, where C-N coupling of benzylamine and iodobenzene using CuO supported on mesoporous CeO_2, CuO/CeO_2, was studied, it was shown that although this solid catalyst can be recycled and reused, the active species was the copper leached into solution. It was also shown that every reagent used in the catalytic reaction, including the solvent, reactants, and base, had a role in causing copper leaching. In Chapter 4, benzylamine oxidative homocoupling was studied using the same supported catalyst, CuO/CeO_2. In that study,[135] it was also shown that the concentration of leached copper into the solution was directly related to the rate of reaction.

Due to the effect of the base observed, it was hypothesized that it has a significant role in copper leaching, in general, and the understanding of the leaching mechanism associated with the presence of the base, could provide important information that could facilitate the design of a stable heterogeneous copper catalyst. CeO_2 was initially chosen as a support because of its basic characteristics and its potential stability under the basic reaction conditions. As mentioned earlier, CeO_2 was stable as a support but copper leaching still occurred, and hence other supports were explored to examine the effect of

the support on copper leaching. Gamma-alumina, γ-Al_2O_3, can be synthesized in mesoporous form such that it has surface basic character, and thus was chosen as a support for this investigation. Also, to test the effect of the degree of interaction between CuO and the support, TiO_2 was chosen as another support for investigation and comparison, as it is known that TiO_2 has strong interaction with some metals[137,138] and metal oxides.[139–141]

Alumina supported copper catalysts have been used for a variety of different coupling reactions including Sonogashira couplings, oxidative coupling of 2-naphthols, S-arylation, and (3 + 2) Huisgen cycloadditions[2,142–145] among others. In most cases, the solid precatalyst was recovered and recycled, and often the catalyst was deemed to be recyclable with some loss of activity after each cycle.[142,143] The reason behind those losses were often not explored,[143,144] or attributed to site blocking effects associated with deposition of reactants or products on the catalyst surface.[142]

Titania supported copper catalysts have also been used for various homo-[133] and cross-coupling reactions.[146] Yamaguchi et al[146] reported a relation between the polarity of solvent and copper leaching from the support in the 1,3-dipolar cycloaddition of organic azides to terminal alkynes, and that by choosing the right solvent, non-polar in that case, the catalysis was intrinsically heterogeneous, as supported by a hot filtration test. Also, they compared the reactivity between TiO_2 and Al_2O_3 as supports and their effect on the catalytic activity of copper. They showed that titania supported copper catalyst had much higher catalytic performance than alumina supported copper for the studied reaction.

For this study, the oxidative homocoupling of terminal alkynes was selected as a model reaction mainly because this reaction can give the product in a good yield both at room and high temperature, which will allow the study of the effect of temperature on copper leaching, along with other factors. Also, this reaction can be run without using polar solvent like DMSO, which is already known from Chapter 3 to have significant role in copper leaching. Diyne derivatives are important materials in the fields of natural products synthesis, materials science, and polymer chemistry because they can be converted into various other structural entities in subsequent steps. Therefore, much attention has been paid to the development of new and efficient methods for the synthesis of diynes in recent years. Catalysts based on copper[11,28,133,134,147–151] as well as other metals[152–156] were used as catalysts. Jia et al[149] used copper acetate as a catalyst and air as oxidant in DMSO at 90 °C for the efficient oxidative homocoupling of terminal alkynes. Room temperature terminal alkyne homocoupling was reported by Li et al[150] using CuI with N-bromosuccinimide and N,N-diisopropylethylamine (CuI/BS/DIPEA) as the catalytic system. An amine functionalized mesoporous silica SBA-15 supported copper catalyst was also used and claimed to be recyclable, despite the fact that copper leached significantly from the support.[134] Adimurthy et al[11] showed that running the reaction at room temperature in acetonitrile as a solvent required base and ligand added to the CuCl catalytic system to achieve high product yield. He and Cai[28] employed an Amberlyst A-21 polymer-supported copper iodide catalyst under solvent-free conditions for room temperature terminal alkyne homocoupling. That catalyst was described as recyclable with some loss of activity after each cycle, with insignificant copper leaching. However, as a result of a filtration test, at least part of the catalytic activity could be

ascribed to a homogeneous pathway. Gelderen et al[157] immobilized copper species on amine functionalized silica and used the catalyst in alkyne homocoupling reactions. They claimed their catalyst to be heterogeneous and used a hot filtration test to demonstrate that no active copper leached to the reaction mixture. Another amine functionalized silica-supported copper catalyst was synthesized by Li et al[158] and used for terminal alkyne homocoupling at room temperature. They reused the catalyst six times and claimed that the catalyst retained its mesoporous structure, but found that its catalytic activity decreased by 40% over the six cycles.

In this study, the activity and stability of unsupported CuO nanoparticles, CuO supported on γ-Al_2O_3 (CuO/γ-Al_2O_3), and on TiO_2 (CuO/TiO_2) were explored in oxidative homocoupling of ethynylbenzene to form 1,4-diphenylbutadiyne (DPBD), Scheme 5.1, at systematically varied reaction conditions, elucidating the nature of the reactive copper species.

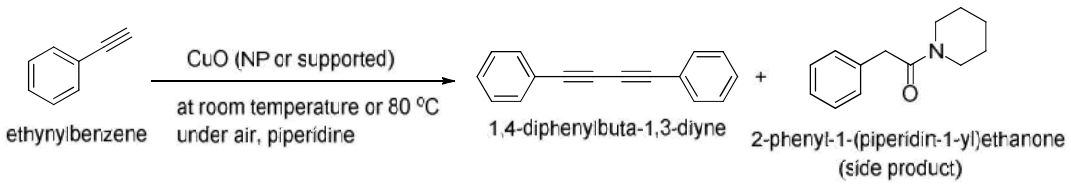

Scheme 5.1 Ethynylbenzene oxidative homocoupling reaction

5.2 Experimental Details

5.2.1 Catalysts Preparation

5.2.1.1 Synthesis of Mesoporous γ-Al_2O_3

Gamma alumina was synthesized as per an earlier reported procedure by employing surfactant P-123® mediated self-assembly of pseudoboehmite nano particles.[159] In a typical synthesis, 13.75 g of pseudoboehmite obtained from Sasol North America (Catapal B, 74.3% Al_2O_3) was peptized in a mixture of 0.9 mL nitric acid (Fischer Scientific, ~70%) and 200 mL distilled water. The suspension obtained was then sonicated for 90 min at room temperature followed by stirring at 60 °C for 17 h. The suspension was then cooled to room temperature and the peptized alumina thus obtained was added to a stirred surfactant solution comprising 15.30 g Pluronic P123® in 200 mL ethanol (200 proof). The resulting solution was further stirred for 24 h at room temperature followed by evaporation of the solvent at 60 °C. The obtained alumina composite was then dried at 75 °C for 24 h. The white sol-gel derived mesoporous γ-alumina was finally obtained by calcination of this composite at 700 °C for 4 h with a heating ramp of 1 °C/min and an intermediate holding step of 150 °C for 1 h for the removal of water and ethanol.

5.2.1.2 Supporting CuO on Mesoporous γ-Al_2O_3

A solution synthesized by dissolving193 mg of copper nitrate tri-hydrate, $Cu(NO_3)_2.3H_2O$ (Sigma-Aldrich, purity > 99%), in 0.60 mL of de-ionized water was added to 500 mg of the above synthesized γ-Al_2O_3, to yield a 10 wt % alumina-supported

copper oxide catalyst. Then, the wet sample was heated to 120 °C at ramp of 3 °C/min, in an air flow and dried at 120 °C for 3 h. Next, the temperature was increased to 500 °C at a ramp of 3 °C/min, and the catalyst was calcined in flowing air at 500 °C for 3 h. This catalyst will be referred to as 10CuO-Al_2O_3.

5.2.1.3 Supporting CuO on Mesoporous TiO_2

Commercial mesoporous anatase TiO_2 (S_{BET} = 127 m^2/g and V_{pore} = 0.25 cm^3/g) was used as a support for CuO. A solution was prepared by dissolving 435 mg of copper nitrate tri-hydrate, $Cu(NO_3)_2.3H_2O$ (Sigma-Aldrich, purity > 99%), in 0.12 mL of de-ionized water. The total volume of this solution was 0.30 mL. To insure good distribution of copper in the pores of mesoporous TiO_2, and avoid depositing CuO on its surface, half of this solution was added to 1 g of commercial mesoporous TiO_2, dried at 75 °C, and then the other half was added, to yield a 10 wt % titania-supported copper oxide catalyst. The wet sample was transferred to a calcination oven, heated to 120 °C at a ramp of 3 °C/min, in an air flow and dried at 120 °C for 3 h. The temperature was then increased to 500 °C at ramp of 3 °C/min, and the catalyst was calcined in flowing air at 500 °C for 3 h. This catalyst will be referred to as 10CuO-TiO_2.

Commercial CuO nanoparticles (Sigma-Aldrich, S_{BET} = 16 m^2/g) were used as received for comparison purposes.

5.2.2 Materials Characterization

Powder X-ray diffraction (PXRD) was carried out with a PAnalytical X'pert PRO diffractometer operating with Cu Kα radiation and an X'celerator RTMS detector. A step size of 0.002° 2θ and a scan rate of 10 s per step were used. Hydrogen-temperature programmed reduction (H_2-TPR) was measured using approximately 150 mg of fresh catalyst in a Micromeritics AutoChem II 2920. The samples were placed in a U-shaped tube and first oxidized in 10% O_2-He flow of 60 mL/min while heating from room temperature to 600 °C at 10 °C/min, then passivated under helium and returned to room temperature. The TPR spectra were then recorded by heating the samples from room temperature to 400 °C at 10 °C/min, under a 60 mL/min flow of 10% H_2-Ar mixture. Nitrogen adsorption isotherms were recorded at 77 K using a Micromeritics Tristar II 3020. BET (Brunauer-Emmett-Teller) surface areas were calculated using the adsorption data. Average pore diameters were determined by the BDB-FHH method (a simplified Broekhoff–de Boer method with a Frenkell–Halsey–Hill isotherm).[79] Elemental analyses by ICP-AES were carried out by ALS Environmental Division (Tucson, AZ). TEM images were recorded on a JEOL 100CX II TEM instrument with a resolution of 2-3 Å at an acceleration voltage of 100 kV. TEM samples were prepared by grinding the samples in a mortar and pestle followed by dispersing them in isopropyl alcohol. Dispersed samples were then deposited on a lacey carbon grid supported on copper grids.

5.2.3 Catalytic Oxidative Homocoupling of Terminal Alkynes

In a typical reaction, the catalyst (0.05 eq. or 0.10 eq. Cu relative to limiting reactant), was added to a 25 mL two-neck round bottom flask mounted with a magnetic stir bar and containing 2 mmol ethynylbenzene (220 μL), 2 mL piperidine, and 1 mmol diphenylether (0.5 eq., 158 μL) as an internal standard. Experiments were run either at 80 °C, where the round bottom flask was attached to a condenser and immersed in an preheated oil bath, or at room temperature (22-24 °C). Samples of the reaction mixture were taken at specified times, filtered over a silica gel column and diluted with a mixture of dichloromethane and ethylacetate, and the reactant (ethynylbenzene) conversion was determined by GC-FID, and calculated by comparing the reactant to an internal standard. The identity of the product was also verified by GC-MS. The product yield is calculated by dividing the product concentration by the initial concentration of the reactant, ethynylbenzene, after calibrating the GC-FID peaks in reference to the internal standard, diphenylether.

5.3 Results and Discussion

5.3.1 Catalyst Characterization

Table 5.1 shows the copper content of each of the supported catalysts. It can be noticed that upon supporting copper on γ-Al_2O_3 and TiO_2, the pore volume decreases by 60%, the average pore diameter decreases by 25-35%, and the BET surface area decreases by 30% in the case of γ-Al_2O_3, and by 60% in the case of TiO_2.This means that copper oxide is mainly deposited inside the pores of the support.

Table 5.1 Catalyst characterization

Catalyst	Copper wt %	Support metal wt %	BET surface area m^2/g	Pore volume cm^3/g	Average pore diameter nm
Bare γ-Al_2O_3	N/A	N/A	221	1.10	20
10CuO-Al_2O_3	10.6	45.3 (Al)	153	0.41	13
Bare TiO_2 pellets	N/A	N/A	127	0.25	24
10CuO-TiO_2	13.0	46.8 (Ti)	42	0.10	18
CuO nanoparticles	N/A	N/A	16	N/A	N/A

5.3.2 Catalyst Heterogeneity Evaluation

In this study, the various catalysts were evaluated in the oxidative homocoupling of ethynylbenzene as a model substrate under a variety of conditions to assess the heterogeneity or homogeneity of the catalysis, with an overall goal of assessing if such solid copper precatalysts can be operated as truly heterogeneous catalysts under some sets of conditions. Piperidine was used as both the base and solvent, and the reaction was conducted under air at ambient conditions or 80 °C. The homocoupling reaction is depicted in Scheme 5.1, showing the desired product as well as a side product, 2-phenyl-1-(piperidine-1-yl)ethanone. The effect of three factors on catalyst leaching was studied in detail. These factors are temperature, support, and solvent.

5.3.2.1 Effect of Temperature on Copper Leaching and Reactivity

As shown in Figure 5.1, when running the reaction using 10CuO-Al_2O_3 as a catalyst at room temperature, the 1,4-diphenylbuta-1,3-diyne (DPBD) yield reached 30% in 7 hours (CuAl-C), while at an elevated temperature, 80 °C, the yield reached approximately 50% in 7 hours (denoted CuAl-H). For long reaction times, some loss of product yield was observed, as the product decomposed to some degree. The same overall behavior was observed when CuO nanoparticles were used as the catalyst, with the difference that the CuO nanoparticles were not active at room temperature. It might be thought that higher temperature is needed to activate the substrate and has nothing to do with the catalyst, but since this reaction is known to be active at room temperature under different conditions,[151,156] and as the 10CuO-Al_2O_3 catalyst was observed to be active here, it was hypothesized that temperature played a role in pre-catalyst activation and not substrate activation. This was the first indication that solid forms of copper may not be active in this reaction under all conditions, and suggested that copper solubilization might be a pre-requisite for activity. This hypothesis was thus explored further, as described below.

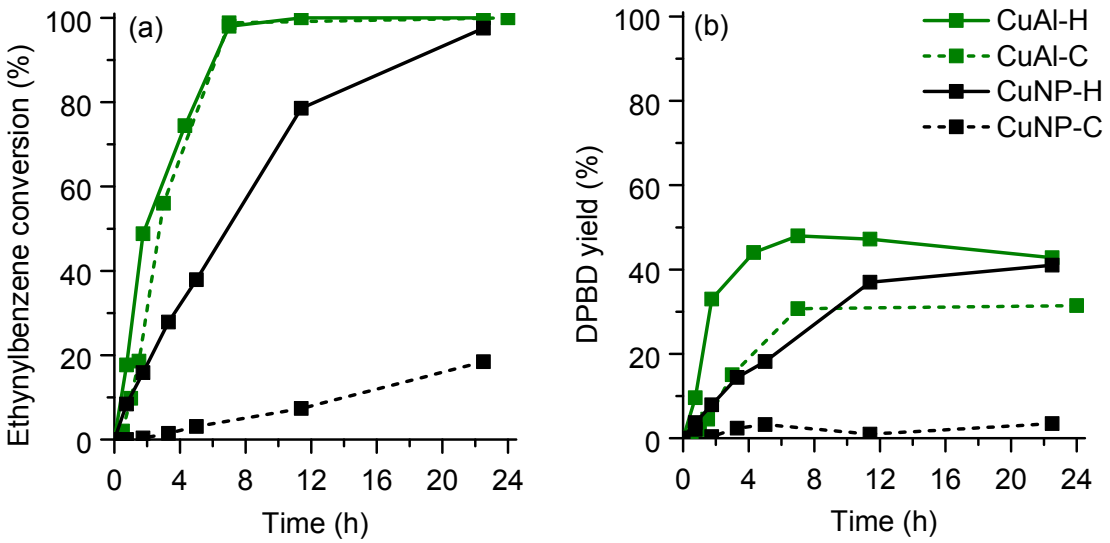

Figure 5.1 **Effect of temperature on the homocoupling reaction of ethynylbenzene using 10CuO-Al_2O_3 (CuAl) and CuO nanoparticles (CuNP) as catalysts. Experiments run at 80 °C are denoted by (H) and experiments run at room temperature are denoted by (C). Figure (a) represents the conversion of ethynylbenzene and figure (b) represents the desired product (DPBD) yield, as a function of time.**

To test this hypothesis and to understand the role and effect of temperature on the reactivity of the precatalyst, several additional experiments were conducted. The same amount of catalysts (CuO nanoparticles and 10CuO-Al_2O_3, separately) used in the previous reactions was mixed with piperidine only, overnight. One aliquot of each precatalyst was mixed at room temperature and another one at 80 °C. Each mixture was then centrifuged and the liquid was decanted. A sample from each of the four decanted liquid mixtures was sent for elemental analysis to quantify the amount of copper in the solution. To 2 mL of each of the decanted liquid, ethynylbenzene (1 mmol) and the internal standard were added, and then the reaction was started with these mixtures.

Table 5.2 shows a summary of the six reactions that were run for this set of experiments, and Figure 5.2 (a and b) shows the conversion of the limiting reactant and yield of the desired product. To make comparison easy, the copper mass content was converted to the equivalent concentration in mol % with respect to the ethynylbenzene.

Table 5.2 Effect of temperature on copper leaching

Experiment	Catalyst	Mixing T (°C)	Reaction T (°C)	Copper content in liquid (mol %)
CuNP-CC	CuO nanoparticles	Room Temp	Room Temp	1.6
CuNP-HC	CuO nanoparticles	80	Room Temp	1.6
CuNP-HH	CuO nanoparticles	80	80	1.6
CuAl-CC	$10CuO\text{-}Al_2O_3$	Room Temp	Room Temp	1.0
CuAl-HC	$10CuO\text{-}Al_2O_3$	80	Room Temp	1.5
CuAl-HH	$10CuO\text{-}Al_2O_3$	80	80	1.5

It can be observed in Figure 5.2 that once the catalyst is mixed with piperidine at high temperature, nearly the same catalytic results were obtained when running the subsequent catalytic reaction either at room or high temperature. This further demonstrates that for this reaction, elevated temperature was mainly required to activate copper precatalyst, most likely by copper leaching, and once it was activated, product could be formed without the need of additional heating. On the other hand, mixing the catalyst with piperidine at room temperature produced a catalytically inactive mixture in the case of

CuO nanoparticles (CuNP-CC) and only a modestly active solution was obtained in the case of 10CuO-Al_2O_3 (CuAl-CC). The fact that mixing CuO nanoparticles at room and high temperatures gave almost the same amount of copper in solution, as noted in Table 5.2, yet at the same time cold mixing did not produce active copper species, required additional investigation.

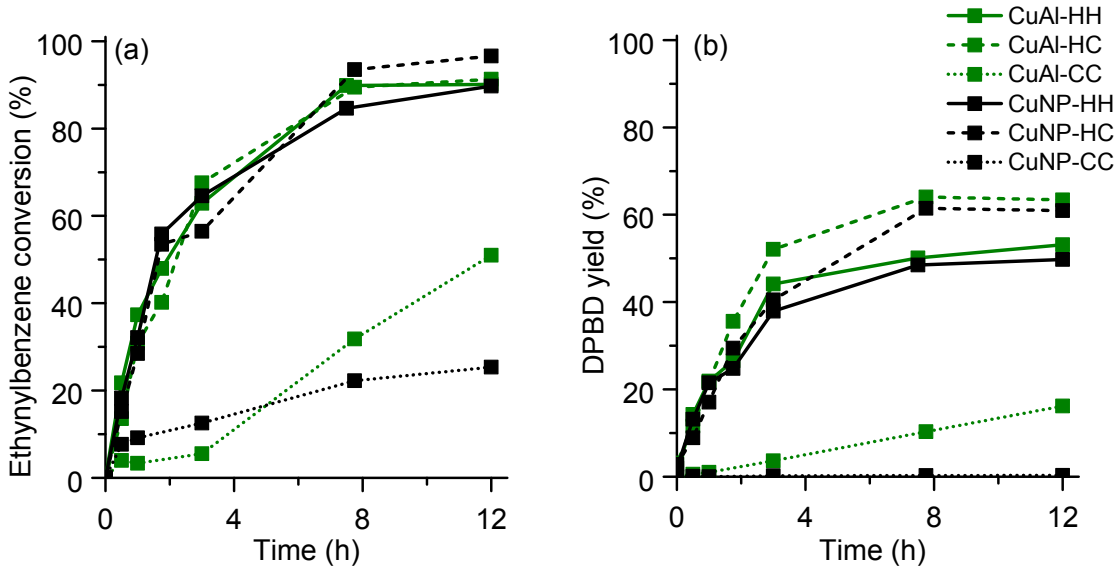

Figure 5.2 **Effect of temperature on copper leaching from CuO nanoparticles (CuNP) and from the γ-Al_2O_3 support (CuAl), for the homocoupling reaction of ethynylbenzene. Figure (a) represents the conversion of ethynylbenzene and figure (b) represents the desired product (DPBD) yield, as a function of time. The first letter represents the mixing temperature and the second letter represents the reaction temperature; (H) is for 80 °C and (C) is for room temperature.**

It was hypothesized that the copper leached into solution in the hot mixed experiment was soluble copper ions ligated with piperidine, whereas in the cold mixed experiment

produced primarily fine, inactive CuO nanoparticles that were not separated by centrifugation. To test this hypothesis, the liquid mixtures resulting from mixing CuO nanoparticles with piperidine at room temperature (CuNP-C) and at 80 °C (CuNP-H) were analyzed by mass spectroscopy, and the spectra were compared with the spectrum for the piperidine reagent alone. It was found that mass spectra of piperidine and CuNP-C are similar to each other, showing mainly peaks associated with piperidine and its dimer, while the solution from CuNP-H has 2 new peaks with molecular weights of 165 and 250 g/mol, circled in red in Figure 5.3. These are likely associated with copper-piperidine complexes, as suggested in in Figure 5.4, supporting the notion that treatment of the precatalyst at elevated temperature produced molecular Cu-piperidine complexes.

To probe the possibility that the copper in the cold mixed mixture CuNP-C were fine CuO nanoparticle, fresh CuO nanoparticles were mixed with deionized water at room temperature overnight and centrifuged to recover the solid nanoparticles, which were dried and further analyzed. If, as hypothesized, fine CuO nanoparticles were removed with the decanted water, then residual, recovered CuO nanoparticles, which were also expected to be shifted in size distribution towards larger sized particles, should be inactive. TEM images of recovered solid CuO nanoparticles (referred to as CuNP-C-W) were taken and compared with TEM images of the commercial CuO nanoparticles before the water treatment.

The particle size distribution of the CuO nanoparticles before and after water treatment, as determined via analysis of TEM images, Figure 5.5, is shown in Figure 5.6. Measuring the diameter of 105 particles in each sample, it was found that the particles diameters ranged from 17 nm to 72 nm, and the volume average particle size of commercial CuO

nanoparticles was 40 nm, where that of CuNP-C-W was 48 nm. The distribution of particles sizes, as shown in Figure 5.6, suggests that the water treatment removed some of the smaller particles from the mixture, as intended. This supports the hypothesis that the copper content of cold mixed mixtures (CuNP-C) above was likely fine copper oxide nanoclusters that could not be recovered from solution by centrifugation, which were inactive at room temperature.

Thus, temperature does not appear to affect the extent of copper leaching (due to leaching of fine CuO particles at all temperatures), but it mainly helps solubilizing leached copper and forming active complexes that are believed to be molecular copper ions ligated by the amine base.

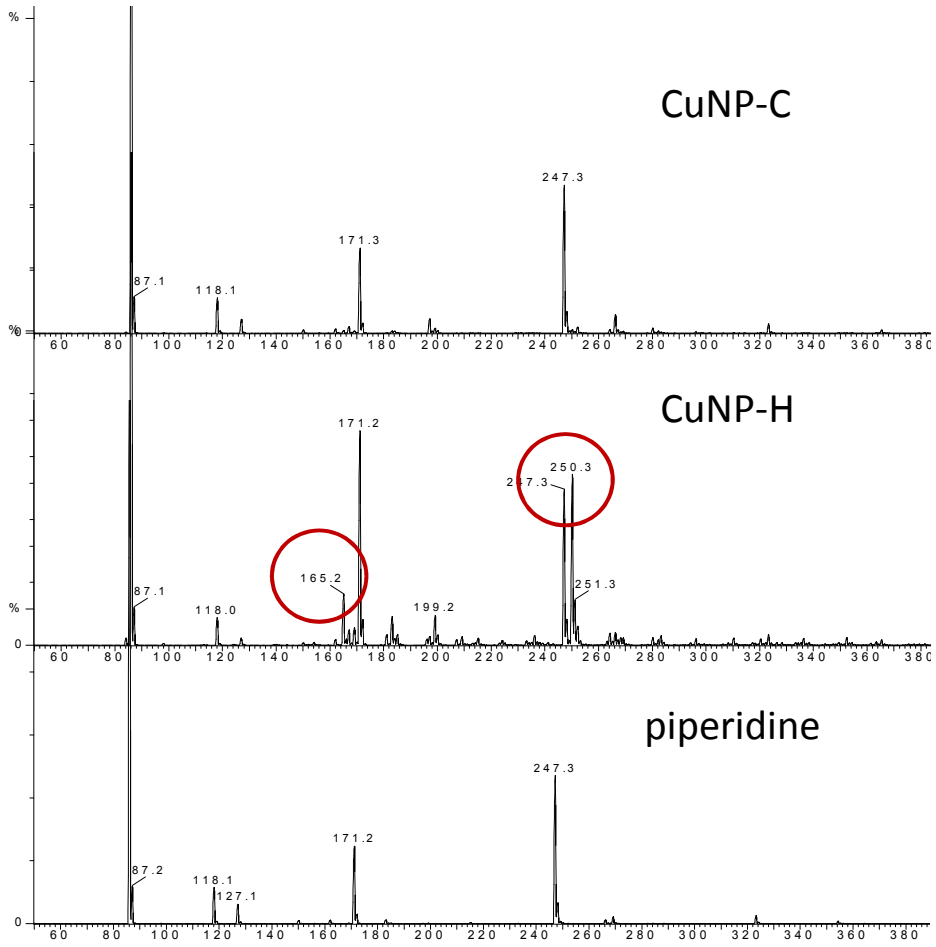

Figure 5.3 **Comparison of ESI MS spectra of pure piperidine, piperidine decanted after mixing it with CuO nanoparticles at 80 °C (CuNP-H), and piperidine decanted after mixing it with CuO nanoparticles at room temperature (CuNP-C) overnight.**

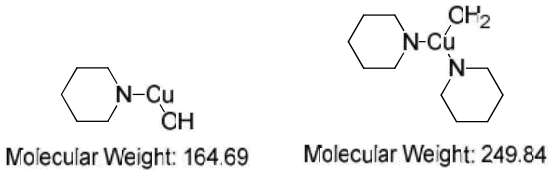

Figure 5.4 **Anticipated copper-piperidine complexes formed by mixing copper oxide with piperidine at high temperature (80 °C).**

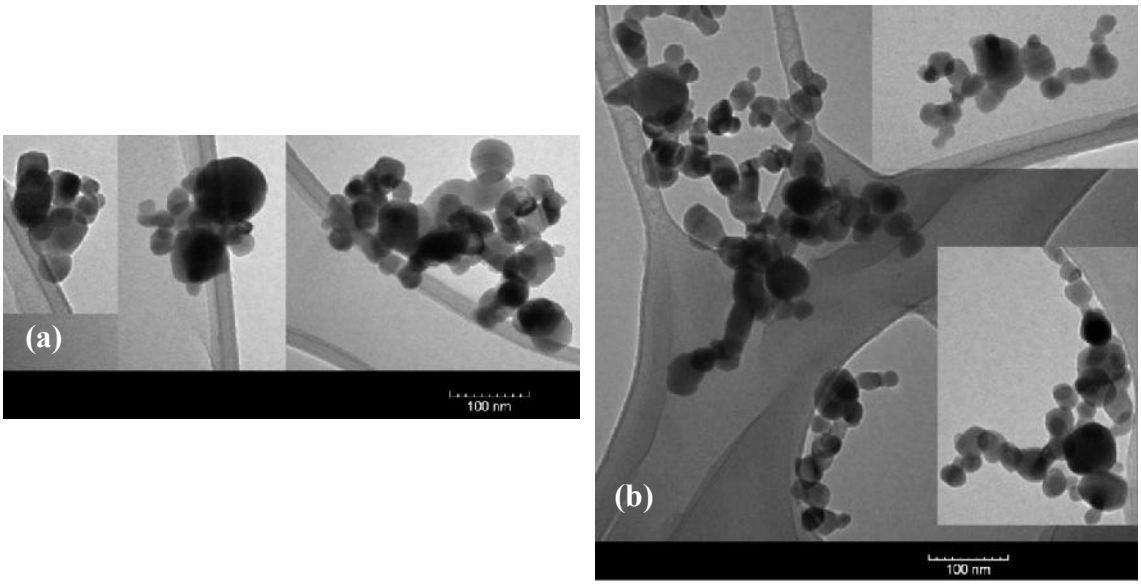

Figure 5.5 **TEM images of (a) CuO nanoparticles after stirring them in water at room temperature and decanting liquid water, and (b) commercial CuO nanoparticles**

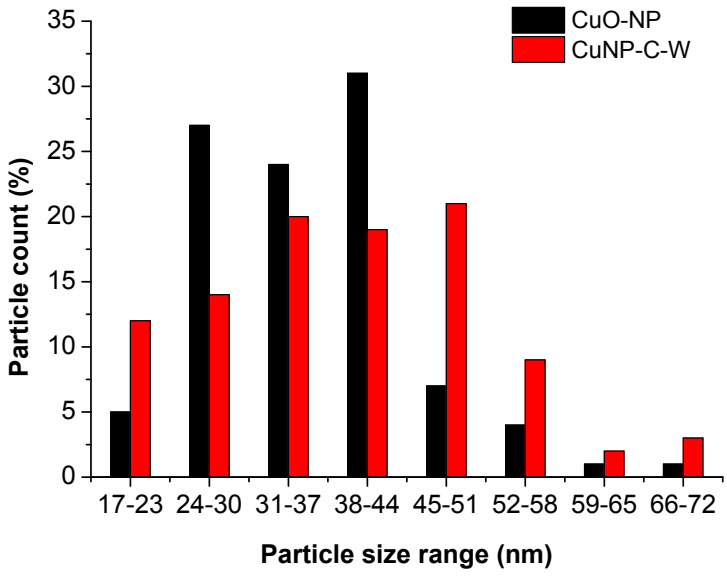

Figure 5.6 **Particle size distribution of commercial CuO nanoparticles (red) and CuO nanoparticles after stirring them in water at room temperature overnight and separating them by centrifugation (CuNP-C-W)**

5.3.2.2 Effect of Support and Support Interaction with Copper Oxide on Copper Leaching

The next factor investigated that can affect copper leaching from the support is the strength of interaction between the support and copper oxide. Yamaguchi et al[146] compared the performance of copper hydroxide supported on titanium oxide, $Cu(OH)_x/TiO_2$ with that supported on aluminum oxide, $Cu(OH)_x/Al_2O_3$ in the 1,3-dipolar cycloaddition of organic azide to terminal alkynes. They showed that $Cu(OH)_x/TiO_2$ is a much more active catalyst than $Cu(OH)_x/Al_2O_3$, demonstrating the potential for significant support effects in coupling reactions.

H_2-TPR is a useful technique widely used to assess the dispersion of metals or metal oxides and to understand the nature and types of reducible metal species on the support.[138,141,160,161] To probe the effect of the copper oxide – support interaction, TiO_2, which has strong interactions with metals and metal oxides[141] was chosen and used to support CuO for comparison to the γ-Al_2O_3 and unsupported precatalysts.

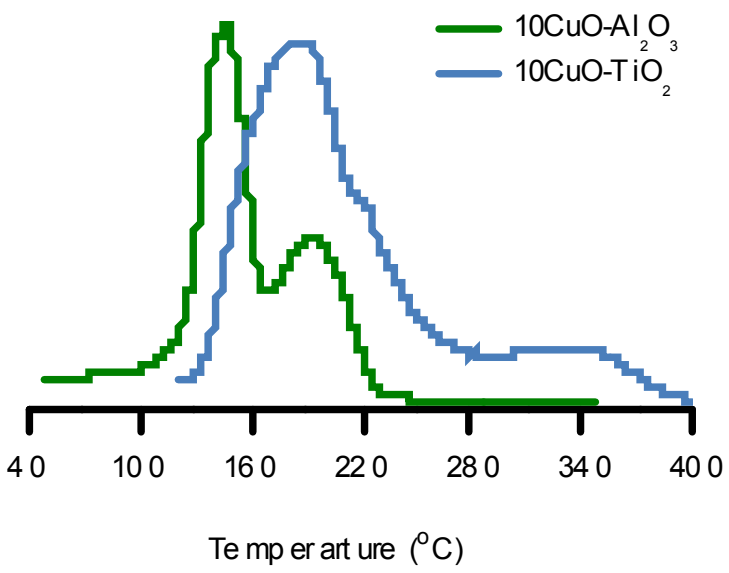

Figure 5.7 H_2-TPR profiles of 10CuO-Al_2O_3 and 10CuO-TiO_2

Figure 5.7 shows H_2-TPR profiles of 10CuO-Al_2O_3 and 10CuO-TiO_2. On Al_2O_3, CuO has two reduction peaks; at 147 °C and 198 °C. The total H_2 consumption calculated from integrating the area under the curve was 0.71 mmol/g, representing ~40% of total Cu in the catalyst. On TiO_2, the CuO reduction peaks were shifted to the right; one peak was at 188 °C with a shoulder at 219 °C, and another peak was at 332 °C. The total H_2 consumption in this case was 1.20 mmol/g, representing ~60% of total copper in the sample. The higher H_2 consumption in 10CuO-TiO_2, given that TiO_2 is not reducible over the range of 40-400 °C, suggests that the copper species in this precatalyst were more accessible than the copper species in 10CuO-Al_2O_3, and the shifting in reduction peaks to higher temperature means that the copper species in 10CuO-TiO_2 were more dispersed than those in 10CuO-Al_2O_3. In addition, and referring back to the literature, the low

temperature peak in 10CuO-Al_2O_3 may be assigned to reduction of CuO particles having little or no interaction with the support, while the smaller peak, at 198 °C, might be assigned to highly dispersed surface CuO species. Also, it can be observed that most H_2 consumption occurs at lower temperature, suggesting that most of CuO species had little interaction with the γ-Al_2O_3 support. Similarly, the first peak in 10CuO-TiO_2 and its shoulder might be assigned to highly dispersed surface CuO species, while the broader second peak at 332 °C might be assigned to highly dispersed cluster or (more) isolated Cu ions that were strongly interacting with the support. In comparing the amount of H_2 consumption in each temperature range, more of the copper can be considered as highly dispersed surface CuO species, with about 15% of it strongly interacting with the support. These results are in good agreement with XRD patterns for each precatalyst shown in Figure 5.8, where the two distinctive crystalline CuO peaks at 35.5° and 38.8° were much more significant in 10CuO-Al_2O_3 pattern than in 10CuO-TiO_2 pattern. The CuO crystalline size was calculated using Scherrer equation and found to be 29 nm and 19 nm in 10CuO-Al_2O_3 and 10CuO-TiO_2, respectively.

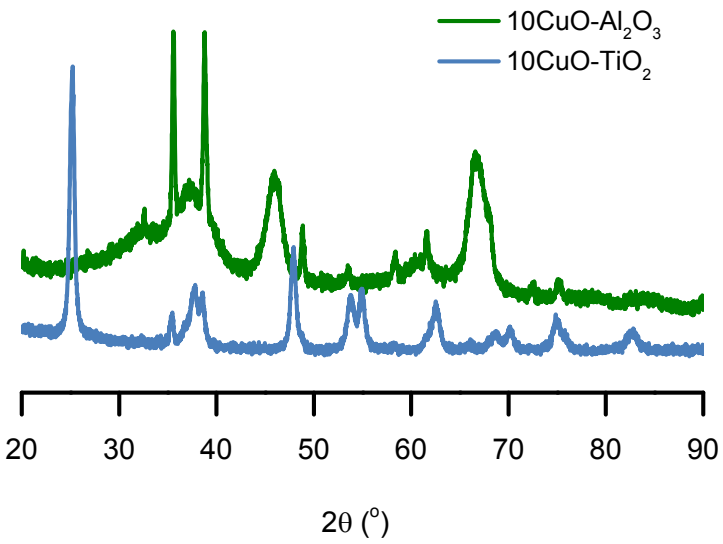

Figure 5.8 XRD patterns of 10CuO-Al_2O_3 and 10CuO-TiO_2

Figure 5.9 shows the effect of the support on the catalytic activities of CuO based precatalysts in ethynylbenzene homocoupling. At high temperature, the support had almost no effect, neither on the conversion nor on the yield of the desired product, DPBD. On the other hand, when running the reaction at room temperature, 10CuO-TiO_2 was more active than 10CuO-Al_2O_3, and produced more of the desired product. To explain these observations and results, additional experiments were conducted. First, to eliminate the possible effect of the support, the same reactions where run with bare supports, and both γ-Al_2O_3 and TiO_2 showed no reactivity. Then, leaching experiment similar to the one described in the previous section was run using 10CuO-TiO_2. Table 5.3 shows a summary of three new mixing experiments that were run and compared with the results described in Table 5.1. The copper contents of each liquid mixture is also shown, after converting the copper mass content to the equivalent concentration in mol % with respect to ethynylbenzene.

Table 5.3 Effect of temperature on copper leaching when using TiO_2 as a support

Experiment	Catalyst	Mixing T (°C)	Reaction T (°C)	Copper content (mol %)
CuTi-CC	10CuO-TiO_2	Room Temp	Room Temp	0.3
CuTi-HC	10CuO-TiO_2	80	Room Temp	3.3
CuTi-HH	10CuO-TiO_2	80	80	3.3

Considering the data in Table 5.1, it can be noticed that at room temperature the amount of copper leached from TiO_2 (CuTi-CC) is less than that leached from γ-Al_2O_3 (CuAl-CC) under similar conditions. This was expected because CuO has stronger interaction with TiO_2 than with Al_2O_3 supports, as depicted from H_2-TPR profiles, shown Figure 5.7. The ability of piperidine to ligate with copper at high temperature and facilitate its leaching from the support makes the system more complicated to draw similar conclusions at high temperature.

Figure 5.10 shows the kinetic curves of six catalytic experiments, three from the TiO_2 supported sample and the other three are from the γ-Al_2O_3 supported sample. Similar to the findings from the previous section and Figure 5.2, comparing CuAl-HC with CuAl-HH, and CuTi-HC with CuTi-HH, it was observed that once the molecular copper species leached to the solution, they had similar performance, whether the reaction was run at room temperature or at high temperature. However, comparing CuAl-CC with CuTi-CC, and knowing that the amount of leached copper in the CuTi-CC is only one-third of that in the CuAl-CC reaction, it is noteworthy that the leached species derived from the

10CuO-TiO_2 precatalyst were more active than those from the 10CuO-Al_2O_3. This suggests that the support affected the nature of the leached copper species.

It was noted above that much of copper in 10CuO-Al_2O_3 was in the form of CuO particles that had little interaction with the support, and furthermore that CuO nanoparticles were not active at room temperature (Figure 5.1), as they cannot form copper-piperidine active species (Figure 5.3 and Figure 5.4). Thus, one can hypothesize that the leached copper in the CuAl-CC sample was mostly inactive CuO nanoclusters.

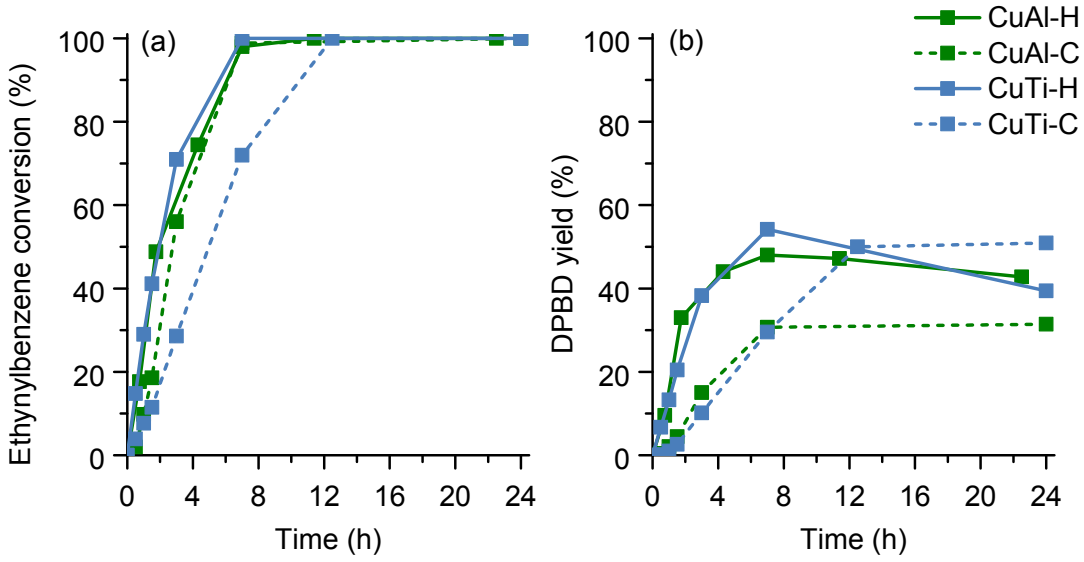

Figure 5.9 **Effect of support and temperature on the catalytic activities of CuO supported on γ-Al_2O_3 (CuAl) and on TiO_2 (CuTi) in ethynylbenzene homocoupling at room temperature (C) and 80 °C (H)**

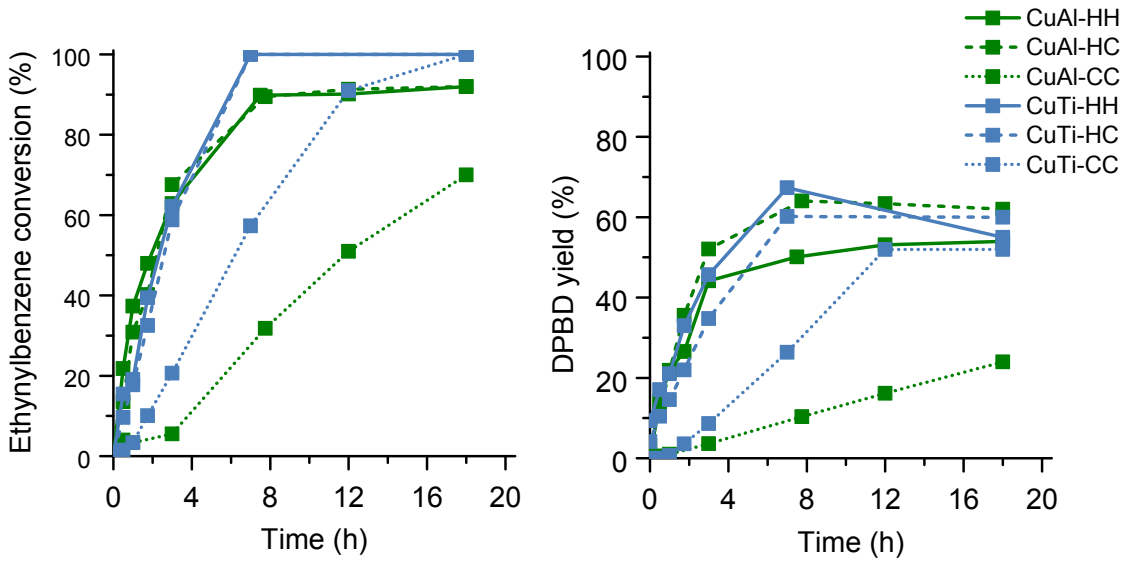

Figure 5.10 Effect of temperature on copper leaching from γ-Al_2O_3 support (CuAl) and from TiO_2 support (CuTi) at room temperature (C) and at 80 °C (H)

To understand the nature of the very active copper species in CuTi-CC, another two experiments were conducted using soluble copper acetate as the catalyst. One experiment was carried out with 0.3 mol% copper from copper acetate for comparison with CuTi-CC (which leached 0.3 mol% of copper species), and the other one was run with 1 mol% copper from copper acetate to compare it with CuAl-CC (which leached 1 mol% of copper species). The results are shown in Figure 5.11, and suggest that copper leaching from TiO_2 was soluble copper similar in nature to that coming from copper acetate (Figure 5.11 (b)) , as they had similar reaction rates. On the other hand, only part of the copper leached from γ-Al_2O_3 was active (Figure 5.11 (a)), while the other part was likely in the form of inactive fine CuO nanoparticles. Finally, comparing the performance of leached copper (CuTi-CC) and solid catalyst (CuTi-C) shown in Figure 5.12 (a), it

appears that essentially all the activity of the solid catalyst was associated with the leached copper. On the contrary, as shown in Figure 5.12 (b), supported copper in CuAl- appeared to have an increasing reaction rate with time, possibly due to additional soluble copper leaching over time, catalyzing the reaction.

From these collected experiments, it is clear that the catalyst support had a significant effect on the activity of the precatalyst, affecting the extent of copper leaching and the nature of the leached copper species.

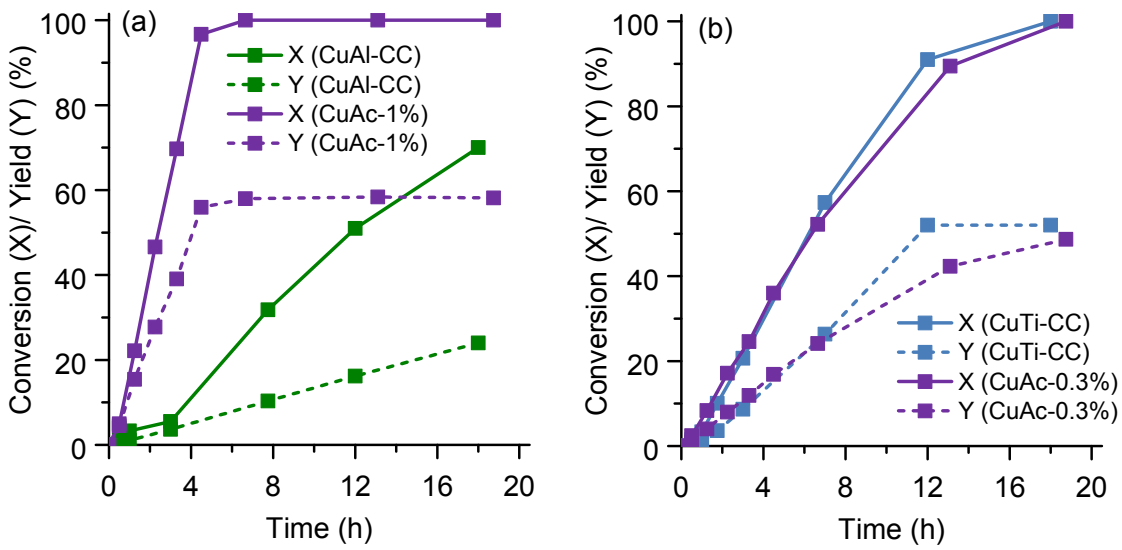

Figure 5.11 Comparison between the activities of soluble copper from copper acetate, CuAC, with copper from (a) solid 10CuO-Al_2O_3 and with copper from (b) 10CuO-TiO_2 at the same concentration

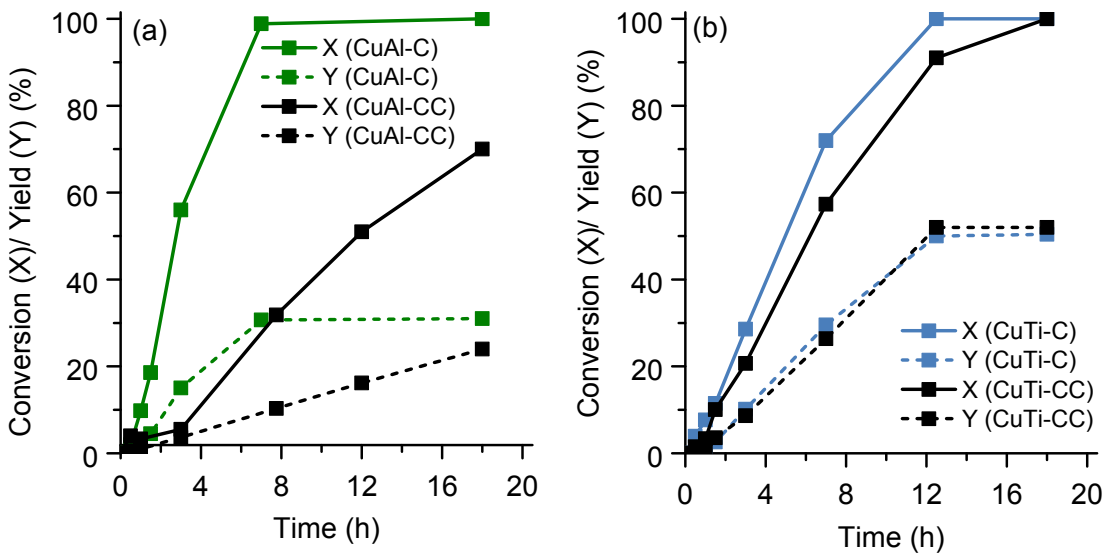

Figure 5.12 Comparison between the catalytic activities of solid catalysts (a) 10CuO-Al_2O_3 and (b) 10CuO-TiO_2 with copper leached from the same catalyst

5.3.2.3 Effect of Solvent and Reactant on Copper Leaching

In the final set of experiments, the effect of the solvent on copper leaching was explored. Three more experiments were conducted. In one experiment, the titania supported copper precatalyst, 10CuO-TiO_2, was mixed with acetonitrile as solvent, as it is one of the most commonly used solvents in the literature for alkyne homocoupling reactions.[11,134,150] In a second experiment, the precatalyst was mixed with the substrate, ethynylbenzene. After mixing overnight and centrifugation in both cases, the decanted liquid was used in the oxidative homocoupling reaction. Four millimoles of piperidine were added to 2 mL of the decanted liquids. No activity was observed in acetonitrile mixture, or in ethynylbenzene mixture, and elemental analysis of the copper content of the liquids showed that there was no copper in the solution. In a third experiment, piperidine was

replaced by 2,2,6,6-tetramethylpiperidine (TMP), as a hindered base that was expected to eliminate the copper ligating effect of piperidine. Although TMP is similar to piperidine in basicity, it was found to be inactive for the oxidative homocoupling of ethynylbenzene, most probably because it cannot ligate with copper and solubilize it from the support. Thus, for this reaction, the piperidine is critical to the activation of the solid copper precatalyst, and the role it plays is that of a ligand that coordinates active species, which are likely molecular copper ions ligated by piperidine in solution. In this work, no definitive evidence for catalysis by the solid surface of supported CuO was obtained.

5.3.3 Does Recyclability Mean Heterogeneity?

In heterogeneity studies, quite often solid catalyst recyclability is used as a "proof" of heterogeneous catalysis. In this work, it was shown that 0.3 mol% copper (Table 5.3 and Figures 5.10, 5.11 and 5.12) leaching from the TiO_2 support was enough to produce 50% of the desired product (DPBD) at room temperature. However, because this catalyst only leached a small amount of the total copper into solution (6%), this catalyst can be seen as reusable (but technically not recyclable, as the same copper species are not used in each cycle) if it were reused and if additional copper can leached in the next cycle.

Figure 5.13 shows a recyclability test of the titania-supported copper catalyst over three consecutive runs, and Table 5.4 tabulates the copper and titanium contents of the catalyst, and the percent copper leaching after each cycle. Although the precatalyst was recoverable and reusable, and the third cycle had an even higher initial rate than the first cycle, one cannot claim it to be a truly heterogeneous catalyst because copper leached

from the support, and this leached copper was the active catalytic species, as shown above.

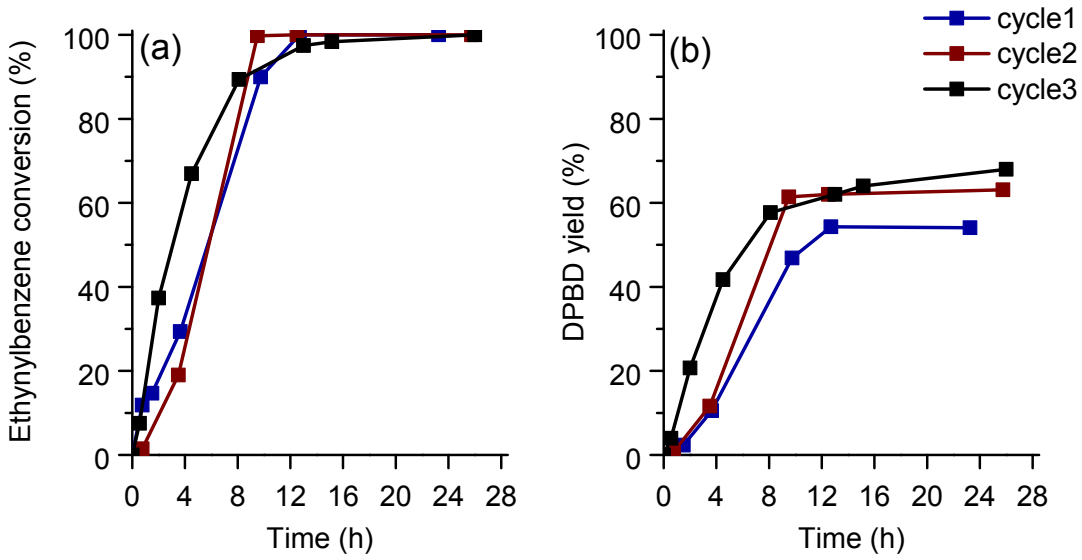

Figure 5.13 **Recyclability test of 10CuO-TiO_2 for oxidative homocoupling of ethynylbenzene at room temperature**

Table 5.4 **Copper and titanium contents of fresh and recycled 10CuO-TiO_2 catalyst**

Catalyst	Cu wt %	Ti wt %	Cu/Ti wt/wt	% Cu leaching
Fresh	13.0	46.8	0.278	-
1st cycle	11.5	48.3	0.238	14%
2nd cycle	8.9	51.5	0.173	27%
3rd cycle	8.3	50.7	0.164	5%

5.4 Conclusions

Supported copper oxide on γ-Al_2O_3 (10CuO-Al_2O_3) and TiO_2 (10CuO-TiO_2) were synthesized and used as precatalysts for the oxidative homocoupling of ethynylbenzene. The heterogeneity of these catalysts was assessed and the effect of temperature, support, and solvent on copper leaching and catalyst reactivity was investigated. It was found that for this alkyne homocoupling reaction, elevated temperature was needed to solubilize copper and activate it by forming copper-piperidine complexes. Once this activation occurred, the reaction could be conducted at room temperature, giving good yields of the desired product. Copper oxide was found to interact differently on the two supports; CuO supported on TiO_2 was more dispersed and accessible than CuO supported on γ-Al_2O_3. Less copper leached from 10CuO-TiO_2 than from 10CuO-Al_2O_3 at room temperature. Nevertheless, copper species leached from 10CuO-TiO_2 were more active than those leached from 10CuO-Al_2O_3. That was probably because the copper leached from the 10CuO-TiO_2 was cationic, molecular copper. In contrast, some of the copper leached from 10CuO-Al_2O_3 was believed to be inactive CuO nanoclusters, with some also in the cationic, molecular form. Piperidine had multiple roles in this reaction: it acted as solvent, base, as well as an important ligand. When using acetonitrile as the solvent, the alkyne homocoupling reaction did not proceed to any significant extent, and in a separate experiment it was found that acetonitrile could not leach copper from the support under the conditions employed. The sterically hindered organic base, 2,2,6,6-tetramethylpiperidine, was also used and found to produce an inactive mixture, as it could not act as a ligand. These results support the hypothesis that soluble, molecular copper-piperidine species catalyze this oxidative alkyne homocoupling reaction. Although the

precatalyst 10CuO-TiO_2 was reused three times, it should not be considered a recyclable catalyst, but rather a reusable solid precatalyst that produced soluble active copper in each cycle.

CHAPTER 6

CONCLUDING REMARKS

Copper is an inexpensive non-toxic metal that have been widely used as an active catalyst. Many copper-catalyzed coupling reactions are used for the construction of important organic molecules, including pharmaceuticals, commodity chemicals and polymers. We tried to understand the homogeneity/heterogeneity of some copper catalyzed reactions using supported copper oxide catalysts. One common thing among all explored reactions was the amine. Amine was used either as one of the reactants (in Ullmann-type coupling reaction) or as a solvent (in oxidative terminal alkyne-homocoupling reaction).

All conducted heterogeneity assessment tests showed that copper leached from the support, and that leached copper was the active catalytic species. Leaching was facilitated by the use of polar solvents, inorganic base, ligating amines, and the high temperature.

Designing a truly heterogeneous catalyst, which is stable, does not leach copper, and recyclable, seems to be a challenging task under these harsh conditions.

Alkyne-azide coupling is one of the copper catalyzed reactions that does not need polar solvent, base, or amine to proceed. In fact, it was shown by Yamaguchi et al[146] that copper hydroxide supported on TiO_2 and Al_2O_3 is a truly heterogeneous catalyst for this reaction, but only when non-polar solvent like toluene is used. The difference between Yamaguchi's catalyst and the catalyst we used for alkyne homocoupling in Chapter 5 is the form of copper. They supported copper hydroxide, while we supported copper oxide.

Therefore, it would be beneficial to use our 10CuO-TiO_2 catalyst to run the azide-alkyne coupling reaction and compare the results with Yamaguchi's result in order to learn about the effect of nature of copper on the catalyst on copper leaching.

Because of the strong interaction between copper and amines, the next catalyst to be investigated should be copper supported on functionalized supports. This was tried by Likhar et al[49] where they used silica tethered copper catalyst for N-arylation of N(H)-heterocycles with aryl halides. Although they claimed that their catalyst to be heterogeneous, depending on hot filtration test, and that it is recyclable, silica is not stable under the basic conditions used, and the lack of catalyst characterization before and after reaction open the door to more improvements. Supporting this copper complex on basic supports might result in truly heterogeneous catalyst.

Finally, more investigation is needed to test the heterogeneity of supported copper catalysts in other types of reactions, like palladium-free Sonogashira coupling, where amine is not part of the reaction system.

REFERENCES

[1] L. Shao, C. Qi, *Appl. Catal. A Gen.* **2013**, *468*, 26–31.

[2] A. Biffis, E. Scattolin, N. Ravasio, F. Zaccheria, *Tetrahedron Lett.* **2007**, *48*, 8761–8764.

[3] F. Ullmann, *BERICHTE DER Dtsch. Chem. GESELLSCHAFT* **1903**, *36*, 2382–2384.

[4] A. J. Hickman, M. S. Sanford, *Nature* **2012**, *484*, 177–185.

[5] X. Fan, N. Li, T. Shen, X.-M. Cui, H. Lv, H.-B. Zhu, Y.-H. Guan, *Tetrahedron* **2014**, *70*, 256–261.

[6] R. Schmidt, R. Thorwirth, T. Szuppa, A. Stolle, B. Ondruschka, H. Hopf, *Chemistry* **2011**, *17*, 8129–8138.

[7] R. Salazar, L. Fomina, S. Fomine, *Polym. Bull.* **2001**, *47*, 151–158.

[8] A. Sharifi, M. Mirzaei, M. Reza Naimi-Jamal, *Monatshefte für Chemie - Chem. Mon.* **2005**, *137*, 213–217.

[9] X. Lu, Y. Zhang, C. Luo, Y. Wang, *Synth. Commun.* **2006**, *36*, 2503–2511.

[10] P. Kuhn, A. Alix, M. Kumarrajaa, B. Louis, P. Pale, J. Sommer, *European J. Org. Chem.* **2009**, 423–429.

[11] S. Adimurthy, C. C. Malakar, U. Beifuss, *J. Org. Chem.* **2009**, *74*, 5648–5651.

[12] K. Okuro, M. Furuune, M. Miura, M. Nomura, *Tetrahedron Lett.* **1992**, *33*, 5363–5364.

[13] G. Chen, X. Zhu, J. Cai, Y. Wan, *Synth. Commun.* **2007**, *37*, 1355–1361.

[14] F. Monnier, F. Turtaut, L. Duroure, M. Taillefer, *Org. Lett.* **2008**, *10*, 3203–3206.

[15] A. Sagadevan, K. C. Hwang, *Adv. Synth. Catal.* **2012**, *354*, 3421–3427.

[16] J. E. Hein, V. V Fokin, *Chem. Soc. Rev.* **2010**, *39*, 1302–1315.

[17] O. Avrutina, M. Empting, S. Fabritz, M. Daneschdar, H. Frauendorf, U. Diederichsen, H. Kolmar, *Org. Biomol. Chem.* **2009**, *7*, 4177–4185.

[18] A. Marra, A. Vecchi, C. Chiappe, B. Melai, A. Dondoni, *J. Org. Chem.* **2008**, *73*, 2458–2461.

[19] T. Miao, L. Wang, *Synthesis-Stuttgart* **2008**, 363–368.

[20] M. Li, P. De, S. R. Gondi, B. S. Sumerlin, *Macromol. Rapid Commun.* **2008**, *29*, 1172–1176.

[21] T. Jin, F. Kitahara, S. Kamijo, Y. Yamamoto, *Chem. Asian J.* **2008**, *3*, 1575–1580.

[22] A. S. Guram, R. A. Rennels, S. L. Buchwald, *Angew. Chemie-International Ed. English* **1995**, *34*, 1348–1350.

[23] J. Louie, J. F. Hartwig, *Tetrahedron Lett.* **1995**, *36*, 3609–3612.

[24] B. Schlummer, U. Scholz, *Adv. Synth. Catal.* **2004**, *346*, 1599–1626.

[25] N. T. S. Phan, M. Van Der Sluys, C. W. Jones, *Adv. Synth. Catal.* **2006**, *348*, 609–679.

[26] C. E. Garrett, K. Prasad, *Adv. Synth. Catal.* **2004**, *346*, 889–900.

[27] J. RICHARDSON, C. JONES, *J. Catal.* **2007**, *251*, 80–93.

[28] Y. He, C. Cai, *Catal. Sci. Technol.* **2012**, *2*, 1126-1129.

[29] S. M. Islam, S. Mondal, P. Mondal, A. S. Roy, K. Tuhina, N. Salam, M. Mobarak, *J. Organomet. Chem.* **2012**, *696*, 4264–4274.

[30] B. M. Choudary, C. Sridhar, M. L. Kantam, B. Sreedhar, *Tetrahedron Lett.* **2004**, *45*, 7319–7321.

[31] G. C. H. Chiang, T. Olsson, *Org. Lett.* **2004**, *6*, 3079–3082.

[32] F. Monnier, M. Taillefer, *Angew. Chemie-International Ed.* **2009**, *48*, 6954–6971.

[33] N. R. Jogdand, B. B. Shingate, M. S. Shingare, *Tetrahedron Lett.* **2009**, *50*, 4019–4021.

[34] N. Xia, M. Taillefer, *Angew. Chemie-International Ed.* **2009**, *48*, 337–339.

[35] R. Hosseinzadeh, M. Mohadjerani, R. Tavakoli, M. Alikarami, *Synth. Commun.* **2010**, *40*, 282–288.

[36] X. Guo, H. H. Rao, H. Fu, Y. Y. Jiang, Y. F. Zhao, *Adv. Synth. Catal.* **2006**, *348*, 2197–2202.

[37] R. Hosseinzadeh, Y. Sarrafi, M. Mohadjerani, F. Mohammadpourmir, *Tetrahedron Lett.* **2008**, *49*, 840–843.

[38] R. A. Altman, E. D. Koval, S. L. Buchwald, *J. Org. Chem.* **2007**, *72*, 6190–6199.

[39] M. T. Wentzel, J. B. Hewgley, R. M. Kamble, P. D. Wall, M. C. Kozlowski, *Adv. Synth. Catal.* **2009**, *351*, 931–937.

[40] M. Kantam, B. Rao, B. Choudary, R. Reddy, *Synlett* **2006**, *2006*, 2195–2198.

[41] S. Jammi, S. Sakthivel, L. Rout, T. Mukherjee, S. Mandal, R. Mitra, P. Saha, T. Punniyamurthy, *J. Org. Chem.* **2009**, *74*, 1971–1976.

[42] F. Monnier, M. Taillefer, *Angew. Chem. Int. Ed. Engl.* **2009**, *48*, 6954–6971.

[43] A. Klapars, J. C. Antilla, X. Huang, S. L. Buchwald, *J. Am. Chem. Soc.* **2001**, *123*, 7727–7729.

[44] H. H. Xu, C. Wolf, *Chem. Commun.* **2009**, 3035–3037.

[45] A. Correa, C. Bolm, *Adv. Synth. Catal.* **2007**, *349*, 2673–2676.

[46] E. Sperotto, J. G. de Vries, G. P. M. van Klink, G. van Koten, *Tetrahedron Lett.* **2007**, *48*, 7366–7370.

[47] L. Rout, S. Jammi, T. Punniyamurthy, *Org. Lett.* **2007**, *9*, 3397–3399.

[48] K. R. Reddy, N. S. Kumar, B. Sreedhar, M. L. Kantam, *J. Mol. Catal. a-Chemical* **2006**, *252*, 136–141.

[49] P. R. Likhar, S. Roy, M. Roy, M. L. Kantam, R. L. De, *J. Mol. Catal. A Chem.* **2007**, *271*, 57–62.

[50] B. M. Choudary, C. Sridhar, M. L. Kantam, G. T. Venkanna, B. Sreedhar, *J. Am. Chem. Soc.* **2005**, *127*, 9948–9949.

[51] M. L. Kantam, G. T. Venkanna, C. Sridhar, B. Sreedhar, B. M. Choudary, *J. Org. Chem.* **2006**, *71*, 9522–9524.

[52] B. Sreedhar, R. Arundhathi, M. A. Reddy, M. L. Kantam, *Synthesis-Stuttgart* **2009**, 483–487.

[53] N. M. Patil, S. P. Gupte, R. V. Chaudhari, *Appl. Catal. A Gen.* **2010**, *372*, 73–81.

[54] T. YAMAGUCHI, *J. Catal.* **1981**, *67*, 324–330.

[55] Q. Dai, X. Wang, G. Lu, *Appl. Catal. B Environ.* **2008**, *81*, 192–202.

[56] P. Bera, S. T. Aruna, K. C. Patil, M. S. Hegde, *J. Catal.* **1999**, *186*, 36–44.

[57] Y. Hu, L. Dong, J. Wang, W. Ding, Y. Chen, *J. Mol. Catal. A Chem.* **2000**, *162*, 307–316.

[58] N. A. S. Amin, E. F. Tan, Z. A. Manan, *Appl. Catal. B Environ.* **2003**, *43*, 57–69.

[59] X. Y. Jiang, L. P. Lou, Y. X. Chen, X. M. Zheng, *J. Mol. Catal. a-Chemical* **2003**, *197*, 193–205.

[60] G. R. Rao, H. R. Sahu, B. G. Mishra, *Colloids Surfaces A Physicochem. Eng. Asp.* **2003**, *220*, 261–269.

[61] M. Khristova, B. Ivanov, I. Spassova, T. Spassov, *Catal. Letters* **2007**, *119*, 79–86.

[62] C. C. Pantazis, D. E. Petrakis, P. J. Pomonis, *Appl. Catal. B Environ.* **2007**, *77*, 66–72.

[63] J. Beckers, G. Rothenberg, *Dalton Trans.* **2008**, 6573–8.

[64] L. J. Liu, B. Liu, L. H. Dong, J. Zhu, H. Q. Wan, K. Q. Sun, B. Zhao, H. Y. Zhu, L. Dong, Y. Chen, *Appl. Catal. B-Environmental* **2009**, *90*, 578–586.

[65] J. F. Chen, Y. Y. Zhan, J. J. Zhu, C. Q. Chen, X. Y. Lin, Q. Zheng, *Appl. Catal. a-General* **2010**, *377*, 121–127.

[66] L. J. Liu, Z. J. Yao, Y. Deng, F. Gao, B. Liu, L. Dong, *ChemCatChem* **2011**, *3*, 978–989.

[67] A. Martínez-Arias, A. B. Hungría, A. Iglesias-Juez, M. Fernández-García, J. A. Anderson, J. C. Conesa, G. Munuera, J. Soria, *Catal. Today* **2012**, *180*, 81–87.

[68] M. F. Luo, J. M. Ma, J. Q. Lu, Y. P. Song, Y. J. Wang, *J. Catal.* **2007**, *246*, 52–59.

[69] M. H. Lu, M. S. Li, Y. H. Shan, K. Seshan, L. Lefferts, *Chinese J. Chem.* **2008**, *26*, 1035–1040.

[70] R. Zhang, T. Haddadin, D. P. Rubiano, H. Nair, C. S. Polster, C. D. Baertsch, *Acs Catal.* **2011**, *1*, 519–525.

[71] P. Djinovic, J. Batista, A. Pintar, *Catal. Today* **2009**, *147*, S191–S197.

[72] R. K. Pati, I. C. Lee, S. C. Hou, O. Akhuemonkhan, K. J. Gaskell, Q. Wang, A. I. Frenkel, D. Chu, L. G. Salamanca-Riba, S. H. Ehrman, *ACS Appl. Mater. Interfaces* **2009**, *1*, 2624–2635.

[73] P. Gawade, B. Mirkelamoglu, U. S. Ozkan, *J. Phys. Chem. C* **2010**, *114*, 18173–18181.

[74] L. Li, L. Song, H. D. Wang, C. Q. Chen, Y. S. She, Y. Y. Zhan, X. Y. Lin, Q. Zheng, *Int. J. Hydrogen Energy* **2011**, *36*, 8839–8849.

[75] R. Si, J. Raitano, N. Yi, L. H. Zhang, S. W. Chan, M. Flytzani-Stephanopoulos, *Catal. Today* **2012**, *180*, 68–80.

[76] L. Wan, X. Cui, H. Chen, J. Shi, *Mater. Lett.* **2010**, *64*, 1379–1382.

[77] J. Zhu, Q. Gao, Z. Chen, *Appl. Catal. B Environ.* **2008**, *81*, 236–243.

[78] E. Sperotto, G. P. M. van Klink, G. van Koten, J. G. de Vries, *Dalt. Trans.* **2010**, *39*, 10338-10351.

[79] W. W. Lukens, P. Schmidt-Winkel, D. Y. Zhao, J. L. Feng, G. D. Stucky, *Langmuir* **1999**, *15*, 5403–5409.

[80] K. W. Anderson, T. Ikawa, R. E. Tundel, S. L. Buchwald, *J. Am. Chem. Soc.* **2006**, *128*, 10694–10695.

[81] S. Maurer, W. Liu, X. Zhang, Y. Jiang, D. Ma, *Synlett* **2010**, 976–978.

[82] J. Chen, T. Yuan, W. Hao, M. Cai, *Catal. Commun.* **2011**, *12*, 1463–1465.

[83] K. G. Thakur, G. Sekar, *Chem. Commun.* **2011**, *47*, 6692–6694.

[84] D. Zhao, N. Wu, S. Zhang, P. Xi, X. Su, J. Lan, J. You, *Angew. Chemie-International Ed.* **2009**, *48*, 8729–8732.

[85] O. Bortolini, G. Fantin, V. Ferretti, M. Fogagnolo, P. P. Giovannini, A. Massi, S. Pacifico, D. Ragno, *Adv. Synth. Catal.* **2013**, *355*, 3244–3252.

[86] G. Jimenez-Cadena, E. Comini, M. Ferroni, G. Sberveglieri, *Mater. Lett.* **2010**, *64*, 469–471.

[87] M. J. Stiff, *Water Res.* **1971**, *5*, 171–176.

[88] N. Habbache, N. Alane, S. Djerad, L. Tifouti, *Chem. Eng. J.* **2009**, *152*, 503–508.

[89] L. Blackburn, R. J. K. Taylor, *Org. Lett.* **2001**, *3*, 1637–1639.

[90] D. Gnanamgari, E. L. O. Sauer, N. D. Schley, C. Butler, C. D. Incarvito, R. H. Crabtree, *Organometallics* **2009**, *28*, 321–325.

[91] H. Sun, F. Z. Su, J. Ni, Y. Cao, H. Y. He, K. N. Fan, *Angew. Chemie-International Ed.* **2009**, *48*, 4390–4393.

[92] S. Kegnaes, J. Mielby, U. V Mentzel, C. H. Christensen, A. Riisager, *Green Chem.* **2010**, *12*, 1437–1441.

[93] M. A. Esteruelas, N. Honczek, M. Olivan, E. Onate, M. Valencia, *Organometallics* **2011**, *30*, 2468–2471.

[94] W. He, L. D. Wang, C. L. Sun, K. K. Wu, S. B. He, J. P. Chen, P. Wu, Z. K. Yu, *Chem. Eur. J.* **2011**, *17*, 13308–13317.

[95] L. Jiang, L. L. Jin, H. W. Tian, X. Q. Yuan, X. C. Yu, Q. Xu, *Chem. Commun.* **2011**, *47*, 10833–10835.

[96] C. Xu, L. Y. Goh, S. A. Pullarkat, *Organometallics* **2011**, *30*, 6499–6502.

[97] G. B. Chu, C. B. Li, *Org. Biomol. Chem.* **2010**, *8*, 4716–4719.

[98] A. Dhakshinamoorthy, M. Alvaro, H. Garcia, *ChemCatChem* **2010**, *2*, 1438–1443.

[99] Q. Cai, H. Zhang, B. L. Zou, X. Xie, W. Zhu, G. He, J. Wang, X. H. Pan, Y. Chen, Q. Yuan, et al., *Pure Appl. Chem.* **2009**, *81*, 227–234.

[100] S. Furukawa, Y. Ohno, T. Shishido, K. Teramura, T. Tanaka, *Acs Catal.* **2011**, *1*, 1150–1153.

[101] R. D. Patil, S. Adimurthy, *Adv. Synth. Catal.* **2011**, *353*, 1695–1700.

[102] X. J. Lang, W. H. Ma, Y. B. Zhao, C. C. Chen, H. W. Ji, J. C. Zhao, *Chem. Eur. J.* **2012**, *18*, 2624–2631.

[103] K. Orito, T. Hatakeyama, M. Takeo, S. Uchiito, M. Tokuda, H. Suginome, *Tetrahedron* **1998**, *54*, 8403–8410.

[104] T. Mukaiyama, A. Kawana, Y. Fukuda, J. Matsuo, *Chem. Lett.* **2001**, 390–391.

[105] H. Choi, M. P. Doyle, *Chem. Commun.* **2007**, 745–747.

[106] B. L. Zhu, M. Lazar, B. G. Trewyn, R. J. Angelici, *J. Catal.* **2008**, *260*, 1–6.

[107] G. Jiang, J. Chen, J. S. Huang, C. M. Che, *Org. Lett.* **2009**, *11*, 4568–4571.

[108] M. H. So, Y. G. Liu, C. M. Ho, C. M. Che, *Chem. Asian J.* **2009**, *4*, 1551–1561.

[109] A. Prades, E. Peris, M. Albrecht, *Organometallics* **2011**, *30*, 1162–1167.

[110] T. Hirao, M. Higuchi, Y. Ohshiro, I. Ikeda, *Chem. Lett.* **1993**, 1889–1890.

[111] K. Nakayama, M. Hamamoto, Y. Nishiyama, Y. Ishii, *Chem. Lett.* **1993**, 1699–1702.

[112] L. Aschwanden, B. Panella, P. Rossbach, B. Keller, A. Baiker, *ChemCatChem* **2009**, *1*, 111–115.

[113] L. Aschwanden, T. Mallat, J. D. Grunwaldt, F. Krumeich, A. Baiker, *J. Mol. Catal. a-Chemical* **2009**, *300*, 111–115.

[114] K. W. Chi, H. Y. Hwang, J. Y. Park, C. W. Lee, *Synth. Met.* **2009**, *159*, 26–28.

[115] Y. Perez, C. Aprile, A. Corma, H. Garcia, *Catal. Letters* **2010**, *134*, 204–209.

[116] H. F. Guo, M. Kemell, A. Al-Hunaiti, S. Rautiainen, M. Leskela, T. Repo, *Catal. Commun.* **2011**, *12*, 1260–1264.

[117] X. J. Lang, H. W. Ji, C. C. Chen, W. H. Ma, J. C. Zhao, *Angew. Chemie-International Ed.* **2011**, *50*, 3934–3937.

[118] M. T. Schümperli, C. Hammond, I. Hermans, *Acs Catal.* **2012**, *2*, 1108–1117.

[119] A. Grirrane, A. Corma, H. Garcia, *J. Catal.* **2009**, *264*, 138–144.

[120] S. Kodama, J. Yoshida, A. Nomoto, Y. Ueta, S. Yano, M. Ueshima, A. Ogawa, *Tetrahedron Lett.* **2010**, *51*, 2450–2452.

[121] S. Minakata, Y. Ohshima, A. Takemiya, I. Ryu, M. Komatsu, Y. Ohshiro, *Chem. Lett.* **1997**, 311–312.

[122] S. Naya, K. Kimura, H. Tada, *ACS Catal.* **2013**, *3*, 10–13.

[123] X. Tang, B. Zhang, Y. Li, Y. Xu, Q. Xin, W. Shen, *Catal. Today* **2004**, *93–95*, 191–198.

[124] H. Zou, X. Dong, W. Lin, *Appl. Surf. Sci.* **2006**, *253*, 2893–2898.

[125] J. L. Ayastuy, A. Gurbani, M. P. Gonzalez-Marcos, M. A. Gutierrez-Ortiz, *Int. J. Hydrogen Energy* **2010**, *35*, 1232–1244.

[126] J. L. Ayastuy, N. K. Gamboa, M. P. González-Marcos, M. A. Gutiérrez-Ortiz, *Chem. Eng. J.* **2011**, *171*, 224–231.

[127] G. Avgouropoulos, T. Ioannides, *Appl. Catal. A Gen.* **2003**, *244*, 155–167.

[128] P. Zhu, J. Li, S. Zuo, R. Zhou, *Appl. Surf. Sci.* **2008**, *255*, 2903–2909.

[129] A. Gómez-Cortés, Y. Márquez, J. Arenas-Alatorre, G. Díaz, *Catal. Today* **2008**, *133–135*, 743–749.

[130] M. Tamura, T. Tonomura, K. Shimizu, A. Satsuma, *Green Chem.* **2012**, *14*, 717–724.

[131] M. K. Patil, M. Keller, B. M. Reddy, P. Pale, J. Sommer, *European J. Org. Chem.* **2008**, 4440–4445.

[132] K. H. V. Reddy, V. P. Reddy, J. Shankar, B. Madhav, B. S. P. Anil Kumar, Y. V. D. Nageswar, *Tetrahedron Lett.* **2011**, *52*, 2679–2682.

[133] T. Oishi, T. Katayama, K. Yamaguchi, N. Mizuno, *Chemistry* **2009**, *15*, 7539–42.

[134] Z. Ma, X. Wang, S. Wei, H. Yang, F. Zhang, P. Wang, M. Xie, J. Ma, *Catal. Commun.* **2013**, *39*, 24–29.

[135] L. Al-Hmoud, C. W. Jones, *J. Catal.* **2013**, *301*, 116–124.

[136] T. Oishi, K. Yamaguchi, N. Mizuno, *ACS Catal.* **2011**, *1*, 1351–1354.

[137] J. A. Rodríguez, J. Evans, J. Graciani, J.-B. Park, P. Liu, J. Hrbek, J. F. Sanz, *J. Phys. Chem. C* **2009**, *113*, 7364–7370.

[138] N. Scotti, D. Monticelli, F. Zaccheria, *Inorganica Chim. Acta* **2012**, *380*, 194–200.

[139] B. M. Reddy, B. Chowdhury, P. G. Smirniotis, *Appl. Catal. A Gen.* **2001**, *211*, 19–30.

[140] S. Matsuda, A. Kato, *Appl. Catal.* **1983**, *8*, 149–165.

[141] K. V. R. Chary, G. V. Sagar, D. Naresh, K. K. Seela, B. Sridhar, *J. Phys. Chem. B* **2005**, *109*, 9437–9444.

[142] T. Sakamoto, H. Yonehara, C. Pac, *J. Org. Chem.* **1994**, *59*, 6859–6861.

[143] S. Bhadra, B. Sreedhar, B. C. Ranu, *Adv. Synth. Catal.* **2009**, *351*, 2369–2378.

[144] I. S. Park, M. S. Kwon, Y. Kim, J. S. Lee, J. Park, *Org. Lett.* **2008**, *10*, 497–500.

[145] T. Katayama, K. Kamata, K. Yamaguchi, N. Mizuno, *ChemSusChem* **2009**, *2*, 59–62.

[146] K. Yamaguchi, T. Oishi, T. Katayama, N. Mizuno, *Chemistry* **2009**, *15*, 10464–10472.

[147] J. D. Crowley, S. M. Goldup, N. D. Gowans, D. A. Leigh, V. E. Ronaldson, A. M. Z. Slawin, *J. Am. Chem. Soc.* **2010**, *132*, 6243–6248.

[148] H. A. Stefani, A. S. Guarezemini, R. Cella, *Tetrahedron* **2010**, *66*, 7871–7918.

[149] X. Jia, K. Yin, C. Li, J. Li, H. Bian, *Green Chem.* **2011**, *13*, 2175–2178.

[150] L. Li, J. Wang, G. Zhang, Q. Liu, *Tetrahedron Lett.* **2009**, *50*, 4033–4036.

[151] R. Xiao, R. Yao, M. Cai, *European J. Org. Chem.* **2012**, *2012*, 4178–4184.

[152] A. Lei, M. Srivastava, X. Zhang, *J. Org. Chem.* **2002**, *67*, 1969–1971.

[153] A. S. Batsanov, J. C. Collings, I. J. S. Fairlamb, J. P. Holland, J. A. K. Howard, Z. Lin, T. B. Marder, A. C. Parsons, R. M. Ward, J. Zhu, *J. Org. Chem.* **2005**, *70*, 703–706.

[154] M. Shi, H. Qian, *Appl. Organomet. Chem.* **2006**, *20*, 771–774.

[155] S.-N. Chen, W.-Y. Wu, F.-Y. Tsai, *Green Chem.* **2009**, *11*, 269–274.

[156] L. Zhou, H.-Y. Zhan, H.-L. Liu, H.-F. Jinag, *Chinese J. Chem.* **2007**, *25*, 1413–1416.

[157] L. van Gelderen, G. Rothenberg, V. Roberto Calderone, K. Wilson, N. Raveendran Shiju, *Appl. Organomet. Chem.* **2013**, *27*, 23–27.

[158] H. Li, M. Yang, X. Zhang, L. Yan, J. Li, Y. Qi, *New J. Chem.* **2013**, *37*, 1343–1349.

[159] S. Bali, T. T. Chen, W. Chaikittisilp, C. W. Jones, *Energy & Fuels* **2013**, *27*, 1547–1554.

[160] G. Fierro, M. Lo Jacono, M. Inversi, P. Porta, R. Lavecchia, F. Cioci, *J. Catal.* **1994**, *148*, 709–721.

[161] F. Boccuzzi, A. Chiorino, M. Gargano, and N. Ravasio, *J. Catal.* **1997**, *165*, 129–139.